Final Report

FDOT Contract No: BD545, RPWO # 31
UF Contract No. 00051239

Prestressed Concrete Pile Installation - Utilizing Jetting and Pressure Grouting

Principal Investigators: Michael McVay
David Bloomquist
Heath Forbes
James Johnson

Department of Civil and Coastal Engineering
University of Florida
Gainesville, Florida 32611

Developed for the

Peter Lai, P.E., Project Manager

January 2009

DISCLAIMER

"The opinions, findings, and conclusions expressed in this publication are those of the authors and not necessarily those of the Florida Department of Transportation or the U.S. Department of Transportation.

Prepared in cooperation with the State of Florida Department of Transportation and the U.S. Department of Transportation."

ACKNOWLEDGEMENTS

The researchers would first like to thank the FDOT for the financial support to carry out this research as well as the guidance of the project manager for its successful outcome. In addition, this research could not have been completed without the aide of the State Materials Office in locating and trucking all the soil to the facility, as well as conduct all the soil monitoring, as well as testing (e.g., nuclear density, compaction, strength, and insitu DMT and PMT tests). Finally, the researchers would like to recognize Coastal Caisson's generous donation (approximately $100,000) for materials and labor (e.g., use of 3/4″ thick steel casing vs. corrugated pipe, 2nd drill rig, crews, etc.) in the construction of the FDOT/UF 12′ × 35′ test chamber used for this research.

SI (MODERN METRIC) CONVERSION FACTORS (from FHWA)

APPROXIMATE CONVERSIONS TO SI UNITS

SYMBOL	WHEN YOU KNOW	MULTIPLY BY	TO FIND	SYMBOL
LENGTH				
in	inches	25.4	millimeters	mm
ft	feet	0.305	meters	m
yd	yards	0.914	meters	m
mi	miles	1.61	kilometers	km

SYMBOL	WHEN YOU KNOW	MULTIPLY BY	TO FIND	SYMBOL
AREA				
in^2	squareinches	645.2	square millimeters	mm^2
ft^2	squarefeet	0.093	square meters	m^2
yd^2	square yard	0.836	square meters	m^2
ac	acres	0.405	hectares	ha
mi^2	square miles	2.59	square kilometers	km^2

SYMBOL	WHEN YOU KNOW	MULTIPLY BY	TO FIND	SYMBOL
VOLUME				
fl oz	fluid ounces	29.57	milliliters	mL
gal	gallons	3.785	liters	L
ft^3	cubic feet	0.028	cubic meters	m^3
yd^3	cubic yards	0.765	cubic meters	m^3
NOTE: volumes greater than 1000 L shall be shown in m^3				

SYMBOL	WHEN YOU KNOW	MULTIPLY BY	TO FIND	SYMBOL
MASS				
oz	ounces	28.35	grams	g
lb	pounds	0.454	kilograms	kg
T	short tons (2000 lb)	0.907	megagrams (or "metric ton")	Mg (or "t")

SYMBOL	WHEN YOU KNOW	MULTIPLY BY	TO FIND	SYMBOL
TEMPERATURE (exact degrees)				
°F	Fahrenheit	5 (F-32)/9 or (F-32)/1.8	Celsius	°C

SYMBOL	WHEN YOU KNOW	MULTIPLY BY	TO FIND	SYMBOL
ILLUMINATION				
fc	foot-candles	10.76	lux	lx
fl	foot-Lamberts	3.426	candela/m^2	cd/m^2

SYMBOL	WHEN YOU KNOW	MULTIPLY BY	TO FIND	SYMBOL
FORCE and PRESSURE or STRESS				
lbf	poundforce	4.45	newtons	N
lbf/in^2	poundforce per square inch	6.89	kilopascals	kPa

APPROXIMATE CONVERSIONS TO SI UNITS

SYMBOL	WHEN YOU KNOW	MULTIPLY BY	TO FIND	SYMBOL
LENGTH				
mm	millimeters	0.039	inches	in
m	meters	3.28	feet	ft
m	meters	1.09	yards	yd
km	kilometers	0.621	miles	mi

SYMBOL	WHEN YOU KNOW	MULTIPLY BY	TO FIND	SYMBOL
AREA				
mm^2	square millimeters	0.0016	square inches	in^2
m^2	square meters	10.764	square feet	ft^2
m^2	square meters	1.195	square yards	yd^2
ha	hectares	2.47	acres	ac
km^2	square kilometers	0.386	square miles	mi^2

SYMBOL	WHEN YOU KNOW	MULTIPLY BY	TO FIND	SYMBOL
VOLUME				
mL	milliliters	0.034	fluid ounces	fl oz
L	liters	0.264	gallons	gal
m^3	cubic meters	35.314	cubic feet	ft^3
m^3	cubic meters	1.307	cubic yards	yd^3

SYMBOL	WHEN YOU KNOW	MULTIPLY BY	TO FIND	SYMBOL
MASS				
g	grams	0.035	ounces	oz
kg	kilograms	2.202	pounds	lb
Mg (or "t")	megagrams (or "metric ton")	1.103	short tons (2000 lb)	T

SYMBOL	WHEN YOU KNOW	MULTIPLY BY	TO FIND	SYMBOL
TEMPERATURE (exact degrees)				
°C	Celsius	1.8C+32	Fahrenheit	°F

SYMBOL	WHEN YOU KNOW	MULTIPLY BY	TO FIND	SYMBOL
ILLUMINATION				
lx	lux	0.0929	foot-candles	fc
cd/m^2	candela/m^2	0.2919	foot-Lamberts	fl

SYMBOL	WHEN YOU KNOW	MULTIPLY BY	TO FIND	SYMBOL
FORCE and PRESSURE or STRESS				
N	newtons	0.225	poundforce	lbf
kPa	kilopascals	0.145	poundforce per square inch	lbf/in^2

*SI is the symbol for International System of Units. Appropriate rounding should be made to comply with Section 4 of ASTM E380. (Revised March 2003)

TECHNICAL REPORT DOCUMENTATION PAGE

1. Report No.	2. Government Accession No.	3. Recipient's Catalog No.

4. Title and Subtitle	5. Report Date
Prestressed Concrete Pile Installation – Utilizing Jetting and Pressure Grouting	March 2009
	6. Performing Organization Code
7. Author(s)	8. Performing Organization Report No.
Michael McVay, David Bloomquist, Heath Forbes, James Johnson	
9. Performing Organization Name and Address	10. Work Unit No. (TRAIS)
Department of Civil and Coastal Engineering 365 Weil Hall – P.O. Box 116580 University of Florida Gainesville, FL 32611-6580	
	11. Contract or Grant No.
	BD-545 #31
12. Sponsoring Agency Name and Address	13. Type of Report and Period Covered
Florida Department of Transportation 605 Suwannee Street, MS 30 Tallahassee, FL 32399	Final Report _9/22/04 -_2/28/09
	14. Sponsoring Agency Code

15. Supplementary Notes

16. Abstract

With increased urbanization, selection of deep foundations (bridges, signage, walls, etc.) is being controlled by the minimization of impact or disturbance, as well as quality assurance and control (e.g., proof testing, etc.). Deep foundations have thus migrated from driven piles to drilled shafts to tip grouted drilled shafts. Recently, a number of European and Asian designers/contractors have begun grouting driven precast concrete piles along their sides and at their tips. The use of these in Florida soils as well as their design is the focus of this research.

Testing of the proposed jet grouted piles revealed problems with both the grout delivery system, as well as the grout mix design. In addition, full scale tests showed greater radial than vertical grout movement as well as poor bonding between the grout and precast member. Subsequently, improvements to the grout delivery system, mix design and the incorporation of a semi-rigid high tensile strength membrane were introduced. Testing on jet grouted piles from 8 to 20 feet in length revealed both excellent grout side grout coverage, as well as unit side resistance under both axial and torsional loading. Using cavity expansion theory and/or insitu Pressuremeter testing, both the grout pressures and skin and tip resistances may be estimated. The new pile has a number of attractive features: 1) know structural cross-section; 2) minimal installation disturbance; and 3) proof testing and higher LRFD ø factors for design.

17. Key Words	18. Distribution Statement
Deep Foundations, Jet Grouted Piles, Axial and Torsional Resistance, Chamber Testing, and Pile soil stresses.	No restrictions.

19. Security Classif. (of this report)	20. Security Classif. (of this page)	21. No. of Pages	22. Price
Unclassified	Unclassified	158	

Form DOT F 1700.7 (8-72) Reproduction of completed page authorized

TABLE OF CONTENTS

page

LIST OF TABLES

LIST OF FIGURES

EXECUTIVE SUMMARY

Most of FDOT structures (buildings, bridges, signage, walls, etc.) are founded on deep foundations. In the past, the foundation of choice for such structures were driven pre-stressed concrete piles. However, with urbanization, noise and associated vibration, pile driving became an issue. Hence, drilled shafts became more common place due to their less intrusive nature. Unfortunately, because of their installation process (e.g., a horizontal stress reduction), axial capacities were questioned.

To address this, the FDOT and industry looked at grouting the drilled shaft tips, which not only increased tip resistance, but provided a proof test for every shaft, resulting in higher LRFD ϕ factors (Load Resistance Factor Design). Still remaining was the issue of quality control (i.e., the structural integrity of the shaft) and the fact that they have the lowest skin friction of all deep foundation types.

This research tries to resolve the above problems of installing foundation units without noise and vibration by jetting; elimating quality control by using precast concrete piles, and also improve the disturbed surounding soils by pressure grouting both the side and bottom of the piles.

Recently, a number of European and Asian designers/contractor have grouted driven or drilled precast concrete piles at both the side and the tip. Pile capacity increases of 100 percent have been reported for these new piles.

However, jetting, grouting, and load testing revealed a number of technical problems:

1) insertion of precast piles by jetting consumed too much water;
2) compaction grout with pea size aggregate caused hydro locking in the precast pile's internal grout pipes,
3) grout flowed radially rather than vertically during perimeter grouting,

4) grouting could only be performed once through a given grout delivery pipe.

5) grout did not bond well to the pile due to soil contamination.

Subsequently, a new jet-grouted pile system was developed. The jetting system was improved by redesigning the nozzle and introducing compressed air to reduce water volume and increase the jet pressure. In case of the grouting system, some of unique attributes include a novel grout delivery and pressure monitoring system that allows for multiple grouting sessions was developed. In addition, the mix design was improved by incorporating micro-fine flyash, which results in excellent bonding of grout to the pile. Finally, a semi-rigid membrane was introduced around the perimeter of the pile in order to restrict radial grout flow, thereby increasing vertical grout movement as well as to prevent soil contamination at the grout pile interface. With these improvements, small jet-grouted piles, i.e., 6″×6″ and 8″×8″ by 8 foot length, could provide axial capacities of 65 kips to 110 kips, respectively,and unit skin friction of 1.2 ksf at 5 ft depth. The piles had excellent grout coverage and bonding along their entire length. In addition, the final side grout perimeters were twice the precast members. Subsequently, a 16″×16″ by 20 foot length precast concrete pile was constructed and tested. It was first grouted along its length, allowed to cure and then load tested in torque to failure. This was followed by grouting the tip and tested axially. The torque test provided 450 ft-kip of resistance or an average shear resistance of 1.6 ksf, and the axial test developed 300 kips of vertical load at 0.01 inch pile head displacement.

Based on cavity expansion theory, a recommended jet grouted pile design methodology was developed. It includes both estimated grout pressures during installation and estimated skin and tip resistance. The research shows that jet-grouted piles have a number of distinct advantages: (1) the reinforced precast concrete member eliminates the quality uncertainty issue inherent in cast-in-place drilled shafts; (2) jetting minimizes noise

and vibration; (3) grouting maximizes the skin and tip resistance; and (4) tip grouting of the pile not only increases tip resistance, but provides a proof test from which higher LRFD ϕ factors may be used in design.

CHAPTER 1
INTRODUCTION

1.1 Background

Deep foundation construction (for bridges, lights/signs, etc.) especially driven piles in metropolitan and/or businesses areas has become sensitive to pile driving vibration and noise. Selection of an alternative bridge foundation system other than driven piles has become an important design and construction issue in Florida. Florida Department of Transportation (FDOT) Standard Specifications Section 455 provides general guidelines for use of water jetting as well as other pile hole formation processes to minimize the effects of vibrations on adjacent structures. However, the Specification requires that all piles jetted or placed in preformed holes be driven the last 10′ as a minimum to ensure that the required capacity is obtained. Moreover, with most piles tipped in strong competent soils, vibrations, and noise are still concerns for such installations.

To provide an alternative, FDOT undertook research on drilled shafts and subsequently post-grouted drilled shaft tips. Although the results indicated that drilled shaft resistances (tip resistance, not skin friction) increased after post grouting, other problems associated with quality of construction were a concern. Moreover, the grouting did not improve side resistance of the drilled shafts which is the lowest of any installed deep foundations founded in soils.

One conceptually feasible pile installation method, which not only can minimize the construction vibration and noise problem, but also can eliminate the integrity issue of drilled shafts (either conventional or post grouted tips) is to install a precast-concrete-pile by jetting and subsequently post-grouting both the shaft and tip of the pile. The advantages of this alternative are that it combines several proven deep foundation installation techniques, good quality control, more economical, as well as significantly diminishing noise and vibration.

The proven installation techniques are (1) use of precast reinforced concrete pile to eliminate the uncertainty of the cast-in-place drilled shaft quality; (2) jetting minimizes noise and vibration; and (3) grouting maximizes skin and tip resistance.

The objective of this research was to develop a jet-grouted precast concrete pile foundation system for Florida soils. The research focused on designing, fabricating, and testing a jetting-grouting system, as well as identifying a recommended design methodology for the foundation system. The system is intended initially for small-precast concrete piles, i.e., 12″ to 24″ in dimensions and depths from 10′ to 25′. A construction procedure as well as specification will be developed at the conclusion of this report.

1.2 Scope of Work

1.2.1 Test Chamber and Reaction Shafts

Since the proposed foundation system has never been used in practice, the research had to involve experimental testing and validation. Generally, a number of deep foundation testing projects are conducted in the centrifuge to replicate stresses and reduce costs; however due to the need to develop jetting and grouting systems, as well as conduct validation tests, it was decided to perform the tests in the largest in-ground test chamber that could be installed. The final installed chamber was 35′ deep and 12′ in diameter. The benefits of the chamber are: 1) it ensures the replication of the pile-soil stresses; 2) it permits soil excavation to characterize pile/soil grout zones; and 3) it allows for repetitive testing or parametric investigation.

The test chamber was welded ½″ thick steel plates, used as a casing in prior drilled shaft construction. The chamber was installed with a drilled shaft rig capable of boring a 12′ diameter hole, 40′ deep. The bottom of the test chamber has a 5′ to 7′ thick concrete plug to

allow for soil removal as well as variation in water level within the chamber different from the surrounding insitu soil.

To conduct top-down axial compression testing on the jet-grouted piles, two 4′ diameter by 45′ long reaction drilled shafts were placed at 28′ centers to the test chamber. The shafts also had four Dywidag bars cast in each to connect to a reaction beam to carry the tension load generated from the axial downward compression loading of the jet-grouted piles. Each reaction shaft has approximately 150 ton skin friction for tension loading. Details of installation and design of the reaction and test chamber are provided in a later chapter.

1.2.2 Development of Jet-Grouted Concrete Piles

The first known published test results of using drilled shaft grouting was by Gouvenot and Gabix (1975). The results of the testing indicated an increase of 2.5 times in shaft friction. A review of published works on pile construction and the benefit of post grouting between 1975 and 1985 were presented by Bruce (1986). More recently, tip and shaft grouting were used for piles/drilled shafts in sands (Robson and Wahby, 1994; Byrne et al, 1998; Gokalp and Savaskan, 1998). A number of different apparatus for injecting grouts along the pile-soil interface have been developed; most appear as in Figure 1.1, from University of West Australia.

Many different apparatus have been developed for tip grouting deep foundations. Most involve grout tubes to the bottom of the pile/shaft connected to a network of smaller tubes which may or may not be enveloped with a membrane (Mullins et al. 2001). Figure 1.2 shows the grouting system developed through FDOT research (Mullins et al. 2001) for drilled shafts and used in the Royal Park Bridge Replacement project in West Palm Beach and the PGA Blvd. project.

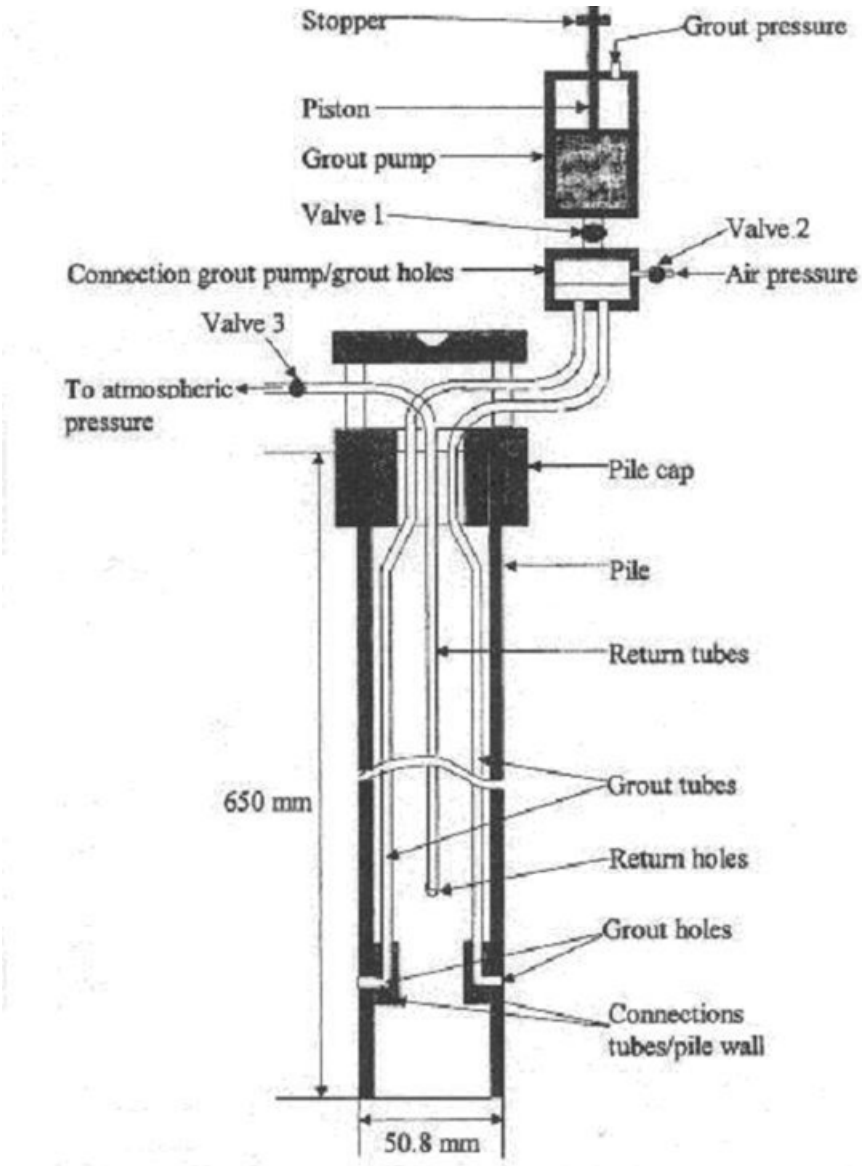

Figure 1.1 Side grouting system for precast pile (Jore et al. 1998).

Also of concern is the grout mix used in the pile or shaft grouting. Typical grout mixes used for grouting drilled shaft tips are combination of cement, sand, and water (water/cement ratio varying between 0.3 and 0.55 for optimum pumpability). Micro fine materials (e.g., fly ash, bentonite, etc.) are also used to improve pumpability (e.g., reduce sand locking); also it may be used as a cementitious replacement material. Generally, grout mixes with aggregate materials greater than 3/8″ are called compaction grouts which are generally used to prevent hydro fracturing of the soil.

Figure 1.2 Grout tipped drilled shaft reinforcement cage (Mullins 2001).

The research effort began with the grouting system shown in Figure 1.1 and the use of compaction grout to prevent hydro fracturing of the soil. It was readily found that the system suffered a number of drawbacks: 1) the pile grout lines could only be used once; i.e., no regrouting was possible; 2) compaction grout is prone to sand locking which generally is overcome by either large diameter delivery lines and/or higher water cement ratios; larger diameter grout pipes in piles becomes prohibitive especially if return lines are employed; and 3) very poor bonding was observed between the delivered grout and the pile which was attributed to grout type (compaction) and the path of grout expansion. The majority of the grouting portion of the research focused on overcoming these three hurdles as well as developing a design nozzle for jetting and a recommended design approach for the grouted pile.

Pile jetting has been widely used to aid pile penetration into dense to very dense sand layers to expedite pile driving and minimize construction vibrations. Jetting is often less effective in firm to stiff clays or soils containing coarse gravel, cobbles, or boulders. Jetting can assist pile installation in several ways. The jetting pressure may loosen (erode) the soil at

the tip of the pile. In addition, the flow of the jetting fluid can reduce the shaft friction along the pile by about 30%. Usually, the jetting tube is attached to the shaft of the pile or sheet pile. If jetting is required for a pile, which "hangs-up" in driving, a separate jet pipe is used. This jetting pipe is then moved up and down close to the side of the pile. An angled jet may be used to ensure that the wash water flows to the pile point. In difficult conditions, two or more jet pipes may be used for a single pile. Tube or box piles driven open-ended can be jetted from within the pile. An adequate quantity of water is essential for jetting. In general, a minimum jet pressure of five bars is required; however, in many cases significantly higher pressures are used.

Recently, Geiken Inc. has developed pushed/jetted pile installation equipment for steel sheet and pipe piles. In soft soils, the pile is pushed, whereas in dense, stiff or hard soils, a disposable jet tip is attached to assist in the pile installation by jetting.

This effort took advantage of the grout delivery system to the bottom of the pile to for water supply for jetting. Like the Geiken System, the research focused on developing a disposable jet tip that would ensure quick pile placement under minimum water needs, as well as provide for optimum grout placement with limited grout sand locking. The developed jet tip also prevented sand/fines ingress to the surrounding soil mass into the grout lines.

1.2.3 Field/Chamber Jet-Grout Pile Testing

Pile testing in the chamber and the field varied from precast pile with widths from 6″ to 16″ and lengths from 4′ up to 27′. All of the tests were performed in sands with density varying from loose to medium dense. Some of the piles were instrumented (strain gages at pile tip) and most had soil stress gages from 1D to 10D from the piles to measure stress changes.

The field/chamber testing began with two 16″ × 16″ × 27′ precast concrete piles with grout delivery system similar to Figure 1.1 and the use of compaction grout. Axially top-down testing of the piles showed improved pile tip resistance, but only limited skin friction improvement. Excavation of the piles revealed side grout bulbs of limited vertical extent near the piles as well as poor bonding between the piles and the grout material.

To improve the jet-grout pile design a series of mini-pile tests (6″ × 6″ × 4′ long piles) were carried out in medium loose sand. The tests involved adding grout return lines to each grout line, changing the grout mix design, and the addition of grout membrane to enclose the perimeter of the pile. The grout return lines allowed for repetitive grouting, and the mix was changed to improve bonding and flowability through the use of fine sand, cement, micro fly ash and a water cement ratio to 0.45. Different membrane materials and thickness were tested with the mini-piles for final grout bulb size, shape and load transfer. The final membrane selected had high tensile strength, and was allowed to inflate (i.e., pleated) to twice the perimeter of precast pile member.

After completion of the mini-pile tests, two larger scale (6″ × 6″ × 8′ and 8″ × 8″ × 8′) jet pile tests were performed in the test chamber in a medium loose Florida sand using the newly developed pile system and grout. The latter tests achieved axial capacities of 65 kips and 115 kips, respectively, with 50/50 skin and tip resistance.

Next, a full-scale 16″ × 16″ × 20′ precast pile was jetted and subsequently grouted in medium loose sand in the test chamber. Prior to grouting the pile tip, the jet-grout pile was subject to 450 ft-kips of torque loading with less than 15° of observed rotation. Subsequently, the tip of the pile was grouted and a top-down compression test was performed. For the grouting phase, the maximum grout pressure was 650 psi and a grout volume of 220 gallons or 29 cubic feet was recorded. Due to uplift limitations of 48″ø × 40′

reaction shafts, only 300 kips of axial top-down load was applied to the pile. For the 300 kips of load, less than 0.1″ of top pile downward deflection was observed and upon unloading 0.07″ of rebound was recorded.

1.2.4 Axial Design of Jet-Grouted Piles

The current limitation of drilled shafts or grout tipped drilled shafts is the available skin friction on the shafts for most soils. Limiting the shaft skin friction is the reduced lateral or radial stress due to excavation or drilling. The latter is also true for jetted piles. However in the case of side grouted piles, the lateral stress is significantly increased (e.g., greater than vertical stress) due to cavity expansion. Moreover the actual required grout pressures may readily be obtained from cavity expansion theory which is a function of depth, relative density (Dr) and strength (angle of internal friction) of the soil. Expansion stresses varying from 80 psi to 1000 psi are possible for Florida silty sands depending on depth. Under limit pressures, a plastic soil zone develops around the perimeter of the pile with the radial stress the highest, followed by vertical and then hoop stresses. Based on the assumed shape of the grout membrane (i.e., barrel or prismatic), the axial skin friction on the grouted pile may be assessed. The most conservative assumption is to assume a prismatic shape, and then the skin friction may be assessed by constructing a Mohr circle touching the strength envelope with the minor principal stress equal to the vertical effective stress. Analysis of all top-down tests gave reasonable estimates of skin friction using the latter approach as well as cavity expansion approach to estimate grout pressures. The latter chapters go into greater detail for each area (e.g., chamber design and installation, grout pile development and chamber/field testing) as well as improvements in grout equipment (e.g., improved grout pressure gages).

CHAPTER 2
CONSTRUCTION OF TEST CHAMBER AND
REACTION SHAFTS

2.1 Design of 12′ø × 35′ Test Chamber and Reaction Shafts

Shown in Figure 2.1 is the plan and cross-sectional view of the originally planned test chamber, reaction shafts, and load frame. The load frame is the FDOT 300 ton system stored at State Materials Office (SMO) in Gainesville, Florida.

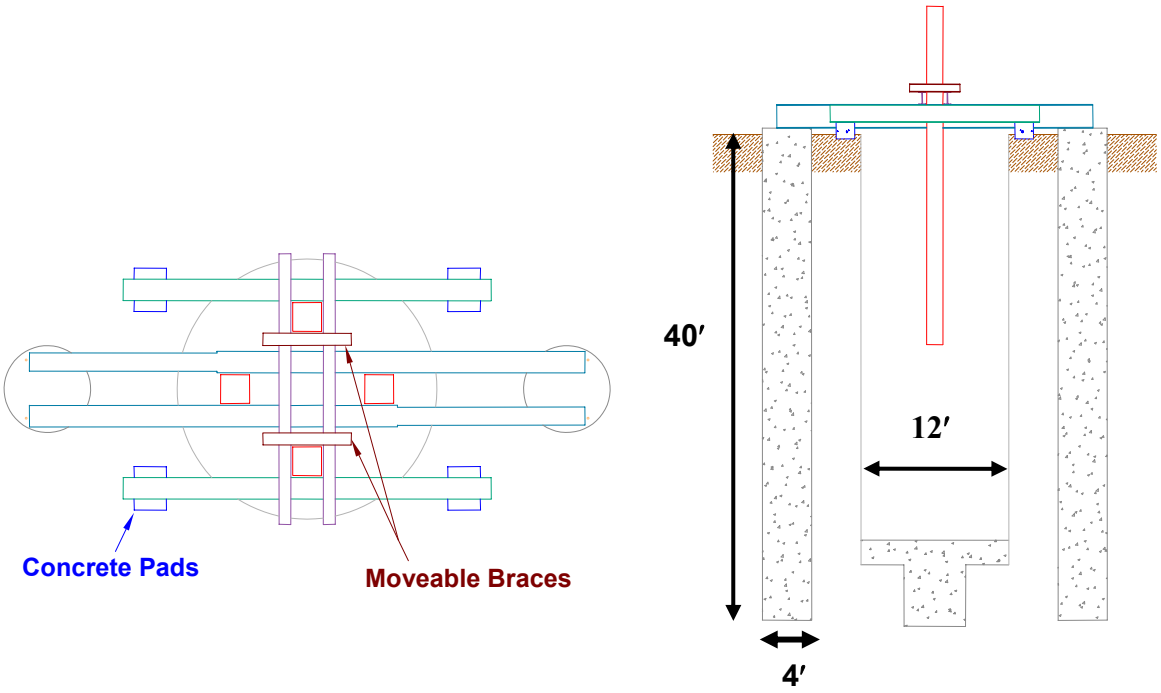

Figure 2.1 Test chamber, reaction shafts and load frame.

The additional outrigger reaction beams which are supported on concrete pads were intended to provide additional uplift loading capacity to the structural frame. Each reaction shaft (4′ø × 40′) in Figure 2.1 was analyzed for uplift capacity based on electric cone data, Figure 2.2, preformed by the SMO FDOT cone rig. Based on FB-DEEP analysis of the cone sounding, each shaft is expected to have an uplift capacity of approximately 150 tons.

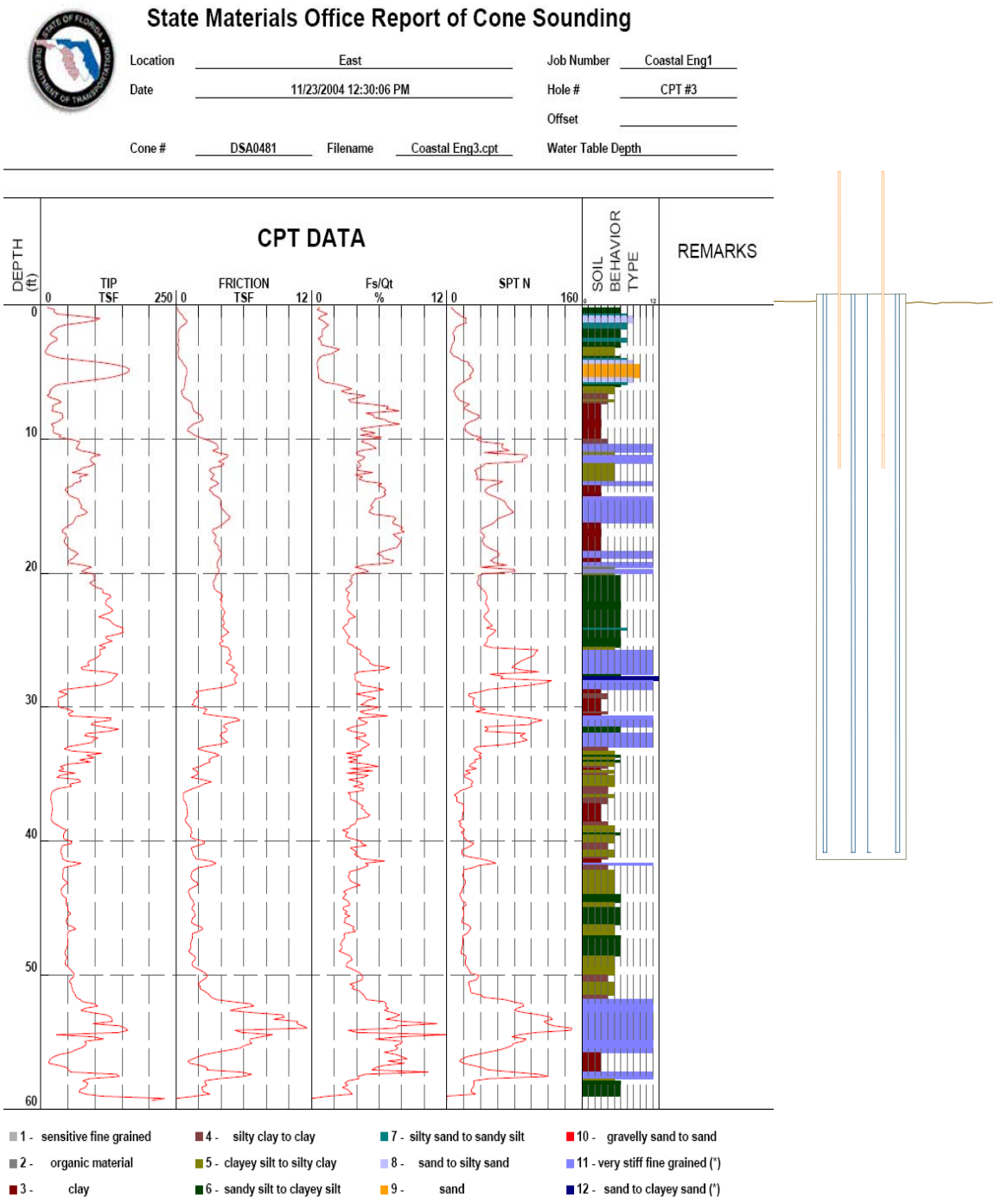

Figure 2.2 ECPT data log for load test reaction shafts.

As part of the contract, anomalies (slurry inclusions, segregation zones) were to be placed within the reaction shafts (Figure 2.3) along with access tubes (PVC and steel) for CSL training. Shown in Figure 2.4 is one of the constructed anomalies, gravel bag (segregation).

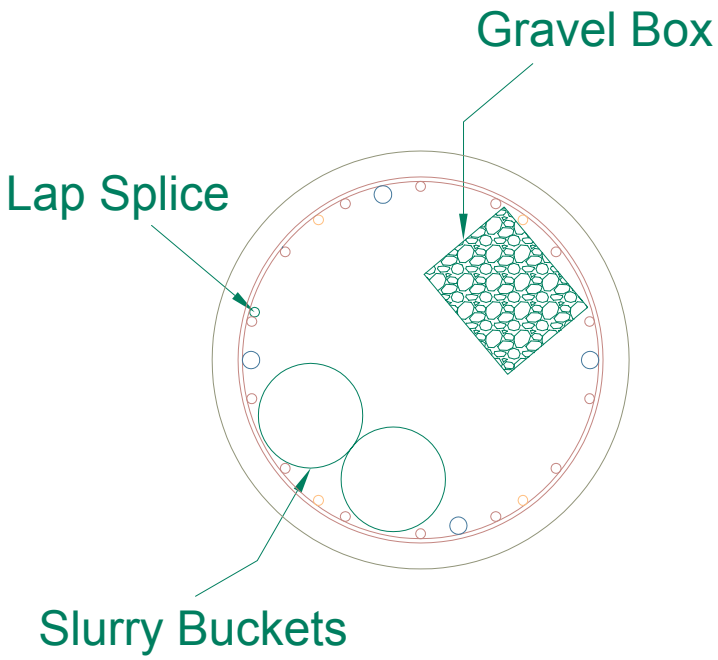

Figure 2.3 Reaction shaft cross-sections with anomalies.

Figure 2.4 Constructed gravel segregation anomalies.

2.2 Construction of the In-ground Test Chamber

In the beginning of 2006, Coastal Caisson arrived at the UF Coastal Laboratory to construct the FDOT test chamber and reaction shafts used for this research. Work began immediately on welding the 3/4″ thick by 12′ diameter sections (four) of the test chamber together (Figure 2.5). Approximately one week later, a truck mounted drill rig and auger (Figures 2.6 and 2.7) arrived on site to drill and install the test chamber.

Figure 2.5 Welding test chamber sections together.

Figure 2.6 Auger for 12′ø test chamber.

Figure 2.7 Drilling 13′Ø × 45′ hole for in-ground test chamber.

On February 3, 2006, Coastal Cassion construction of the in-ground test chamber began by setting temporary casing and drilling of a 12.3′ diameter hole using the "wet-hole" method of construction with KB polymer (Figure 2.7. The excavation proceeded to a depth of 43′ (Feb. 3 and 4, 2006), whereupon the bottom was belled (over reamed) to a diameter of 14′. The over reaming ensured that the concrete plug at the bottom of the test chamber had sufficient uplift soil resistance for the case of hydrostatic uplift and no soil within the test chamber. Figures 2.8 and 2.9 show the installation of the test chamber into the excavation, and Figure 2.10 shows the pouring of the concrete bottom plug.

Figure 2.8 Steel test chamber.

Figure 2.9 Steel test chamber installation.

Figure 2.10 Pouring the concrete floor of the test chamber.

Concrete cylinders from the plug were recovered and tested 14 days after casting with concrete strengths of 4 ksi and 5 ksi, respectively.

2.3 Construction of the Reaction Shafts

The original intent of the research was to test the installed piles using the upward force of the grout exiting the tip (pressure × area) as would be utilized in production piles. However, after discussions with FDOT personnel, it was felt that confirmation of skin friction, in both an upward and downward direction should be assessed. Hence, a supplement for the construction of two reaction shafts was submitted and approved. After completion of the test chamber, Coastal Caisson began construction of the twin reaction shafts for the top-down testing of the jet-grouted research piles. As part of this activity, anomalies, which did not affect the shafts axial capacity, were added to the shafts. These were placed at the request of the FDOT State Materials Office (SMO) to evaluate and train NDT operators in

shaft inspection at no additional cost to the project. They included non-cleaned bottoms (Figure 2.11) slurry inclusion (e.g., improper slurry unit weight and viscosity, Figure 2.12) as well as a gravel box to model segregation of the concrete (Figure 2.13).

Figure 2.11 Inclusion of soft tip (sand bags) and bottom of reaction shaft.

Figure 2.12 Inclusion of slurry anomaly.

Figure 2.13 Wire mesh gravel bag to simulate segregation.

Shown in Figure 2.14 is one of the steel reinforcement cages of the reaction shaft (looking down shaft) with anomalies. Also shown are the access tubes (2″ PVC pipes) that would be used for NDT testing.

The construction initiated on the east shaft (Figure 2.15) using KB polymer slurry. However, during the construction, the bottom of the hole began to heave excessively. The latter was attributed to the belling activity for the test chamber, as well as disturbance to the surrounding soil (clayey sand with excess pore water pressure). Work was stopped, the hole was refilled, and construction of the west shaft initiated. Since this shaft was in predominately sand, no drilling concerns (heave, loss of slurry) was observed, and placement of the cage (Figure 2.16) and subsequent concreting (Figure 2.17) occurred as planned.

Figure 2.14 Reaction shaft reinforcement and CSL access tubes.

Figure 2.15 Drilling the east reaction shaft.

Figure 2.16 Placement of reinforcing cage on west shaft.

Figure 2.17 Completion of west reaction shaft.

Due to concerns of disturbance, heaving, etc. for the construction of the east shaft, it was decided to employ temporary casing and mineral (bentonite) slurry for its subsequent construction. The latter required a different drill rig and operators. On March 1, 2006,

Coastal Caisson began construction of the east reaction shaft. The construction occurred without any difficulties and was finished on March 3, 2006.

2.4 CSL Testing of the Reaction Shafts

After final construction of the reaction shafts, each shaft was investigated with a PDI's cross-hole sonic (CSL) analyzer. This work was carried out by SMO with both their personnel and equipment. The work involved slowly lowering an acoustic emitter down one access pipe and a receiver down an adjacent access pipe. The emitter continuously sends an acoustic signal which is picked up by the receiver and time of wave transmission is recorded, e.g., Figures 2.18 and 2.19. Since the distance between the access pipes are known, and the signal time (travel time from emitter to receiver) is known (right side of Figs. 2.18 and 2.19), the wave travel speed is computed (distance/time), left side (Figs. 2.18 and 2.19). Typical wave travel speeds (c) for concrete are 15,000 ft/sec (e.g., prestressed concrete piles), i.e.,

$$C = (E / \rho)^{0.5}$$

Evident from figures are the anomalies with depth. For instance, the anomaly at 13′ in the west shaft (Figure 2.18) was due to the slurry inclusion, and at 35′ to 40′ was the soft tip due to the sand bags (Figure 2.18). In the case of the east shaft (Figure 2.19) the anomalies at 22′ and 27′ were the slurry, and concrete segregation (Figure 2.12), respectively. However, the anomaly at 5′ was due to reinforcing steel bond breaker (i.e., wrapped with saran wrap).

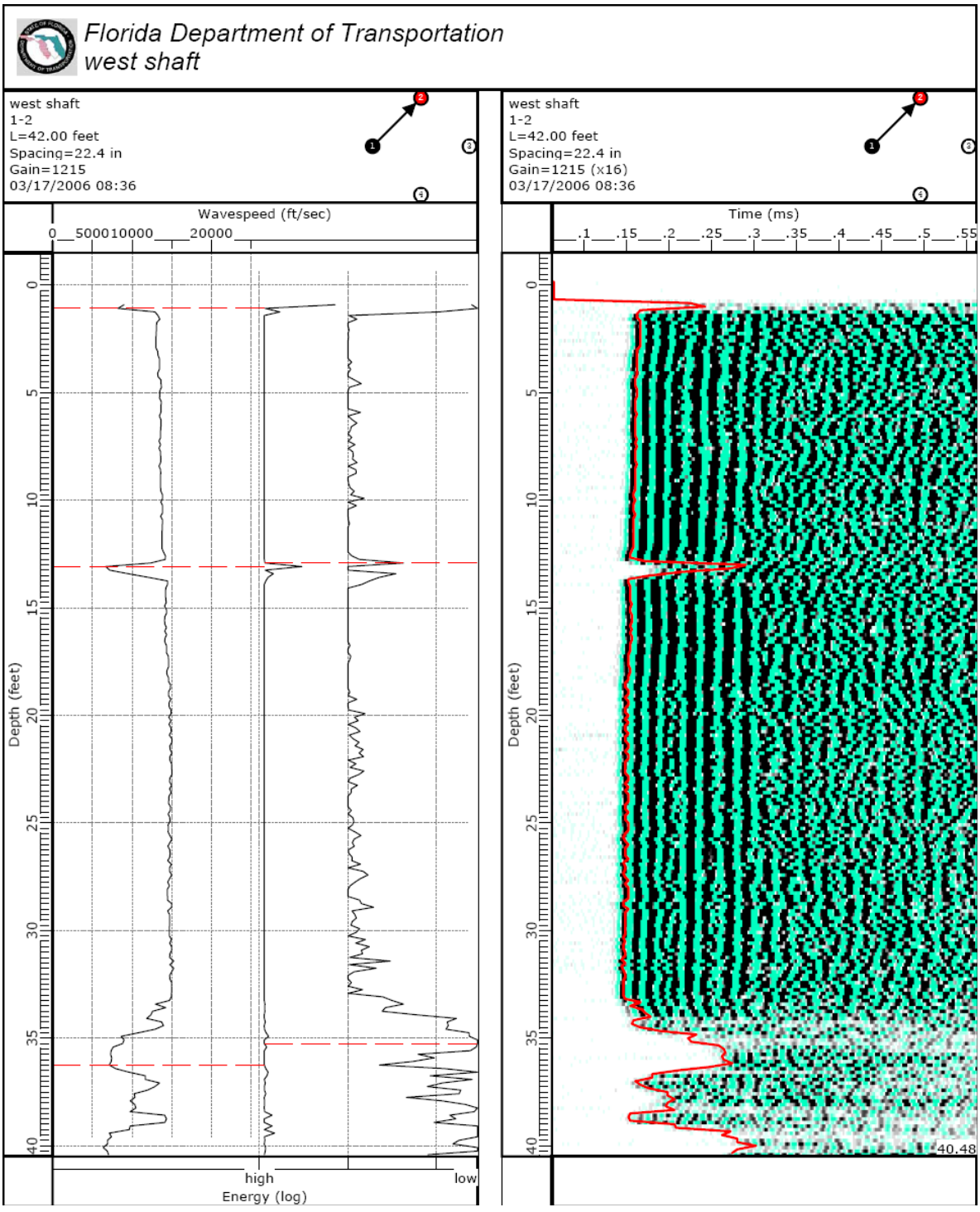

Figure 2.18 CSL log of west shaft with depth.

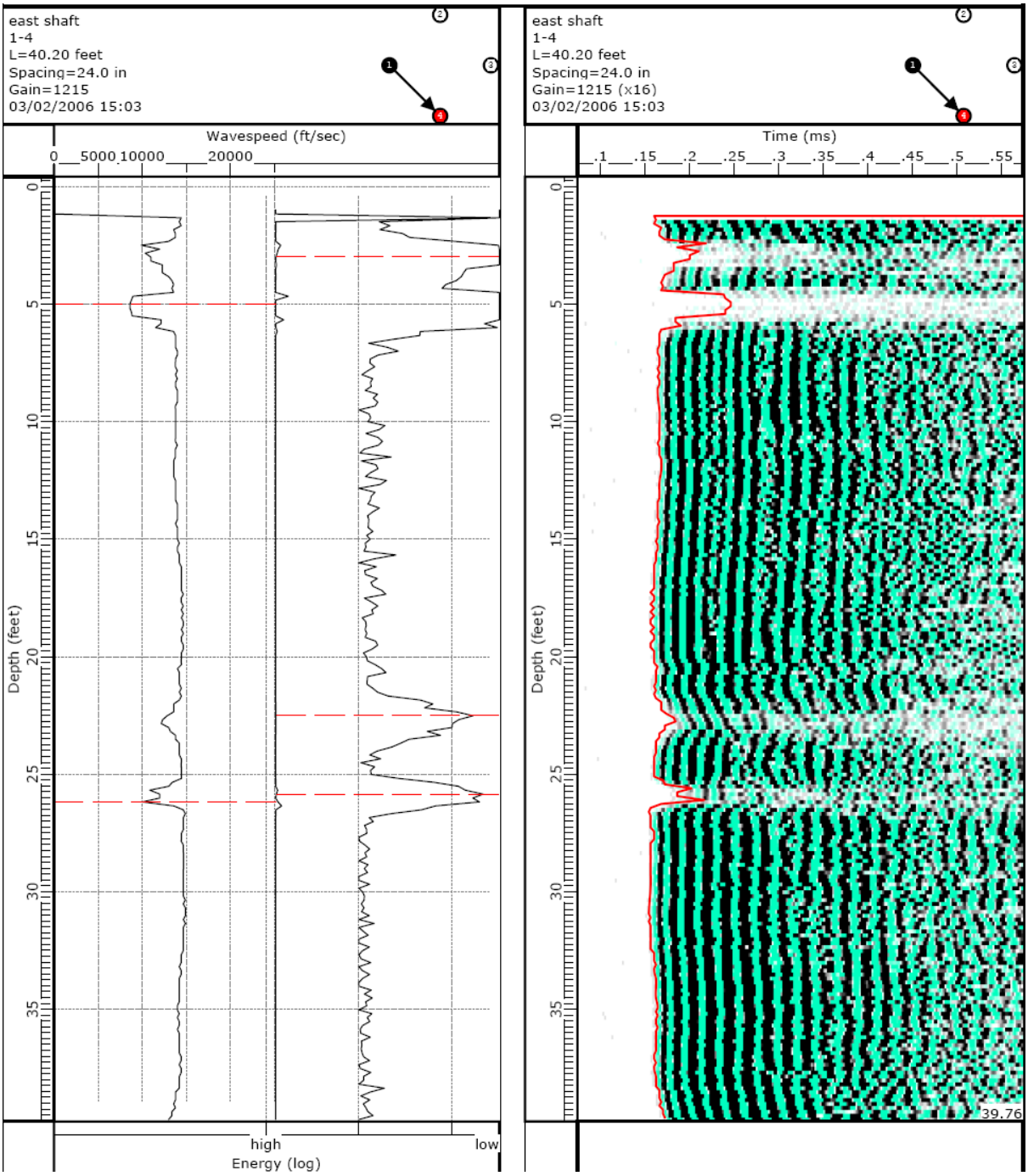

Figure 2.19 CSL log of east shaft with depth.

CHAPTER 3
TEST CHAMBER SOIL PROPERTIES, PLACEMENT, AND INSTRUMENTATION

3.1 Properties of Silty-Sand Used in Test Chamber

One hundred and sixty-five cubic yards of a silty-sand (A-2-4) obtained from a District 2 borrow pit (Figure 3.1) was trucked to the UF coastal facility and stored inside under constant moisture conditions.

Figure 3.1 Silty-sand for test chamber and jet-grout pile tests.

Shown in Figure 3.2 is the grain size distribution of the soil performed on a number of separate samples. The fines in these smaples were classified as non-plastic. In addition, five laboratory relative density tests showed a minimum dry density of 92 pcf and a maximum dry density (γ_d) of 115 pcf. Direct shear tests on the soil at minimum and maximum dry densities showed angles of internal friction of 30° and 36°, respectively. The State Materials Office preformed compaction and triaxial testing on the soil as well. The maximum dry density was 120 pcf.

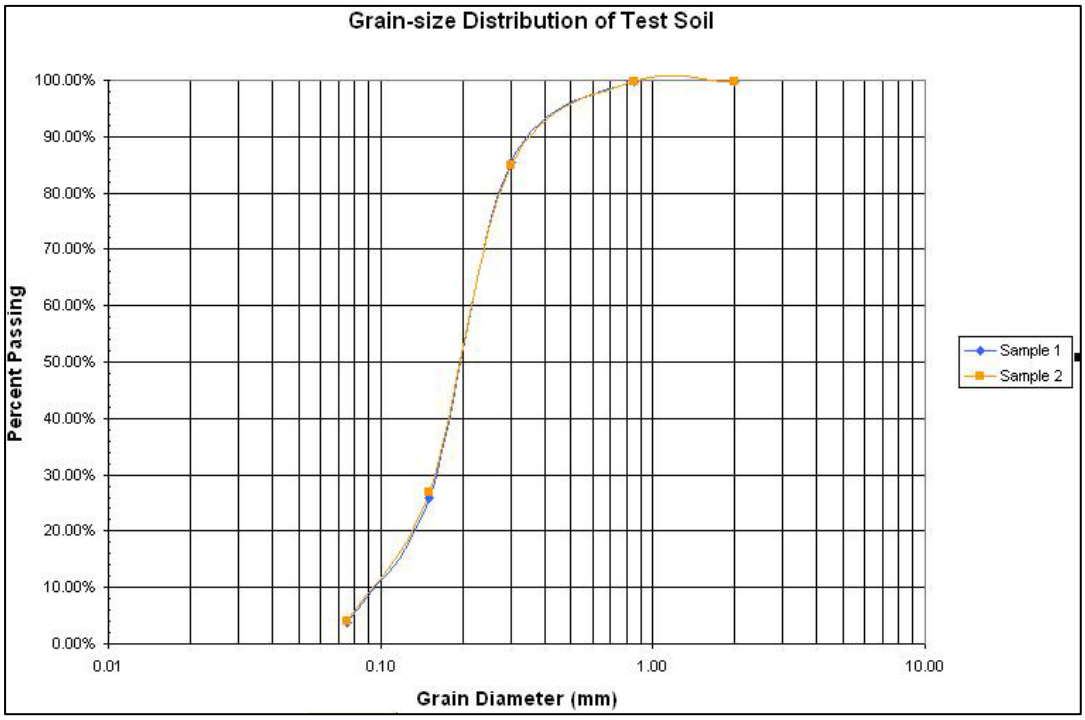

Figure 3.2 Grain-size distribution of test chamber soil.

3.2 Geokon 4800 Stress Gages

To measure both the lateral and vertical stress within the test chamber, ten Geokon model 4800 earth pressures cells were acquired (Figure 3.3). The gages are made from two 12″ flat plates, compressing a fluid monitored with a vibrating wire. The gages are capable of being installed in the dry or fully saturated conditions. The cell calibrations were verified in a 40′ column of water held at 76° F as shown in Figure 3.4. For all testing, eight of the gages were employed to measure horizontal stresses and two of the gages measured vertical stresses. Four of the eight lateral stress gages were placed at one elevation (i.e., N, S, E, and W) (e.g., 6′) within the tank and the other four at a different elevation (e.g., 15′), but at similar positions (i.e., N, S, E, and W). The other two gages were installed horizontally to measure vertical stresses beneath the jet-grouted piles.

Figure 3.3 Geokon soil stress gages.

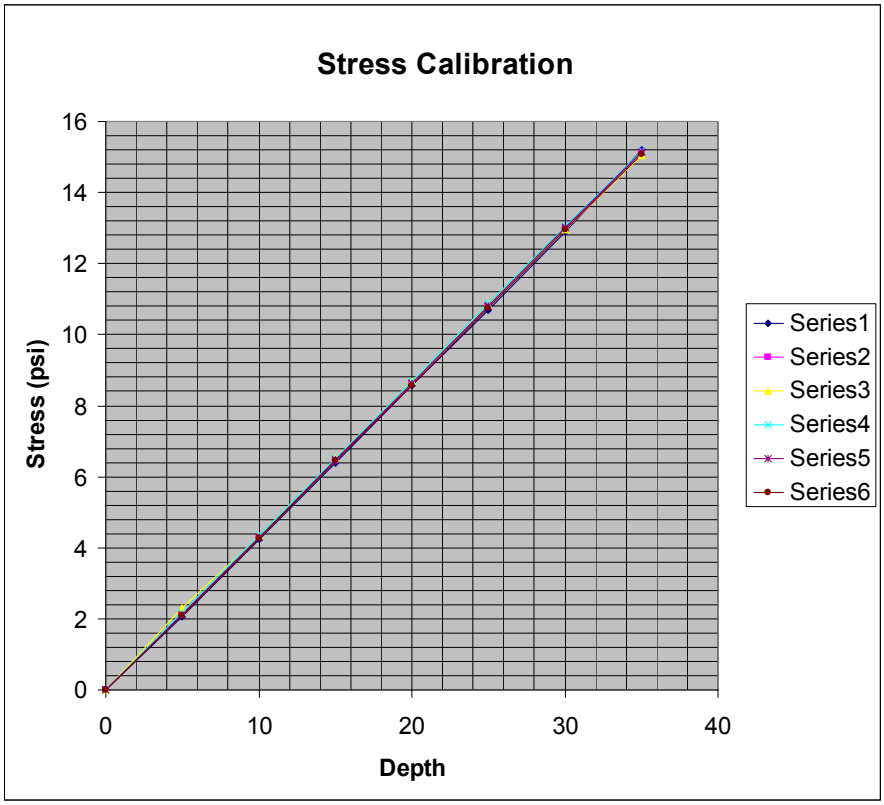

Figure 3.4 Calibrations of Geokon gages.

3.3 Filling the Test Chamber

The test chamber was completely emptied and filled twice for this research project. The first placed the soil in a loose state (i.e., dry density of 92 pcf) and the second in a medium state (i.e., dry density of 100 pcf). It should be noted that while the chamber was only completely emptied twice, portions of chamber (i.e., top 10′) were emptied and filled multiple times for the smaller scale tests; whereas the 20′ pile tests required full removal of the soil and piles for study.

For the loosest possible case, the sand was initially hydraulically placed by dropping the soil through 10′ of water (tank one-quartered filled). However, upon removal of the water for placement of stress gages (Figure 3.5) the soil could not be walked on without dewatering the soil which subsequently altered the soil's density.

Figure 3.5 Placement of stress gages 30′ down from top of the chamber.

Subsequently, the soil was removed and it was decided to place the soil in the dry. To obtain the loosest possible stress state, the soil was loaded into a hopper and then lowered to approximately 6″ to 8″ from the soil surface and allowed free fall while the hopper was

moved around the tank. The latter process resulted in a dry density of approximately 98 pcf. In the case of medium relative density, the soil was allowed to free fall to the bottom of the tank and then lightly compacted in 18″ lifts. The latter resulted in dry densities of approximately 105 pcf. Figure 3.6 shows SMO personnel performing nuclear density measurements on the placed soil.

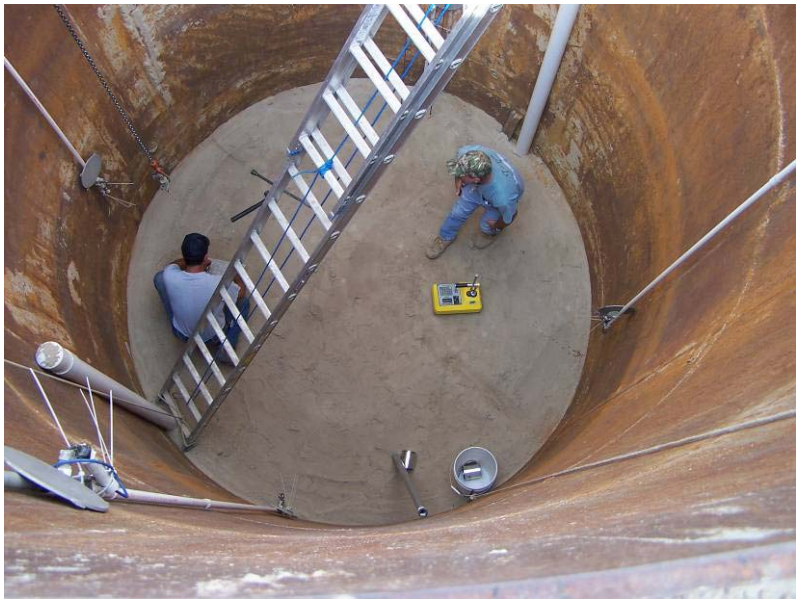

Figure 3.6 Nuclear density measurements of soil within test chamber.

With approximately 6′ of soils within the test chamber, 2 Geokon stress were placed 3′ and 4′ from the bottom of the test chamber to measure vertical soil stresses when the test piles were grouted as well as load transfer to the soil during top-down static load testing. Also at this time, four 6″ diameter slotted PVC pipes wrapped in filter fabric were placed along the walls of the tests chamber (Figure 3.7) to control water levels within the test chamber. A small submersible pump was purchased to fit within the 6″ diameter PVC pipes for water removal. In the case of the medium dense soil (Figure 3.6), the PVC pipes were reduced to two and PVC grid (5) of pipes were placed at the bottom of the tank and covered

Figure 3.7 Four 6″ diameter drainage system to control test chamber water levels.

with crushed stone. The latter system gave much better control of moisture within the tank. Specifically, the water within the tank could be lowered much quicker, e.g., after jetting.

Once the tank had approximately 12′ to 14′ of soil placed, the next level of stress gages were installed (Figure 3.8, loose state). The gages at this elevation were installed vertically to measure horizontal insitu stresses away from the jet-grouted piles. The gages were placed approximately 6″ off the wall of the test chamber. Note the gages could not be placed directly on test chamber wall, since their impedance (stiffness) matched the soil. In the case of medium dense state, it was decided to protect the gages with two steel rods (Figure 3.9) with gages hang between to protect the gages when the soil is removed from the test chamber. After placement, the gages were read to ensure their functionality.

Figure 3.8 Lateral stress gages – 20′ down from top of test chamber.

After placement of the stress gages at a depth of 16′ (medium) to 18′ (loose), more soil was added to the test chamber until the sand surface was 6′ from the top. Subsequently, the final four Geokon stress gages were placed around the perimeter of the test chamber (Figure 3.10). After filling the test chamber with the loose or medium dense sand, a number of hand cones were performed to a depth of approximately the 15′. The tip resistance (qc) were approximately 20 tsf and 60 tsf for loose and medium dense sand, respectively.

After placement of the stress gages, all the instrumentation wiring was routed (Figure 3.11) to an enclosed facility. Note, all of the stress gage wiring (Figures 3.9 and 3.10) were enclosed within 1/2″ø PVC pipes to protect the wiring during jetting/grouting as well as soil removal after load testing. All of the Geokon stress gages were monitored with a Campbell scientific data logger with a laptop running Geokon proprietary software.

Figure 3.9 Steel grillage to protect lateral stress gages.

All gages were read prior to placement, as well as during filling of the chamber with soil to ensure their proper functionality.

Figure 3.10 Lateral stress gages – 6′ down from top of test chamber.

Figure 3.11 Routing of stress gage wiring to central readout.

CHAPTER 4
FIRST GENERATION JET-GROUTED PILES
WITH COMPACTION GROUT

4.1 Introduction

The research started from the Grouting System developed by Jore et al. (1998), (which employed side exit ports along the pile for post grouting activities (Figure 1.1). Since only single grout pipes (no returns) at variable depths are used, it was planned jetting the pile in and subsequently grout the pile in stages from the top-down. Consequently, early research focused on the diameter of the grout tubes to limit "sand locking" during compaction grouting as well as jetting for pile installation.

4.2 Jetting Research

Of interest in the jetting phase is the required water flow rates, and nozzle diameters, for a given pile diameters. FDOT construction specification require center hole pipe for internal and dual jet pipes for external jetting as well as adequate pump for sufficient pressure and flow rate to "freely erode" the soil. Discussion with contractors suggest a pump capable of generating at least five bars of water pressure on a 2″ø water line with a nozzle that reduces the delivery line to one-half of its original diameter. In 1988, Tsinker published the following flow rate equation to estimate water requirements for jetting:

$$\frac{Q}{D} = \left[530 \left(d_{50} \right)^{1.3} l^{0.5} \right] + 0.017 \pi l k$$

$$Q = flow\ rate \left(m^3 / hr \right)$$

$$D = pile\ diameter, or\ width \left(m \right)$$

$$d_{50} = avg.\ size\ of\ sand\ particles \left(mm \right)$$

$$l = desired\ submerged\ length\ of\ pile \left(m \right)$$

$$k = \frac{\sum k_n l_n}{l} = avg.\ filtration\ coefficient \left(m / day \right)$$

Using Tsinker's equation, a number of different jet pipe diameters and nozzles were investigated. Besides water, the inclusion of air at a pressure less than water was found to reduce water requirements, but provide similar pile penetration rates. Also of concern was the size of the disturbance zone adjacent and below the piles due to the jetting process. For instance shown in Figure 4.1 is a 12″ diameter circular pile being jetted into the ground at the FDOT Fairbanks test site.

a) Pile jetting **b) Monitoring flow rates and pressure**

Figure 4.1 Jetting of 12″ø circular pile into silty-sand, Fairbanks, Florida.

Shown in Figure 4.2 is the pile jetted in the ground and Figure 4.3 identifies the zone of disturbance based on Cone Penetration Testing performed radially around and beneath the jetted pile.

Figure 4.2 Jetted pile with soil tailings.

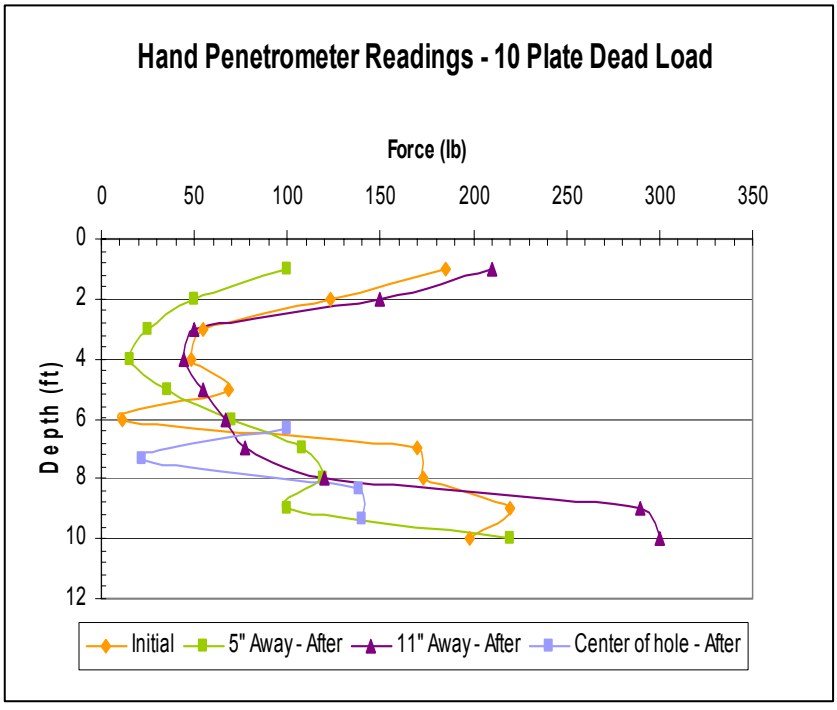

Figure 4.3 CPT tip resistance as function of radial distance.

Evident from Figure 4.3, the disturbance zone extends one-half the pile diameter radially and approximately four diameters below the pile tip. It is expected that any disturbed zones will be filled with compaction grout during the grouting phase.

Based on jetting experiments, as well the cross-sectional limitations of the pile and the other grouting pipes, it was decided to have one 2″ø jet-grout pipe going to the tip of the pile were it was attached to two sets of "T" that split and formed four exit ports on the bottom of the pile. Each exit port would be covered by a rubber nozzle to restrict water flow, increasing the velocity of exiting water. Under high pressures, it was expected the rubber nozzle would expand allowing passage of the compaction grout during the grouting of the pile tip.

4.3 Design and Construction of the Jet-Grout Concrete Piles

Shown in Figure 4.4 is the plan view of the 1st generation jet-grout concrete piles that were tested. The picture on the left shows the 2″ø center jet-grout tube with the two sets of "T" to form the bottom four exit ports. On the right of Figure 4.4 are the 1 1/2″ø PVC pipes used for side grouting of the piles. Two of the PVC pipes go to depth of 8′ and the other two go to a depth of 22′ (8′ +14′) for bottom side grouting. Figure 4.5 shows the cross-section of the piles at various depths. The diameter of the center jet pipe was selected to handle water/air flow rate requirements and associated losses. The diameters of the side grout pipes (e.g., 8′ and 22′) were selected to handle the compaction grout mix maximum particle size (3/8″) and expected pressures (maximum 800 psi).

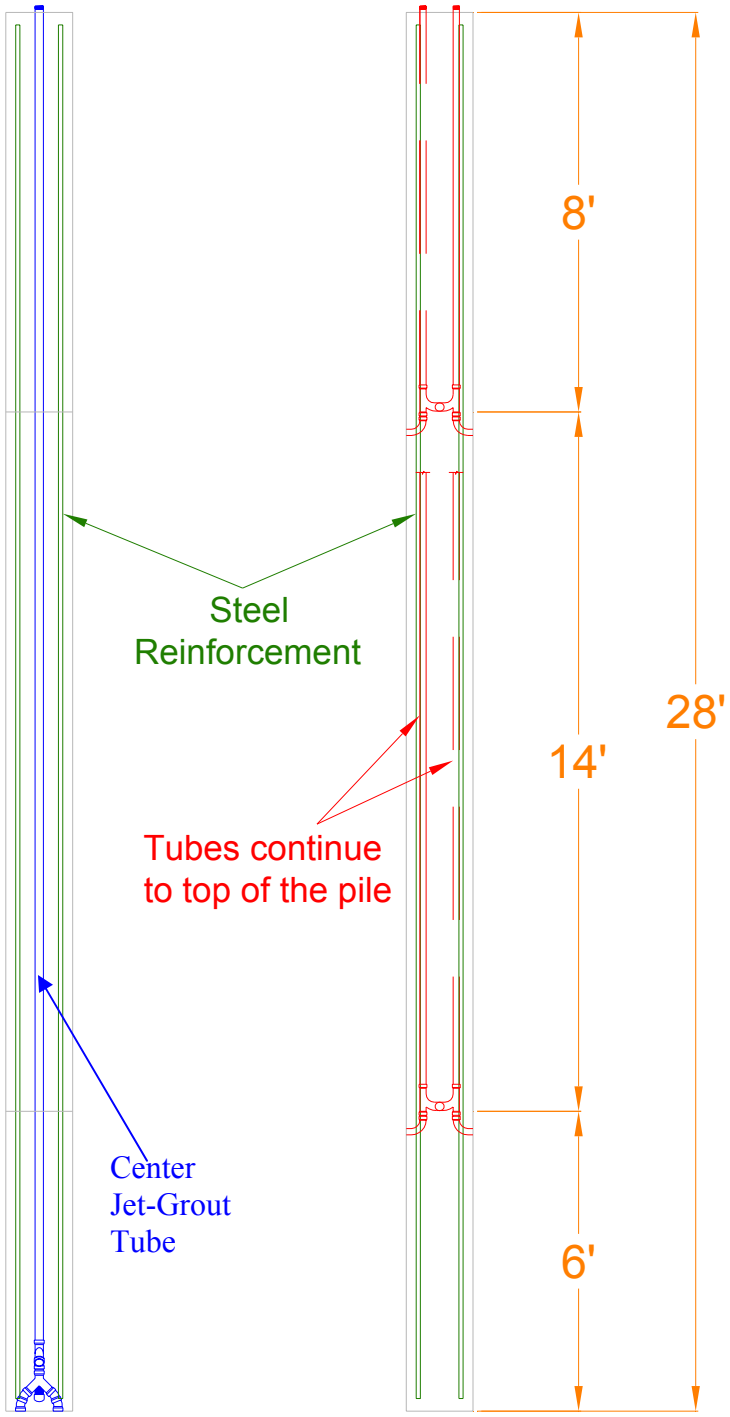

Figure 4.4 16″ × 16″ × 28′ jet-grout piles.

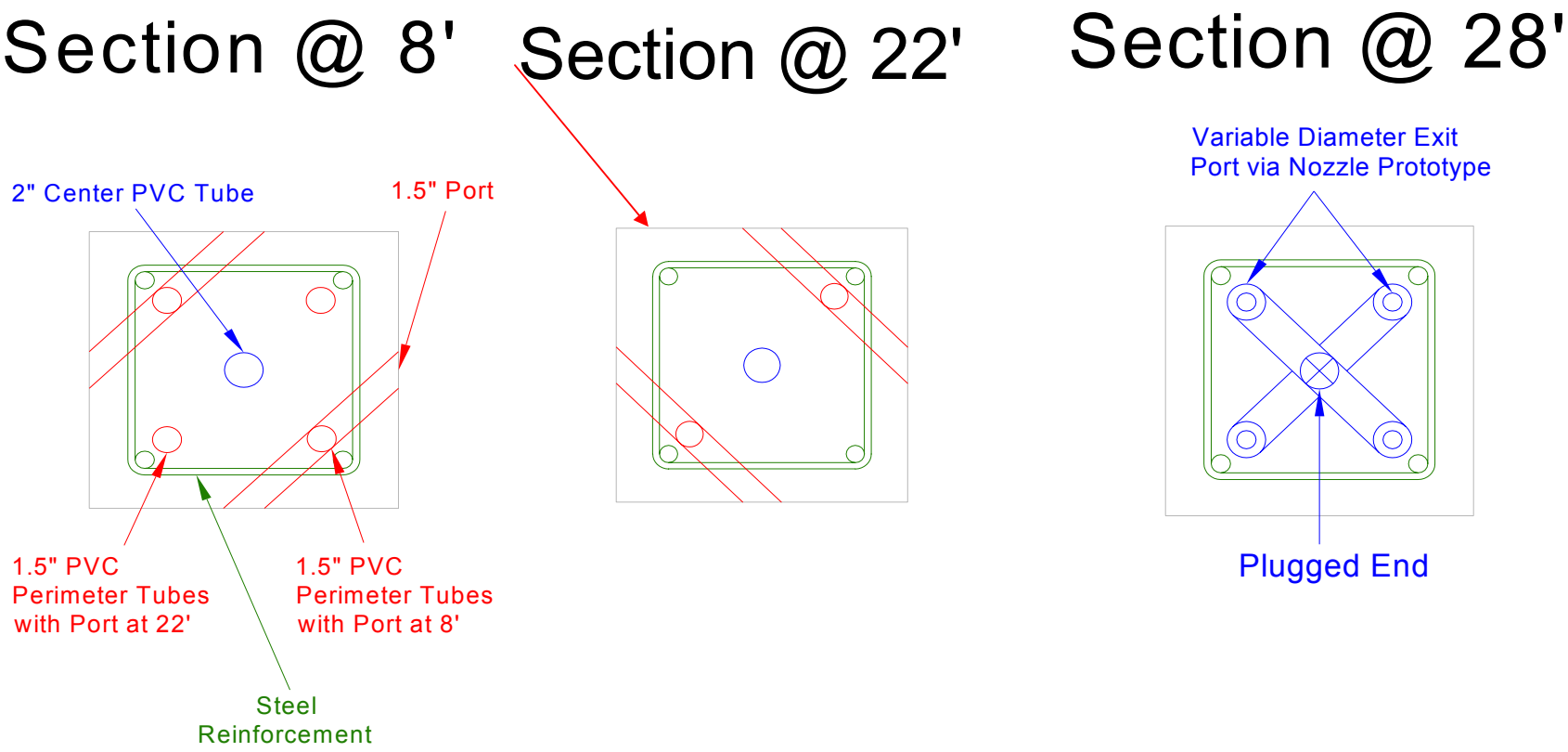

Figure 4.5 Jet-grout pile cross-sections.

To provide the required exit reduction (i.e., nozzle velocity), the exit ports of the tip jet-grout tubes were covered with 1/2″ thick rubber membrane (Figure 4.6) with a 3/4″ elliptic opening. Holding the rubber membrane to the exit port was a 3″ × 3″ welded steel plate. Note, the rubber nozzle and steel plate were attached to the bottom of pile over each port after the pile has been cast.

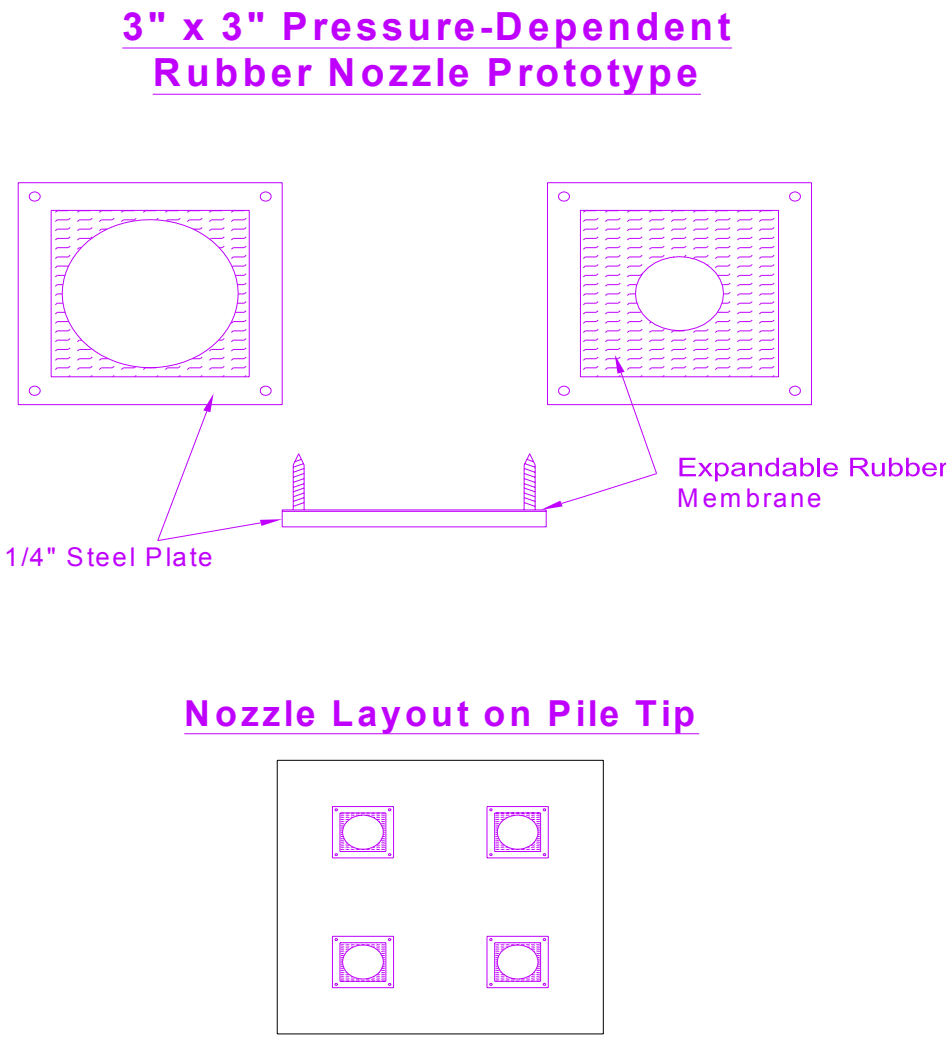

Figure 4.6 Pile tip nozzles for jetting-grouting.

After having obtained FDOT approval for the jet-grout pile design, the piles were subsequently constructed. Shown in Figure 4.7 is the prefabrication of reinforcing cages, as well as attachment of jet and grout pipes to rebar cage for constructing two piles. Next, a 3/4″ thick plywood form was constructed and the rebar cages with grout tubes were set within the formwork. A typical 4000 psi ready-mix was poured and vibrated within the two molds. After one week the piles were removed from their molds.

a) Top of piles

b) Depth 8′ and 22′

Figure 4.7 Construction of two jet-grout pile rebar cages and grout pipes.

Shown in Figure 4.8 is the bottom of one the jet-grout piles prior to placement of jet nozzles. Each pile tip had four 1 1/2″φ exiting ports which are equally spaced on the bottom of the pile. Next, the nozzles (Figure 4.9) were attached to the bottom of the piles with eight 1 1/2″ lag bolts that are drilled after concrete reached 3500 psi strength. Each nozzle had a 2″ × 1/2″ elliptic opening.

Figure 4.8 16″ × 16″ × 28′ reinforced concrete jet-grout pile.

Figure 4.9 Rubber nozzles with elliptic openings.

Shown at the 22′ mark on the side of the pile in Figure 4.10 is one of the 1 1/2″ø exit ports on the side of the pile near the pile tip (28′). The bottom ports will be grouted after the top ports (Figure 4.6) in order to increase lateral confinement of the soil around the pile.

Figure 4.10 Compaction grout port on side of the pile.

One of the jet grouted piles was installed with the nozzle design given in Figure 4.6 and penetration beyond 22′ was found difficult due to loss of water return to the surface. Subsequent testing of the elliptic nozzles showed them to develop a good spray pattern in the long dimension of the ellipse (Figure 4.11) but a very weak or poor spray pattern for the short dimension of the ellipse (Figure 4.12). Consequently, it was decided to redesign the rubber nozzles.

Figure 4.11 Nozzle spray pattern for long dimension of ellipse.

Figure 4.12 Nozzle spray pattern for short dimension of ellipse.

Shown in Figure 4.13 are different orifice sizes and locations within each rubber section. The nozzle which showed the largest spray pattern was the layout in the bottom left of the pile. The smaller holes drilled in the edges of the membrane resulted in significant directional spray due to curvature of membrane under pressure. The final nozzle design spray pattern for test pile # 2 is shown in Figure 4.14. Each grout pipe (Figure 4.13) had

multiple smaller holes in the perimeter of the rubber member to angle the spray direction as well as smaller holes to increase water exit velocity (similar to a bathroom shower head).

Figure 4.13 Testing different jetting nozzle designs.

Figure 4.14 Final nozzle design and spray pattern for test pile # 2.

Since the grout was not capable of flowing through the water exit holes in the rubber, it was expected that the grout would rip the rubber membrane under pressure and subsequently grout the jet void beneath the pile, as well as a load (i.e., bottom up) the test piles.

4.4 Jetting the Test Piles into the Test Chamber

Pile jetting began by positioning a pile over the test chamber (Figure 4.15) with the 22,000-lb capacity Taylor Forklift purchased by FDOT for this project. One end of the pile was placed on a specially constructed steel frame (Figure 4.15) in order that a steel collar could be placed around the pile, which would hold the pile when picked up in a vertical alignment. Also at this time, the jet piping was attached to the top of the pile. Subsequently, the pile was picked up on one end and positioned over the test chamber with the steel cross bracing (Figure 4.16) used for alignment.

Figure 4.15 Test pile positioning prior to jetting with forklift.

Figure 4.16 Aligning the test pile prior to jetting.

Water was provided for the jetting process from a 3000-gallon water tank. The water was provided to the test piles through water pumps (Figure 4.17). For Test pile # 1, a 400 gallon/minute at 30′ head, gas powered pump was used. For Test Pile # 2, a 1000 gallon/minute at 155′ head, diesel powered pump was employed (Figure 4.17). Both water pumps had a 6″ø feed and a 4″ø exit pipe, which was split into a 2″ø return to the water tank and another 2″ø line going to the test pile. Attached to the 2″ø return line was a ball valve allowing the restriction on the 2″ø return line. The latter was used to control the flow and pressure to the jet pile. Connected to the 2″ø water pipe going to the test pile was 5/8″ø air inlet from an air compressor to provide high pressure air entrainment. The latter was used to reduce the volume water required for jetting.

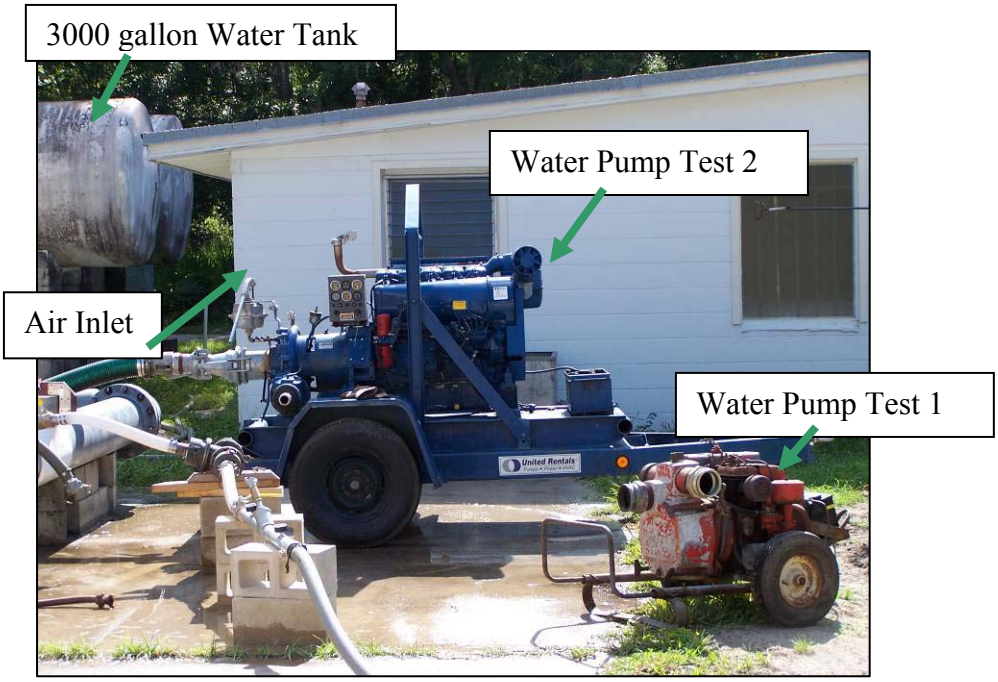

Figure 4.17 Water tank and pumps used in jetting.

Jetting initiated with flow of water from the water tank through the pump to the test pile. Subsequently, air entrainment (pressure and flow rate) was adjusted and the test pile was lowered with the forklift as penetration occurred. Generally, after 10 to 20 minutes of jetting, the test pile had penetrated up to the steel collar (Figure 4.18). Subsequently, the test pile was attached to the steel cross bracing, and the collar was moved upward, out of the way of the soil.

In the case of Test Pile # 1, jetting occurred at a uniform constant rate up to approximately 20′ of pile penetration. At the latter depth, free penetration stopped under self weight. To penetrate the last 5′ to 8′, the pile had to be rocked back and forth to assist the penetration process (Figure 4.19). The loss of penetration was attributed to the bottom jet nozzle design (Figures 4.11 and 4.12). The jetting of the second test pile used the improved nozzle design (Figure 4.14) and larger water pump (Figure 4.17). The jetting of the second test pile did not require any human assistance (Figure 4.20).

Figure 4.18 Moving steel collar up the pile during jetting.

Figure 4.19 Assisting in test pile # 1 jet penetration.

Figure 4.20 Jetting test pile # 2 with new nozzle and water pump.

In addition, it was estimated that approximately half the water was used in jetting test pile # 2 as that for test pile # 1.

4.5 Grouting of the Test Piles

After jetting of the test piles, it was planned to grout the piles immediately. Unfortunately, the grout mix designs of all of the local ready-mix providers did not meet published compaction grout recommendations. Specifically, the fly ash or fine fraction was much lower, and generally the slump was too high. Shown in Figure 4.21 was the proposed aggregate gradation mix along with the range of published compaction grout mix designs. The latter was developed from tests on a number of grout batches which varied sand, fly ash, cement, and water proportions to meet 2500 psi strength as well as 3″ slump for pumpability. After discussion with both the ready mix plants and their associated labs, Rinker agreed to try the proposed mix with a 2″ to 3″ slump.

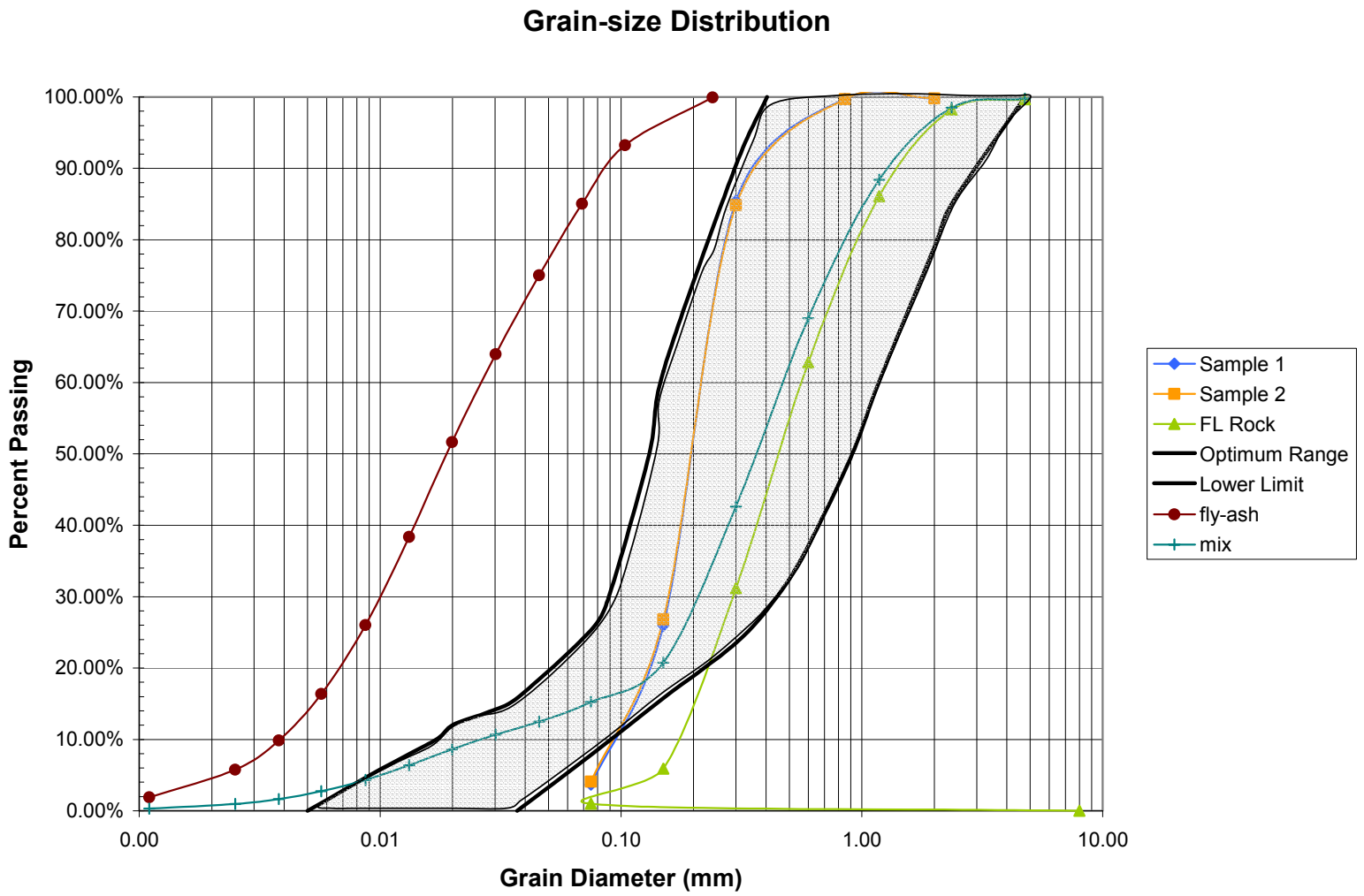

Figure 4.21 Grain-size distribution of sand and fly ash mix proportions.

In September of 2007, American Geotechnical, provider of the Schwing 750 concrete pump (Figure 4.22), began the grouting of the test piles. The grout was poured from the ready-mix truck into the Schwing 750 concrete hopper, and pumped out of a 5″ø line through a reducer to the 1 1/2″ø pile side exit ports (Figure 4.23). The procedure involved grouting the top ports (embedded 8′) on both piles in the morning (10:30 am), and then grouting the bottom sides of each pile in the afternoon (2:00 pm). Control of the grouting process was performed with the pressure gage mounted at the top of the pile (Figure 4.23) and monitoring the stroke rate on the concrete pump. Grouting of the top test pile ports stopped when heave and cracking of ground surface was noted (Figure 4.24).

Figure 4.22 Delivery of grout and start of test pile # 2 grouting.

Figure 4.23 Grout pipe, grout pressure gage, and grouting side of test pile.

Figure 4.24 Heave and ground cracking of grouting top ports of test pile # 2.

Grouting of the bottom ports on the test piles either resulted in ground heave or in the case of Test Pile # 2, the grout came up the adjacent parallel port after progressing completely around the perimeter of the pile (Figure 4.25).

Figure 4.25 Grout coming up opposite port after being injected 20′ into the ground.

After grouting the sides (top and bottom) of both test piles, the tips of the test piles were grouted the following morning to replicate the planned future installation process. After injecting approximately 1 yard of grout below Test pile # 2 (Figure 4.26) the grout pressure reached 150 psi to 200 psi, and the pile heaved (moved up) approximately 1/4″. Test pile # 1 had higher grout pressure (over 400 psi). Presented in Table 4.1 is a summary of the grout takes and pressures used in grouting Test pile # 1 (west pile) and Test pile # 2 (east pile).

Shown in Figures 4.27 and 4.28 are the measured soil pressures for both test pile 1 and 2 during side grouting of the piles. The upper gages are approximately 8′ down and the bottom gages are 16′ below the ground surface. Each level had four gages equally spaced around the chamber at a 1′ stand off.

Figure 4.26 Grouting test pile # 2 with 150 psi-200 psi grout pressure at pile tip.

Table 4.1 Summary of grouting 28′ test piles.

			Max. Grout Pressure (psi)	# of Strokes	Grout Take (gallons)	Remarks
East Pile	Upper Grout Zone	North Pipe	20	10	59.8	grouting stopped when 3/8" ground crack formed
		South Pipe	45	9	53.8	grouting stopped when 1/4" ground crack formed
	Lower Grout Zone	East Pipe	30	29	173.4	grouting stopped when grout came up through the West Pipe
		West Pipe	40	1	6.0	grouting stopped when grout came up through the East Pipe
	Pile Tip		120-150	31	185.4	1/8" pile movement @ 18 stroke; 1/4" movement @ 31 strokes; 1/8" ground cracks formed around pile
West Pile	Upper Grout Zone	West Pipe	60	5	29.9	grouting stopped when small ground cracks formed
		East Pipe	>200	1.5	9.0	sharp pressure increase, pipe may have clogged
	Lower Grout Zone	North Pipe	200	2	12.0	grout build-up in gage saver gave incorrect readings; pressure gage was disassembled and cleaned
		South Pipe	150	1	6.0	grouting stopped when gage blew apart; caused by a stripped fitting
	Pile Tip		400	0	0.0	no grout take; no visible pile movement

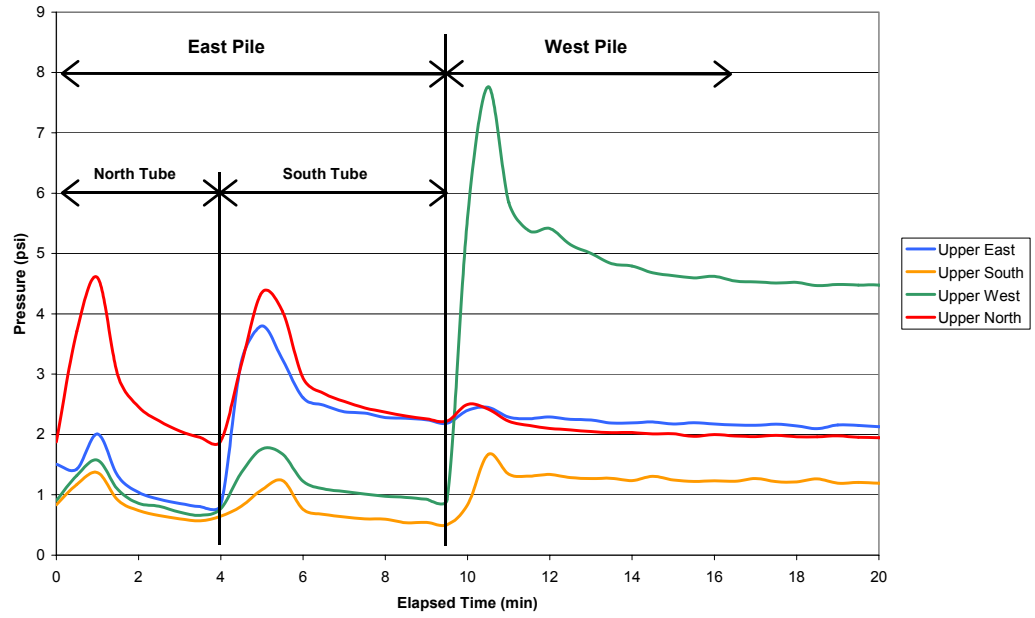

Figure 4.27 Changes in earth pressure during upper level grouting.

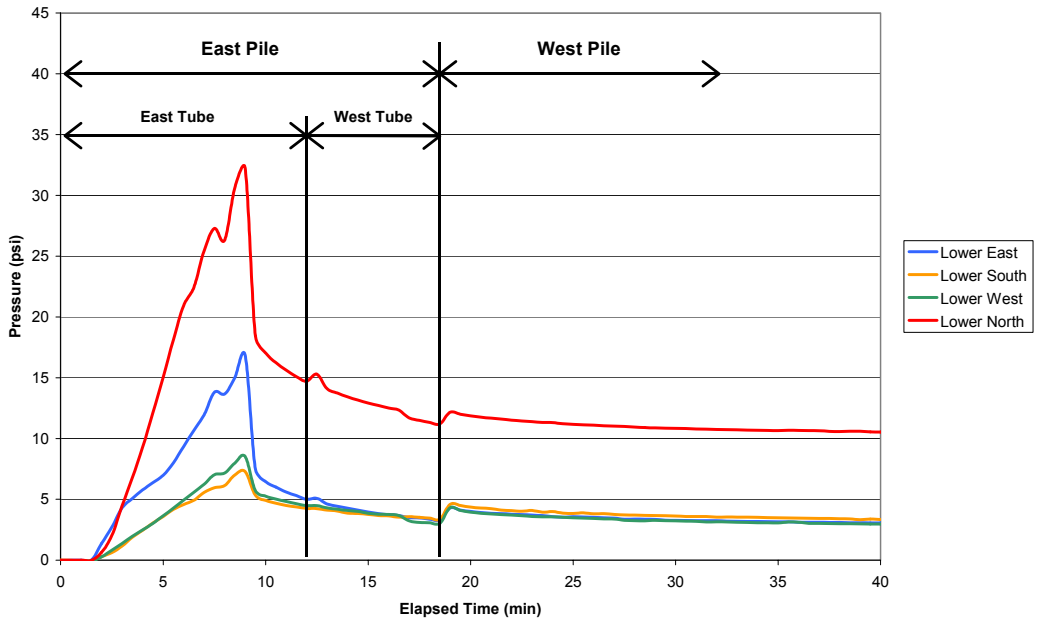

Figure 4.28 Changes in earth pressure during lower level grouting.

The magnitude of soil pressures was as expected (i.e., greater with depth); however the variability at any given elevation was more than expected.

Although the effects may be minor, it is believed that the pressure gage setup was not the best for this type of application. Figure 4.29 shows the pressure gage used during the pile grouting. In order to get an accurate pressure reading, the gage is separated from the grout line with T and rubber membrane with grout on one side and ATF fluid on the other side with the gage. Since both fluids are incompressible, it is expected that the grout pressure is transferred through the fluid to the pressure gage as the grout flows by the T-fitting and the membrane. Over time, however, it was observed grout collects behind the rubber membrane (indicated in Figure 4.29 by the red oval), which reduces the pressure readings (bridging), as well as impede or block the flow of grout.

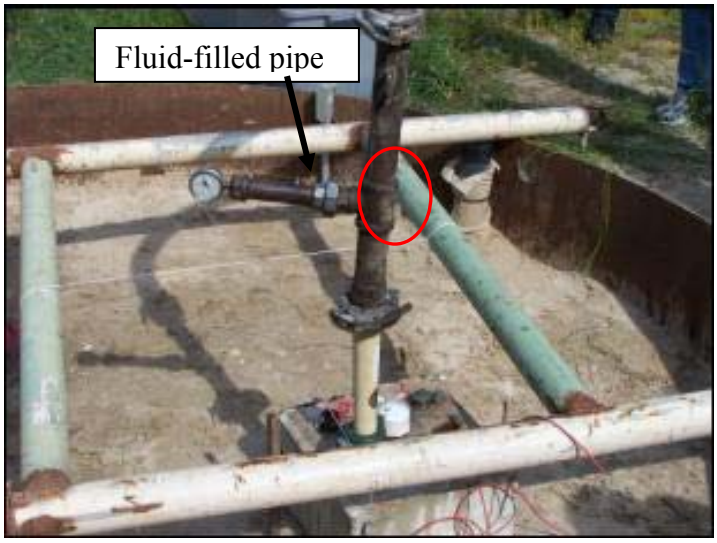

Figure 4.29 Grout pressure gage setup.

During the grouting process grout samples (4″ × 8″ cylinders) were collected from the ready-mix truck prior to pumping. Four days after pouring, three of the cylinders were tested in compression, and grout strengths of 1700 psi were recorded.

4.6 Load Testing the Jet-Grouted Piles

After jetting the test piles into the test chamber, the soil was leveled within the chamber and the tops of each pile were grouted to provide a smooth surface for load testing (Figure 4.30). Next steel cribbing (Figure 4.31) was brought in to support the 500 ton FDOT test beam which would be used to push down (i.e., axial compression) on the test piles.

Figure 4.30 Two jet-grouted test piles being prepared for load testing.

Figure 4.31 Steel cribbing to support 500 ton reaction beam.

It was important that the cribbing was level and provided enough clearance for the jack, load cell, and instrumentation, as well as be lined up over both test piles. Subsequently, the 500 ton reaction beam was trucked from FDOT's SMO facility to the test chamber site. Using the 20 ton FDOT forklift, the reaction beam was placed on the cribbing (Figure 4.32). Approximately 5′ clearance was used between the bottom of the reaction beam and the top of the test piles. Two 4′ × 4′ × 1″ steel plates were fabricated and placed on the top the reaction shaft on each end (Figure 4.33). Connected from the top of each reaction plate to the underlying reaction shafts were four Dywidag bars (75 kips each) (Figure 4.34). The 300 ton FDOT which was sent to Jacksonville for calibration, was subsequently placed on top of the test pile (Figure 4.35).

Figure 4.32 Placement of the 500 FDOT reaction beam.

Figure 4.33 Steel plates to transfer load from beam to reaction shafts.

Figure 4.34 Four Dywidag bars connecting reaction shaft to drilled shafts.

Figure 4.35 Jack, load cell, and vertical deformation instrumentation.

Also shown in Figure 4.35 is the vertical displacement monitoring instrumentation: two LVDTs, and a 0.0001 digital dial gage supported from rectangular steel channel which was attached to two 4″ × 4″ wood posts. The LVDTs were borrowed from LoadTest in Gainesville, Florida.

4.7 Axial Load Test Results of 1st Generation Jet-Grouted Piles

In December of 2007, load testing of both jet-grout piles was performed (Figure 4.36). Instrumentations included a Load Cell, Jack Pressure Gage, LVDT, and Digital Dial Gage at the top of the piles, and Geokon strain gages cast at the bottom of each pile. The top-down test was performed in 12 load steps with 5-minute wait time between increments, followed by an unloading phase. The latter testing regime was adopted to ensure complete capture of the soil stresses within the test chamber.

Figure 4.36 Load testing jet-grout piles.

Shown in the Figure 4.37 is the applied top load vs. vertical deformation at the top of the first jet-grout pile. This was the eastern most pile in the chamber, which was the last pile jetted. Evident from the figure, the 16″ × 16″ × 26′ (embedded length) pile carried a significant axial load at failure (160 kips = 80 tons). It is estimated for a similar pile driven in a very loose silty-sand (qc = 20 tsf), a capacity of 25 tons or 50 kips (FB-Deep) would be achieved (i.e., one-third of jet-grouted pile) or an increase by a factor of two to three.

Also shown in Figure 4.37 is the load transferred to the tip of the pile. Based on a comparison of top and bottom load, approximately two-thirds of load was transferred to the tip of pile. The latter is common for tip grouted foundations (i.e., drilled shafts, etc.); however, with grouting on the side of the pile, it was thought that higher side resistance would occur. However, as shown in the next section, there were a number of reasons why the higher side friction did not develop.

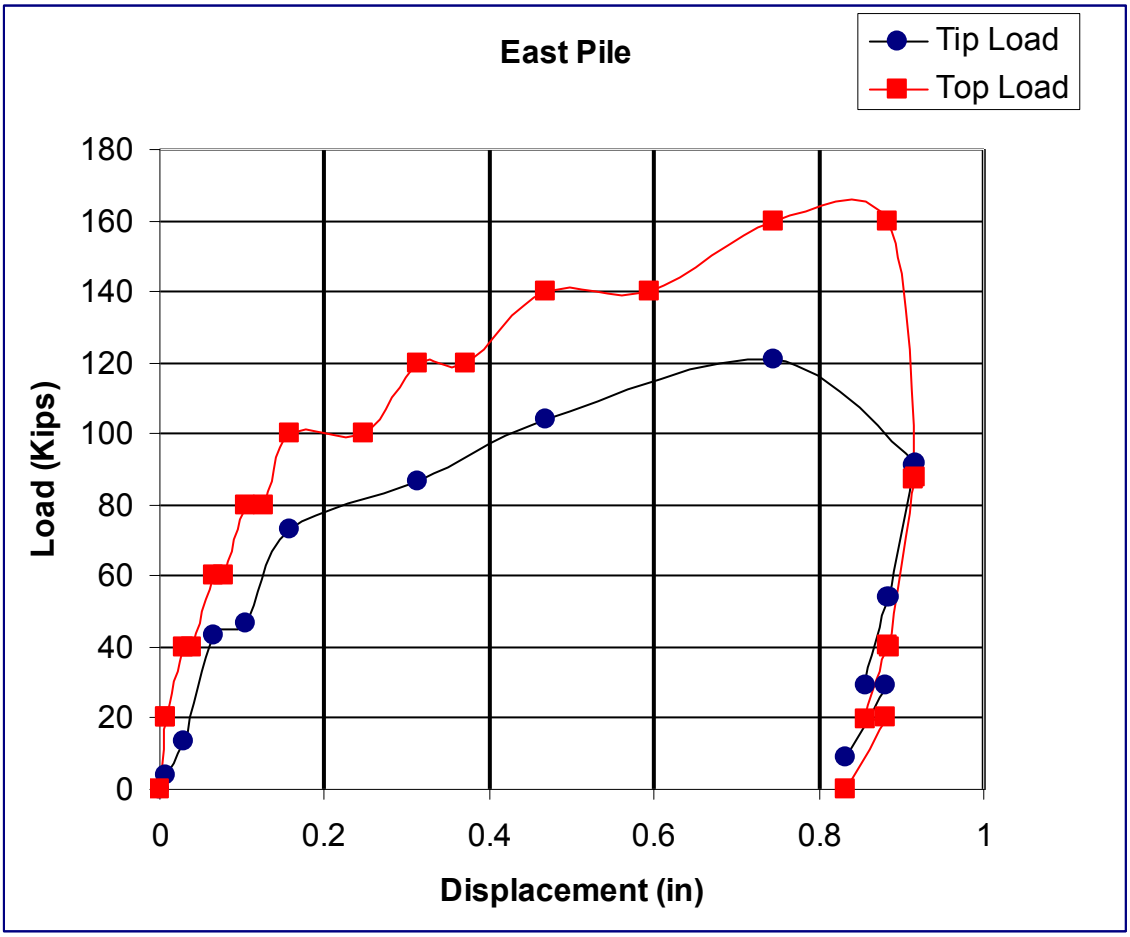

Figure 4.37 Load test results for east pile (last pile jetted – first grouted).

Shown in Figure 4.38 is the load displacement response of the west pile which was the first pile jetted, but the second pile grouted in the test chamber. Evident from a comparison of Figure 4.37 to Figure 4.38, the west pile carried one-half the load of the east pile, but was still greater than a conventional driven pile (50% improvement over 50 kips). Again, the end bearing carried approximately two-thirds of the applied load.

It is believed that the difference in capacity between the east and west piles was attributed to the volume of grout pumped into the ground between both piles (three to four times the volume, see Table 4.1). Since the west pile was the first pile installed, jetting (nozzles, plugs for side nozzles, etc.) had changed/improved between the 1st to the 2nd pile installation.

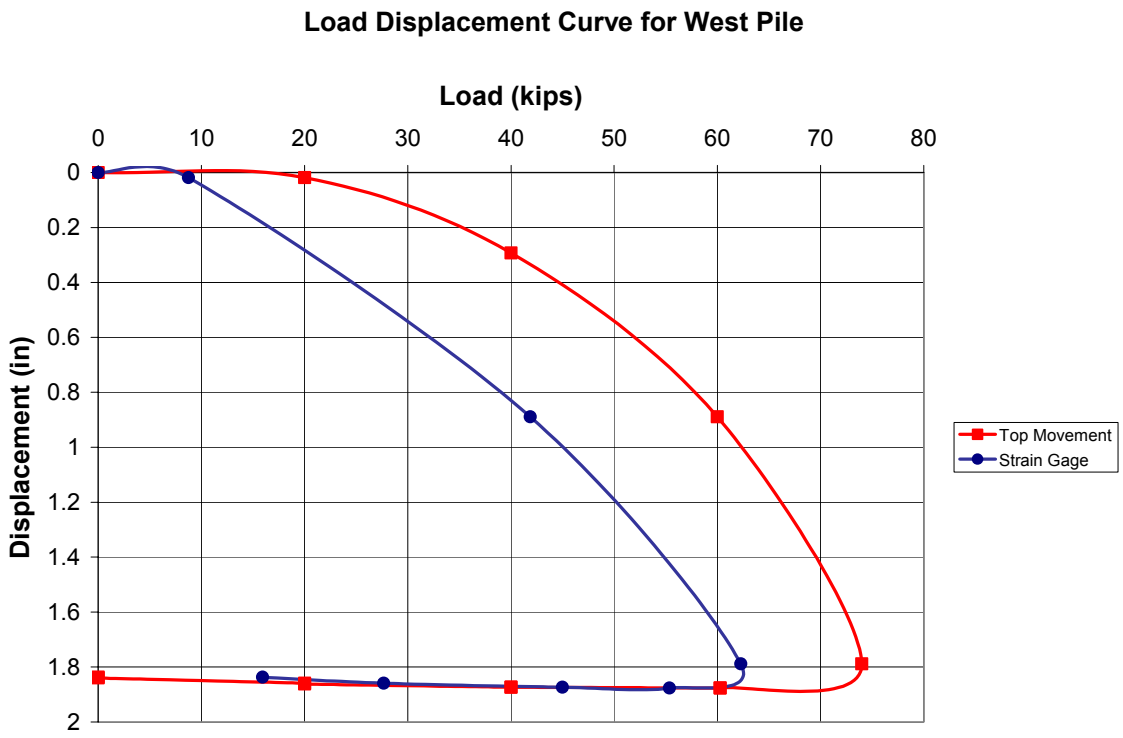

Figure 4.38 Load test results for west pile (first pile jetted – last grouted).

4.8 Excavation of 1st Generation Jet-Grout Piles

After conducting the top-down axial testing of the piles, excavation of the test chamber was undertaken in order to expose the grout around each pile for study. Note, the latter was only possible with the use of the test chamber, i.e., which ensured that the grout bulbs were not damaged due to pulling, etc. A company in south Florida which owned a Vertex vacuum system, Figure 4.39, was hired to remove the silty-sand within the chamber. Discussions with the manufacturer and website information (http://www.vector-vacuums.com/) identified a flow rate of 1000 cfm and vacuum of 28″ of Hg. The approach was thought to be the least disturbing, require no water, and least costly. Unfortunately, due to prior commitments, the company delayed the excavation process by three weeks.

Figure 4.39 Vacuum soil extraction system.

It was discovered that even though the system was capable of moving the silty-sand (Figure 4.40), however, was extremely slow. This was attributed to the time required for the material to travel from the test chamber to the vacuum unit. After observing the unit, it was estimated it would take two weeks to remove the material with the unit which at $1,400/day and was deemed cost prohibitive. Consequently, the tank was excavated manually (Figure 4.41) and took approximately two weeks.

Figure 4.40 Soil removal from test chamber using vacuum.

Figure 4.41 Manual removal of soil from around the piles in the test chamber.

Shown in Figure 4.42, is a typical exposed grout exit port on the east pile which was the last pile jetted. Evident from the excavation is the fact that the grout had a tendency to

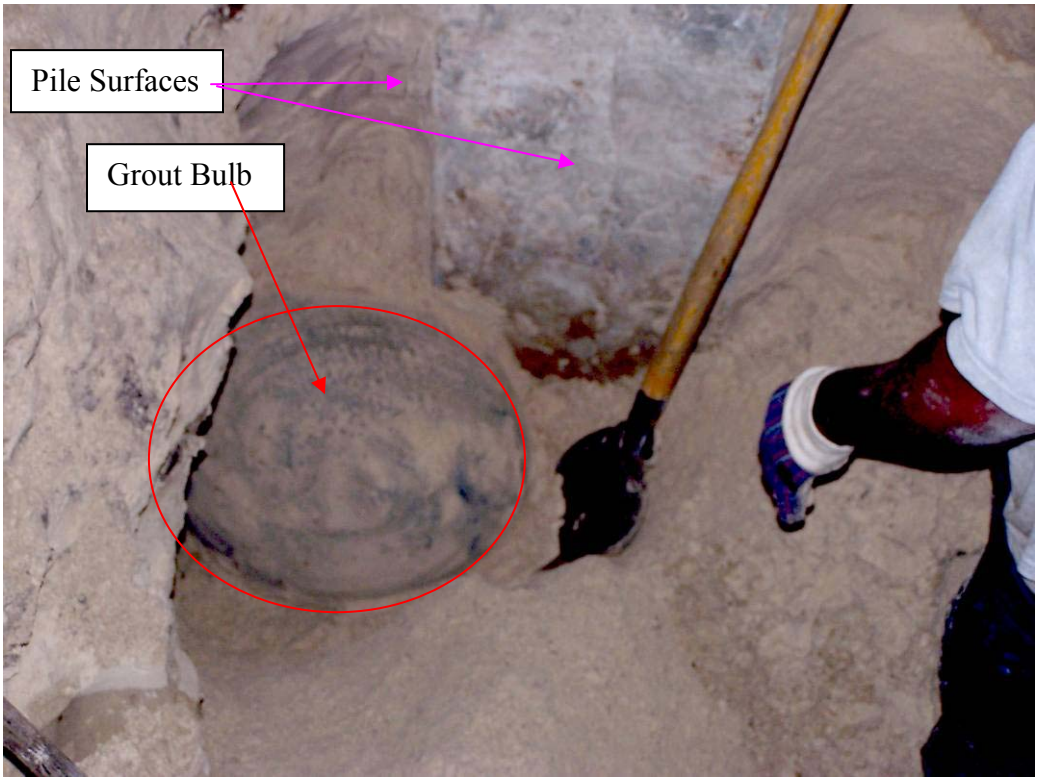

Figure 4.42 Grout bulb on east pile at depth 10′.

flow laterally (i.e., hydraulically fracture the soil) instead of traveling vertically between the soil-pile interface. The latter was believed to be influenced by the applied grout pressure (> 200 psi at pump), the grout slump (5″ vs. 2″) and the aggregate grain size (silt size to prevent sand locking) of the grout.

On a number of the jet-grout orifices on the west pile (1st pile jetted), it was found that the grout orifices were plugged with sand (Figure 4.43). The latter was believed to be affected by poorer jet design of the first installation jet nozzles (Figure 4.13), inadequate pump flow rates, and the minimal if any protection of orifice during insertion. However, prior to grouting, the PVC grout pipes were cleaned out with a hose and fresh water. Figure 4.44 shows the complete exposure of east pile after soil removal within the test chamber. Of major concern besides the plugged orifices (Figure 4.43) was the potential for poor bonding between the grout and the pile as shown in Figure 4.45. All of the load transfer from the bulb to the pile occurs only through shear at the narrow 1 1/2″ø grout exit port.

Figure 4.43 Plugged grout orifice, east pile depth 20′.

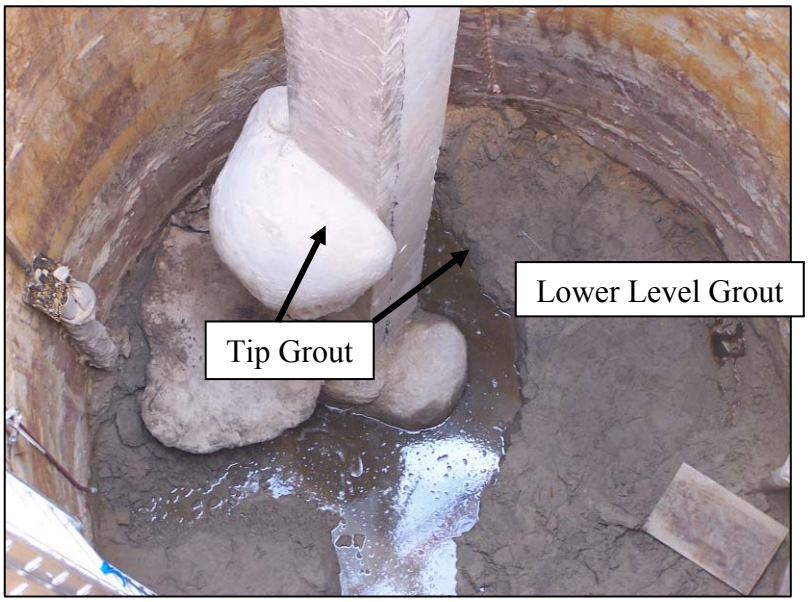

Figure 4.44 Grout bulb at the tip of the east pile.

Figure 4.45 Grout bulb west pile at 8′ depth.

CHAPTER 5
REDESIGN OF JET GROUT PILE SYSTEM AND SMALL SCALE PILE TESTING

5.1 Background

The full-scale testing (16″ × 16″ × 28′) of the compaction grouted jet piles revealed an increase in axial capacity over traditional driven piles. However, analysis of the data revealed the majority of capacity increase (2/3) was due to tip resistance. Since the intended use of the jet-grout technique was to replace sign and lighting foundations (i.e., drilled shafts) which are controlled by torsional resistance, higher skin friction was a high priority. Excavation of the grouted piles (Figure 5.1) revealed that a majority of the grout flowed horizontally outward from the grout port and very little if any bonding occurred between the grout bulb and the side of the pile. Consequently, any load transfer which occurred between the grout bulb and the pile had to pass through the small diameter shear zone at the grout tube (1 1/2″ø) – pile interface.

Figure 5.1 Grout bulbs adjacent to 16″ × 16″ pile.

The first step in the redesign of the grout-pile was to improve both the contact area and the adhesion between the grout and the pile. The latter required that the grout move alongside the pile and that no mixing occurs between the grout and the soil. One way to ensure the latter was to use a membrane around the pile into which the grout could be pumped. It was expected that the membrane would not only provide a path for the grout to move along the pile, but keep the soil from mixing with the grout. It was not known if a stiff or flexible membrane should be used, so both had to be tested. Also, with the use of a membrane which separated the soil from the pile, the grout mix design could be changed to improve pumpability as well as bonding.

5.2 Redesign of Grout Mix and Grout Delivery System

In order for the grout to move more freely around and alongside the pile as well as bond to the pile, it was decided to increase the grout's slump (i.e., water/cement ratio). In addition, to reduce the likelihood of sand locking at the expected pressures and grout pipe sizes, it was decided to remove sand from the grout mix for grouting the side membranes along the pile. Note, sand is an integral part of compaction grout mix designs, but because of the use of the membrane, the fluidity of the grout could be greatly increased without worrying about hydraulic fracturing of the soil. Since the shear transfer between the grout – pile was proportional to an expected skin friction of 1 to 2 ksf, the strength of the grout could be reduced as well as the cost by replacing a percentage of cement in the mix by fly ash. Multiple percentages were investigated; a final of 10% by weight was used. To increase the fluidity of the grout for pumping in small diameter grout pipes, i.e., 1 1/2″ø, the water cement ratio of the mix was varied from 0.3 to 0.6. It was found that a water cement ratio of

0.45 resulted in grout pumping pressures in excess of 400 psi without any locking issues found in the 1 1/2″ø lines.

In the case of tip grout mix, the grout delivery pipe was 2″ diameter and the use of sand in the mix design was thought to be beneficial (i.e., prevent hydraulic fracturing). However, grouting the first few mini-piles always resulted in sand locking or limited grout pressures at the pile tip. The latter becomes untenable for longer or deeper embedded piles. Consequently, the sand was also removed from the grout mix for tip grouting of all the piles. Pressures in excess of 800 psi were readily achievable with 2″ø line.

It was evident for the mini-pile testing that a new grout pump system was required. That is the use of a ready mix truck and a large grout pump to place 50 to 100 gallons of grout (i.e., 6 ft^3 to 12 ft^3) was not viable. The researchers searched for possible rental equipment to place the grout. However none had the operational pressures (i.e., 200 psi) that were required for this work. Consequently, a hydraulic grout pump was developed and constructed for this application (Figure 5.2).

Figure 5.2 Grout pump for grouting mini-piles.

To ensure that the pile could be grouted to any size or pressure of interest, as well as multiple times, it was decided to have a return pipe to the top of the pile for each grout tube. The return lines allowed the grout pipes to be flushed with water and reused. In addition, every exit hole in the grout tube was covered with a gum rubber membrane. The latter acted as a one way valve. That is, grout could exit the tube under pressure, but would not re-enter once grouting finished and flushing occurred. Shown in Figure 5.3 is the grout tube and associated gum rubber covering within the mini-pile formwork.

Figure 5.3 Side grout tubes in mini-pile.

As shown in Figure 5.3 the grout pipes are located in the corners of the pile, outside of the rebar cage, diametrically opposed. Each of the grout pipes (entry and exit) had a series of 1/2″ and 3/4″ holes drilled into the 1 1/2″ø PVC tubes in pairs at 5″ intervals. The larger diameter holes (3/4″) were located at the bottom of the grout pipes and the smaller holes at the top. The gum rubber covering each hole extended approximately 2.5″ to each side. The exit of grout from beneath the gum rubber occurred at grout pressure at approximately 20 psi.

Shown in Figure 5.4 is the testing of the grout lines, and gum rubber membranes that were subsequently used in all next generation jet-grouted piles. Also revealed in Figure 5.4 is the use of a new grout pressure monitoring device. Instead of the current technology of a pipe T and union, covered by rubber membrane and ATF fluid (Figure 4.29) the grout pipe was threaded into a coupling with a rubber membrane which allowed grout to pass through with an incompressible fluid (water/glycol mix) on the other side. Threaded to the body that had the water/glycol mix was a pressure gage to monitor pressures. The new gage was found to work quite well at both low (10 psi) and high (1000 psi) pressures.

Figure 5.4 Pressure gage and grout pipe and gum rubber used for grouting.

Shown in Figure 5.5 is the new grout pipe-system cast into a 4′ section of mini-pile. At top of the pile, a water line was attached to the inlet grout tube. Next, the grout exit line had a ball valve attached, and was closed initially. The water was turned on and the ball valve slowly opened. At approximately 20 psi, the gum rubber expanded and water was found to flow out of the grout exit ports (Figure 5.5). For all subsequent mini-pile, small scale and

large scale piles, the grout pipe system used in Figures 5.3 through 5.5 was employed. Noted for longer piles that employed multiple grout delivery systems, all inlet and exit grout pipes were located flush with the outer surface of the pile and the rebar cage.

Figure 5.5 Water exiting grout pipes cast into mini-piles.

5.3 Testing of Flexible and Semi-Rigid Pile Membranes

Two different membranes were used around the mini-piles: 1) flexible neoprene and 2) semi-rigid canvas material (Figures 5.6 and 5.7). The intent of the membranes was to ensure there are no contamination of the grout and the good adhesion to the pile, as well develop a sufficient grout zone to develop increased skin friction on the final jet-grout pile design.

A number of 6″ × 6″ by 4′ mini-piles with grouting system shown in Figures 5.3 and 5.5, were cast and tested with the proposed membranes. To replicate expected field conditions, the mini-piles were first jetted into the ground and subsequently grouted. Both tests employed the same grout mixes, and pumped volumes. Shown in Figure 5.6 is the excavation of one of the grouted mini-piles.

Figure 5.6 Canvas membrane mini-pile excavation.

Figure 5.7 Neoprene outer membrane on mini-pile.

Shown in Figures 5.7 and 5.8 are the mini-piles in the laboratory with their outer membrane removed. Evident from the pictures, both mini-piles showed excellent bonding

between the precast pile and the grout. To further test the bonding, the piles were struck with a large sledge hammer to see if the grout could be debonded. Interestingly, in order to remove the grout, large pieces of the precast pile had to be broken off with the grout (Figure 5.9).

Figure 5.8 Canvas outer membrane on mini-pile.

Figure 5.9 Testing of bond between grout and pile.

A study of the grout membranes revealed that both did an excellent job of keeping soil away from the perimeter of the pile (i.e., improve bonding); however, the semi-rigid canvas membrane, limited the lateral grout spread and associated grout bulb shape, see Figures 5.7 and 5.8. In the case of the canvas membrane, the shape of the bulb is depended of the number of pleats and the diameter of the membrane. To limit the potential for tearing or splitting of the membrane, the tensile strength of the membrane is very important. The expected stress in the membrane is a function of grout pressure and the diameter of the bulb.

5.4 Small Scale Jet-Grout Pile Testing

Based on the results of the mini-pile tests, it was decided to construct and test two larger 8′ long piles. One of the piles was 6″ square by 8′ long and the other was 8″ square by 8′ long. The different widths were selected to identify size effects in order to develop the design criteria for jet-grout process.

Shown in Figure 5.10 is a rendering of the components for each of the constructed jet-grout pile system. It was composed of two separate grouting systems (each 4′ long) making up the 8′ pile. Each system had its own grout entry and exit pipe, along with semi-rigid covering membrane. Shown in Figure 5.11 is the formwork and grout piping for each 4′ system. The far left pipe and the far right pipe at the bottom are the entry and exit pipes for the bottom grout system; whereas the top far right pipe and the bottom far left pipe makeup the top grout system. After the placement of all the grout pipes in the formwork, a mild steel reinforcing cage was placed, along with threaded steel bars to clamp the semi-rigid membrane (Figure 5.10) to the pile. Subsequently, the concrete was placed and care was taken to ensure that the grout pipes, and jet pipe did not move while the concrete was fluid.

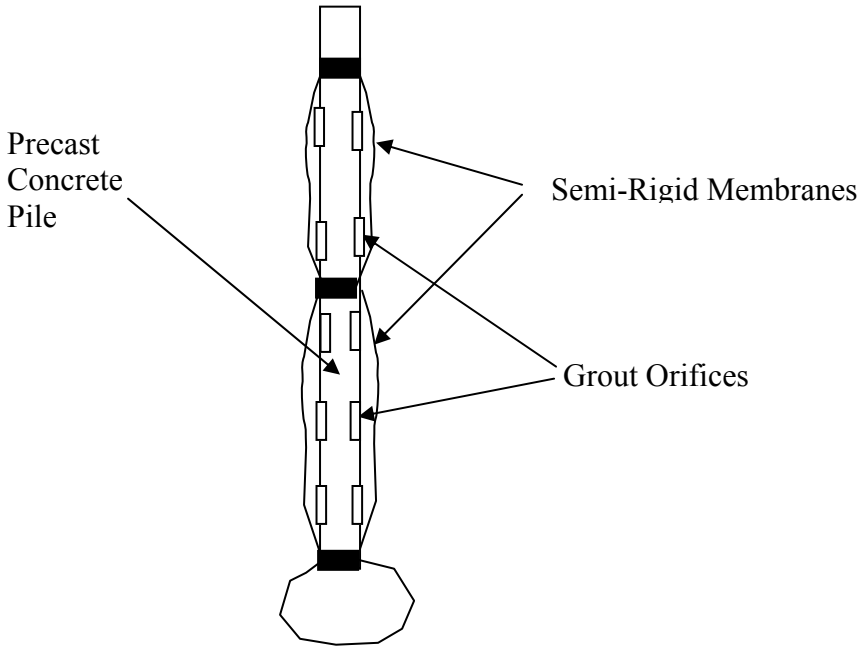

Figure 5.10 Jet-grout mini-piles.

Figure 5.11 Grout delivery pipes for top and bottom ejection ports.

After casting the concrete, the piles were left to hydrate for one week and then the forms were stripped. Excess concrete was removed from the side grout ejection ports (i.e., gum rubber), the piles were stood up and water was flushed through each grout system under pressure as shown in Figure 5.12. The latter ensured that each grout system (i.e., top and bottom) was working correctly (i.e., holes had no obstructions and gum rubber allowed fluid to exit the pile).

Figure 5.12 Flushing the bottom side grout delivery system.

Next, the semi-rigid membranes were attached to the upper and lower sections of the pile. This was accomplished by first folding a 4′ × 10 2/3′ piece of canvas twice, such that perimeter had length of 64″. Subsequently, the top and bottom of the 64″ diameter canvas cylinder was pleated (i.e., folded) to provide a snug fit to the 32″ perimeter of the piles. Then, the canvas is attached at the top and bottom of the piles with threaded rods as shown in

Figure 5.13. Evident from the picture, the membrane is folded thereby providing a minimal width for jetting, but under grouting will fully expand to the 64″ perimeter at its center and taper off toward the ends. Also note, the canvas is not sewn or glued together at any location. Holding the canvas down between each threaded rods/side is a 2″ × 8″ × 1/4″ steel plate to prevent grout from exiting the membrane under the design pressure (i.e., 200 psi). Shown on the bottom of the pile in Figure 5.13 is the jet nozzle attached to the pile for pile insertion. Shown in Figure 5.14 is one of the piles ready for jetting/grouting.

Figure 5.13 Attachment of the semi-rigid membrane to a pile.

Figure 5.14 Test pile prior to jet-grouting.

5.4.1 Test Chamber Soil Preparation

Discussions between the researchers and FDOT resulted in the decision to do the next set of tests in denser soils, i.e., D_r (relative density) at least 50% or above.

Filling the test chamber began by first removing all the previous soil within the tank (approximately one month), and recalibrating all the stress gages in the chamber (ten gages: eight along the sides and two at the bottom) as shown in Figure 5.15. Next, the soil was placed in 2′ lifts and compacted with a vibratory plate compactor. The soil that was placed in the chamber was the same soil which was removed with a natural moisture content of approximately 5 to 7%. Typical dry densities in any lift varied from 101 pcf to 105 pcf due to lift thicknesses and variability in moisture content. Based on the dry densities, the relative densities varied from 50% to 65%. While filling the test chamber a number of hand cone penetrometer tests were also performed on the compacted silty-sand. Cone tip resistances

varied from 50 k_g/cm^2 to 70 k_g/cm for all the lifts. Based on typical relationships of relative density with SPT N values, (Figure 5.16) it is estimated the N values ranged from 10 to 15.

Figure 5.15 Emptying and placing instrumentation within the test chamber.

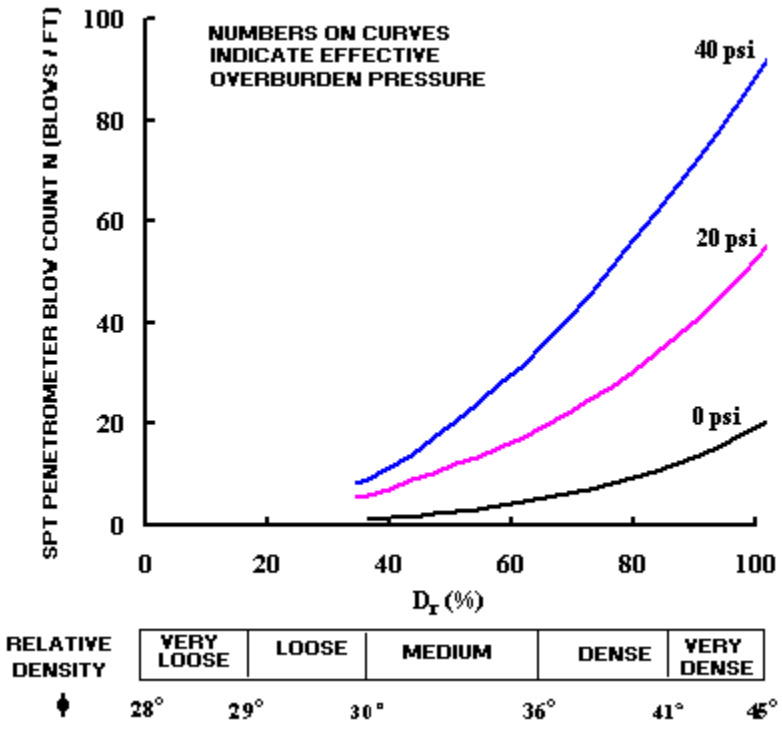

Figure 5.16 SPT N values vs. relative density.

5.4.2 Jet-Grouting Two 8′ Piles

Shown in Figure 5.14 is the 8″ × 8″ × 8′ test pile held up with the FDOT large forklift prior to jetting in the test chamber. The pile had two separate grout systems (i.e., upper and lower) with each having a maximum perimeter of 64″.

The installation began with the jetting and took approximately three minutes and ten seconds using a 2″ø flexible hose connected to the city water supply at a constant pressure of 60 psi. Next, the top grout system (Figure 5.10) was grouted by first mixing 50 gallons of grout by hand in a mortar mixer which had a maximum capacity of 30 gallons. Thus the mix had to be done in two batches; while grouting the first batch (30 gallons) the second batch (25 gallons) was in preparation (cement, 10% fly ash, and w/c = 0.45). Due to physical labor constraints, the grouting took approximately two hours. The maximum recorded grout pressure using the new pinch valve gage was 110 psi on the pump and 80 psi on the return line from the pile. The process was repeated for the lower side grout system on the pile. Again, fifty gallons of grout was mixed and pumped into the lower semi-rigid membrane. Since the lower side grout system was four feet deeper than the top system, grout pressures on the order of 200 psi were observed at the pump and 140 psi on the return line from the pile. Grouting the top semi-rigid membrane caused visible rising of the ground surface around the pile (approximate 3″ to 4″ heave radiating out 4′); however little if any ground motion was observed for the lower system. In addition, no grout was observed coming up through the ground or at the bottom of the pile's jet tube.

To allow for hydration, and increase in grout strength alongside the pile, the tip of the pile was grouted the following morning. Approximately 30 gallons of grout were mixed and loaded into the grout pump (Figure 5.2). Since, the tip jet-grout pipe did not have a return line, the grout pressure gage was mounted as close to the pile as possible, i.e., at the pile top.

Initial grout pressures were approximately 60 psi, and with increased volume of grout the pressure began to climb. At approximately 130 to 150 psi and 30 gallons of grout, the top of the pile and surrounding soil started to move upward and grouting was suspended.

The process described for the 8″ × 8″ × 8′ pile was also performed on the 6″ × 6″ × 8′ pile. Since the 6″×6″ pile had semi-rigid membrane perimeters that were 48″, only 25 gallons of grout were used in each grout system (i.e., 25 gallons top and 25 gallons bottom). Pressures of 80 psi and 140 psi were recorded on the exit grout pipes during grouting. However, when grouting the tip of the 6″ × 6″ × 8′ pile, the grout mix included a sand to fly ash ratio of 1.6 (1.6 sand/fly ash). After pumping approximately 10 gallons, the gage reached its maximum pressure range of 750 psi and flow stopped. Removal of the grout hoses to the pile revealed sand locking and it was decided to remove sand from the grout mix design for tip grouting. The new mix, similar to side grouting mix design was used on the 8″ × 8″ × 8′ pile.

5.4.3 Load Testing the 8′ Jet-Grouted Piles

Approximately two weeks after grouting the test piles, the load frame for the vertical top-down testing was again setup (Figure 5.17). Measurement of both applied top load and vertical deformation (dial gages) were recorded for each test. Shown in Figure 5.18 are the recorded loads versus deformations for both the 6″× 6″ and 8″× 8″ piles. Evident from the plots, ultimate loads in the range of 110 to 120 kips are possible with the 8″× 8″ and 60 to 70 kips for the 6″× 6″ pile depending on the amount of vertical deformation.

Of interest is the distribution of skin and tip resistance on the piles. It was noted when grouting the tip of the 8″× 8″ pile that the top of the pile began to move upward at peak pressures and grout volumes of 150 psi. If, the total ultimate resistance is equally balanced

between side and tip resistance (i.e., down force is balanced by up force during grouting), then side resistance of 16 to 48 kips are achievable (150 psi × A_{cross}: 104 in^2 – pile or 320 in^2 –membrane). One possible check of tip?? vs. skin friction is DeBeer's procedure for

Figure 5.17 Setup reaction beam for top-down testing.

estimating pile capacity. The method identifies the change in slope on log of load vs. log of displacement as the transition from skin to tip resistance. From DeBeer's log-log plot (Figure 5.19), the 6″× 6″ pile would have a skin friction of 30 kips and the 8″× 8″ pile would have a skin friction of 45 kips.

Of interest is a comparison of side resistance on standard driven piles and drilled shafts, versus the jet-grouted piles in similar soil conditions. Using the maximum SPT N values presented earlier (i.e., N=15), FDOT's FB-Deep software gives skin friction of 9 kips and 12 kips for 6″× 6″ and 8″× 8″ driven piles, respectively. In the case of equivalent diameter drilled shafts used for high mast signs and lights, FB-Deep gives 7 kips and 9 kips. Consequently, the new jet-grout piles have increased the side friction by a factor of 3.3 to

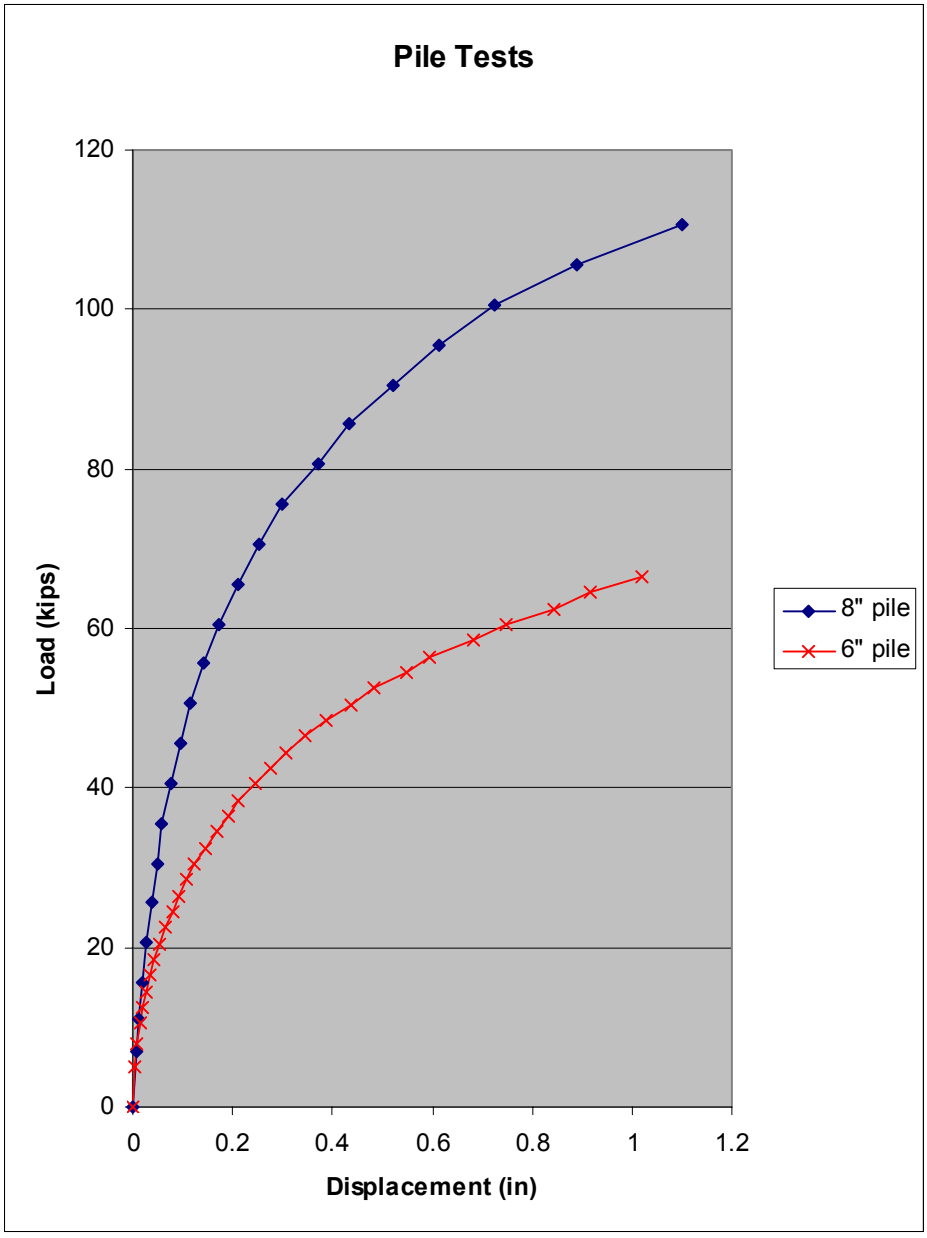

Figure 5.18 Load test results for 6″ and 8″ piles.

3.75 for driven piles and a factor of 4.2 to 5 for drilled shafts. The latter is significant since it will greatly reduce the required embedment lengths. In addition, typical signs and lighting designs are controlled by torsion (i.e., skin friction), and as will be shown in Chapter 6 and 7, the new pressure grouted pile will carry the same torque/ torsional load as axial skin friction.

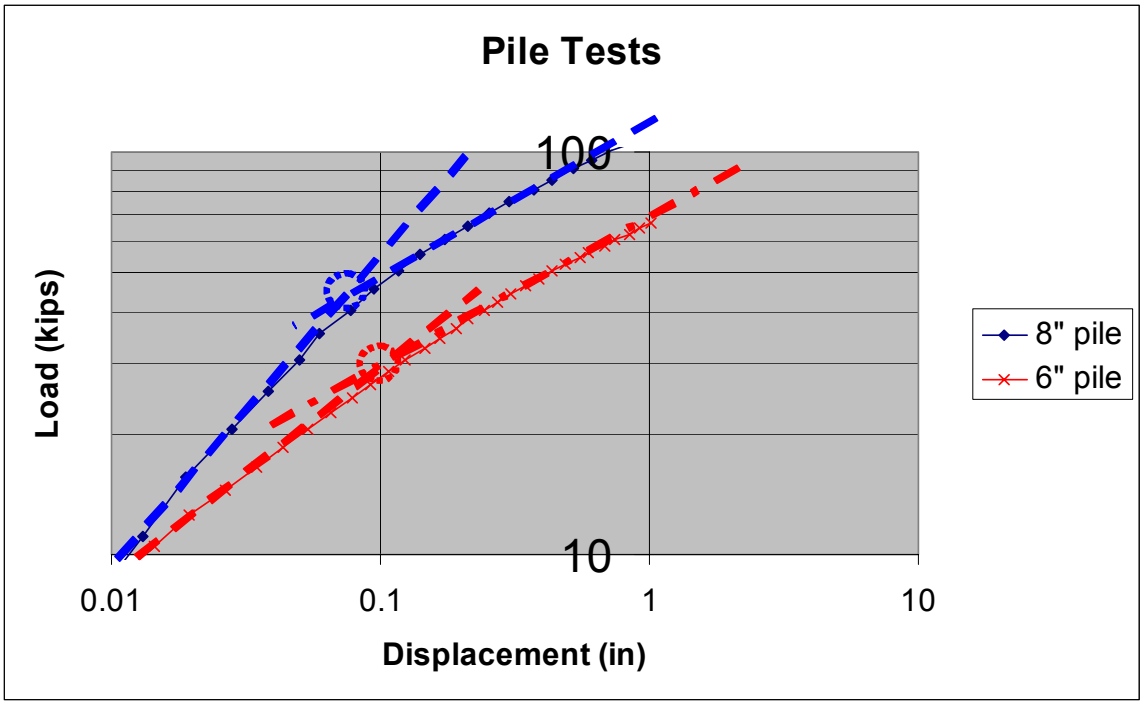

Figure 5.19 Log-log plot of mini-pile load tests and estimated skin friction.

The increase in skin friction on the jet-grout pile is due to the newly developed grout bulb around the perimeter of the pile. Comparison of the bulb of earlier tests, (e.g., Figure 5.1) shows significant differences. The earlier tests (1st generation) had bulbs that extended outwards, whereas, newer system with semi-rigid membrane had grout extending around the complete pile. For instance, shown in Figure 5.20 is the insitu grout bulb around the 8″ × 8′ test pile. Figure 5.21 shows the completely excavated 8″square × 8′ jet-grouted pile. Evident, the bulb engulfs the whole pile and is bonded to the pile, even after testing it to failure (i.e., 120 kips axial load). A discussion on estimating jet-grout pile capacity and design is given in Chapter 7.

Figure 5.20 Insitu grout bulb around 8″ × 8″ test pile.

Figure 5.21 Excavated 8′ jet-grouted pile.

CHAPTER 6
TORQUE AND AXIAL COMPRESSION LOAD TESTINGS OF THE 16″× 16″ × 20′ JET-GROUTED PILE

6.1 Design of 16″ × 16″ × 20′ Jet-Grout Pile

After having successfully installed and tested small scale piles (i.e., 6″× 6″× 8′, and 8″× 8″× 8′) with the improved grout delivery system and membranes, it was decided to test the system full scale (i.e., 16″× 16″ × 20′). Also, since the foundation is planned to support sign, lighting and wall scenarios, it was decided to test the pile under torsional loading, since failure due to wind force times a torque arm is of major concern. A 36″ diameter (grout bulb) by 20′ long jet grouted pile was selected. The latter diameter is smaller than typical drilled shaft diameters (48″); however with the increased skin friction on the grouted pile, comparable or greater torsional resistances are expected. In addition, due to boundary effects of the test chamber, larger diameters will not be representative of field conditions.

Current pile/shaft design involves integrating the torsional shear resistance (typically assumed equivalent axial skin friction) times the radius of the shaft over the surface area of the pile/shaft. Therefore, a 36″ (3′) pile/shaft diameter with a 20′ length should have a torque resistance of 1.2 ksf (unit skin friction from small scale tests) × 36″/2/12 (radius) × π × 36″/12 (diameter) × 20′ (length) or approximately 350 ft-kips of torsional resistance. Note, the axial side friction of the jet-grout pile should be 1.2 ksf (unit skin friction from above) × π × 3′ (diameter) × 20′ (length) or 225 kips.

The planned 16″ precast section of the jet-grouted pile had a structural torsional resistance of approximately 150 ft-kips (i.e., #5 stirrups at 2″ spacing), which is significantly less than the 350 ft-kip torsional resistance provided from 36″ diameter grout membrane. A 24″ diameter pile (#5 stirrups at 2″ spacing) is capable of carrying 400 ft-kip of torque or

sustaining a 40″ diameter grout membrane (i.e., 8″ of grout on each side of pile). However, since the test was to investigate the torsional shear resistance at the interface of the grout membrane and the soil, as well as the bonding between the precast pile and the grout, it was decided to employ a composite steel pipe and a precast 16″ reinforced concrete pile as shown in Figure 6.1.

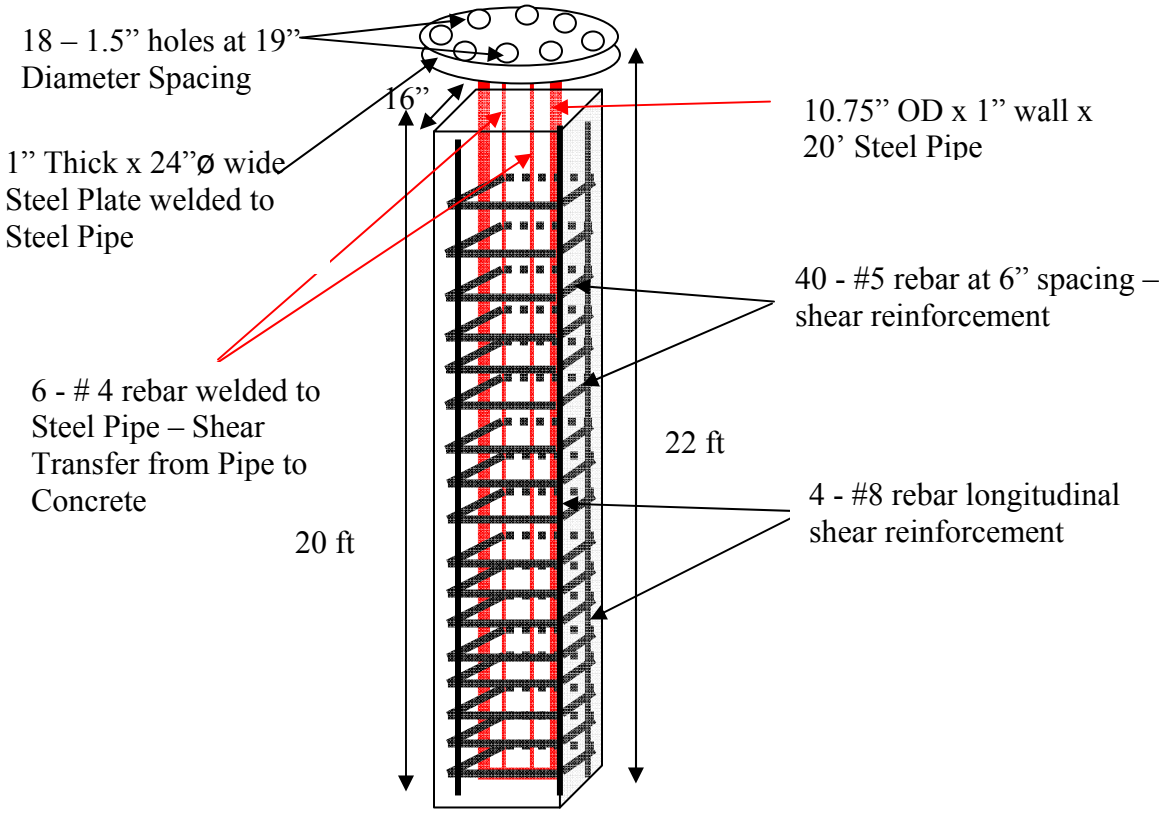

Figure 6.1 Design of 16″ × 16″ × 20′ jet-grout test pile.

The pile consists of a 10.75″ OD × 1″ wall × 20′ long steel pipe running the full length of the pile is capable of carrying a linear decreasing 550 ft-kips torque (F.S. = 1.5) from the top to the tip of the pile. Transferring the torsional shear stress from the pipe to the concrete are six #4 rebars welded along the length of the pile, Figure 6.1, and forty shear stirrups

welded to the pipe. The pile is designed for 50 kips of lateral force which accompanies the 550 ft-kips of torque. Four #8 bars run in the longitudinal direction within the stirrups (Figure 6.1) to assist with the flexure loading. The shear (50 kips), flexure (300 ft-kips), and torque (550 ft-kips) loadings are designed for the test setup as shown in Figure 6.2.

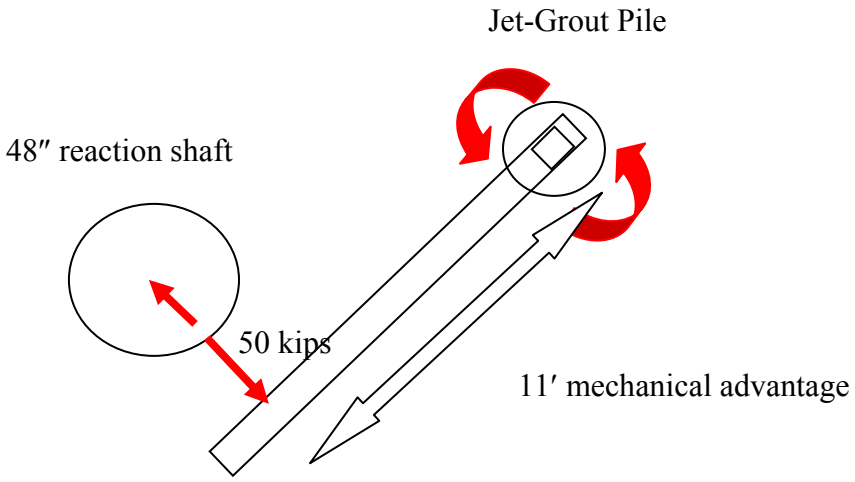

Figure 6.2 Proposed torsion test on jet-grout pile.

6.2 Construction of 16″× 16″ × 20′ Jet-Grout Pile

Construction of the jet-grout pile began with the welding of the six #4 rebars to the 10.75″ OD × 1″ wall × 20′ steel pipe as shown in Figure 6.3. Next, the forty #5 rebars were bent on a frame and subsequently welded to the steel pipe (Figure 6.3) at 6″ spacing. Then, the #8 longitudinal rebar was placed within the shear stirrups and wire wrapped to the shear stirrups. The steel core of the pile (Figure 6.3) was then lifted and placed within the concrete framework, which contained the grout delivery and jetting PVC pipes assembly as shown in Figure 6.4. Placement of the top half grout delivery system required that a 1 1/2″ø hole be cut through the steel pipe. Note the grout delivery tubes travel along the edges of the pile and return to the top of the pile for grout pressure measurement, cleanout if necessary for regrouting.

Figure 6.3 Construction of jet-grout pile.

Figure 6.4 Grouting pipes and steel reinforcement in jet-grout mold.

After the placement of the top and bottom grout delivery systems and the steel reinforcement in the mold, the central jetting system was placed, Figure 6.5. The top of the 1 1/2″ jetting pipe was centrally located within the top of the top torque plate, Figure 6.6. After construction of the steel reinforcement, grout delivery, and jetting systems, the pile was cast with five thousand psi concrete obtained from a nearby ready-mix yard (Rinker). Both the outsides and the inside of the steel pipe were filled with concrete using vibrators. The mold was subsequently stripped (Figures 6.7 and 6.8) and the concrete was allowed to cure for 28 days.

Figure 6.5 Central jet pipe and piping for four nozzles at pile tip.

Figure 6.6 Top torque transfer plate and central jetting pipe.

Figure 6.7 Mid section of cast 16″×16″ × 20′ jet-grout pile.

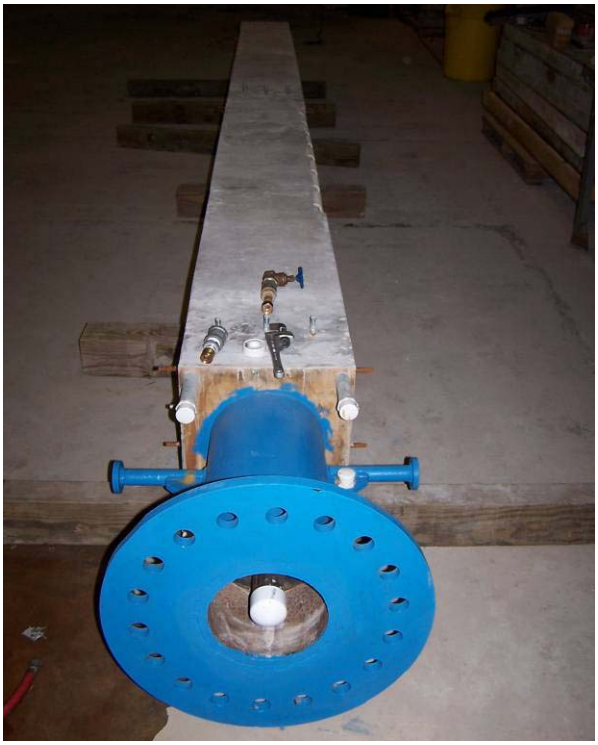

Figure 6.8 Top of cast 16″×16″ × 20′ jet-grout pile.

After curing, the grout delivery tubes were hooked up to the city water supply and flushed to test the system (Figure 6.9). After flushing and testing both sections of the grout system, the membranes were attached to the pile (Figure 6.10). Subsequently, the jet nozzles

Figure 6.9 Flushing and testing grout delivery tubes.

were attached (Figure 6.10) and the pile was transported outside to the test chamber where they were tested (Figure 6.11).

Figure 6.10 Attaching grout membranes and tip jetting nozzles.

Figure 6.11 Testing jet nozzles prior to jetting.

6.3 Refilling the Test Chamber with Soil

For the planned torsional test, it was decided to again prepare the soil in the test chamber at a Dr of 50% or medium dense, or a dry density about 101 pcf. The soil was subsequently placed in the chamber in 18″ lifts at a natural moisture content of approximately 5% to 7% and compacted with a vibratory compactor and tested with a nuclear density meter (Figure 6.12).

Figure 6.12 Performing nuclear density measurements.

Typical dry densities throughout the lifts varied from 101 pcf to 105 pcf due to lift thicknesses and variability of the soil's natural moisture content.

Again, the soil instrumentation was placed near the walls of the tank at two elevations 8′ and 15′, and 1′ standoff. The latter gages measured horizontal stress change. Below the planned jet depth of the pile, approximately 22′ and 23′, and at the center of the tank, two Geokon stress gages were buried to measure vertical stress changes.

6.4 Jetting and Grouting

After filling the test chamber and testing the jet and grouting tubes of the pile, the pile was lifted upright with the large UF/FDOT forklift. A 2″ø water line was hooked to the top inlet of the tip jet-grout nozzles (Figure 6.13). For the jetting, it was decided to use city water

Figure 6.13 2nd generation test pile prior to jetting in test chamber.

supply with 60 psi pressure. However, it was found that once the city water valve was opened and jetting commenced, the pressure in the line dropped to 40 psi. It took approximately 42 minutes to complete the pile insertion. During jetting process, the pile was lowered and raised with the forklift in a cyclic pattern. Shown in Figure 6.14 is the pile near the final tip elevation during the jetting pile insertion process. Evident the runoff and disturbance was not excessive. Note, the rate of insertion may be increased significantly by

Figure 6.14 Jetting the last 2′ of test pile.

increasing the pump flow rate and pressure; however, it is expected that the disturbance and spillage will also increase.

After the pile being jetted to its final tip elevation, the grouting of the pile commenced with the assistance of Applied Foundation Testing personnel and equipment (grout pump) as shown in Figure 6.15.

Figure 6.15 Haney grout mixer and pump with AFT personnel.

The grout mix consisted of cement, micro fine fly ash and water at a water/cement ratio of 0.5. The grout was pumped from a holding tank (Figure 6.15) through a 1 1/2″ø high pressure line to the pile. At the pile head, (Figure 6.16) there were two pressure gages to measure the inlet and outlet grout pressures as well as ball valves to shutoff grout flow.

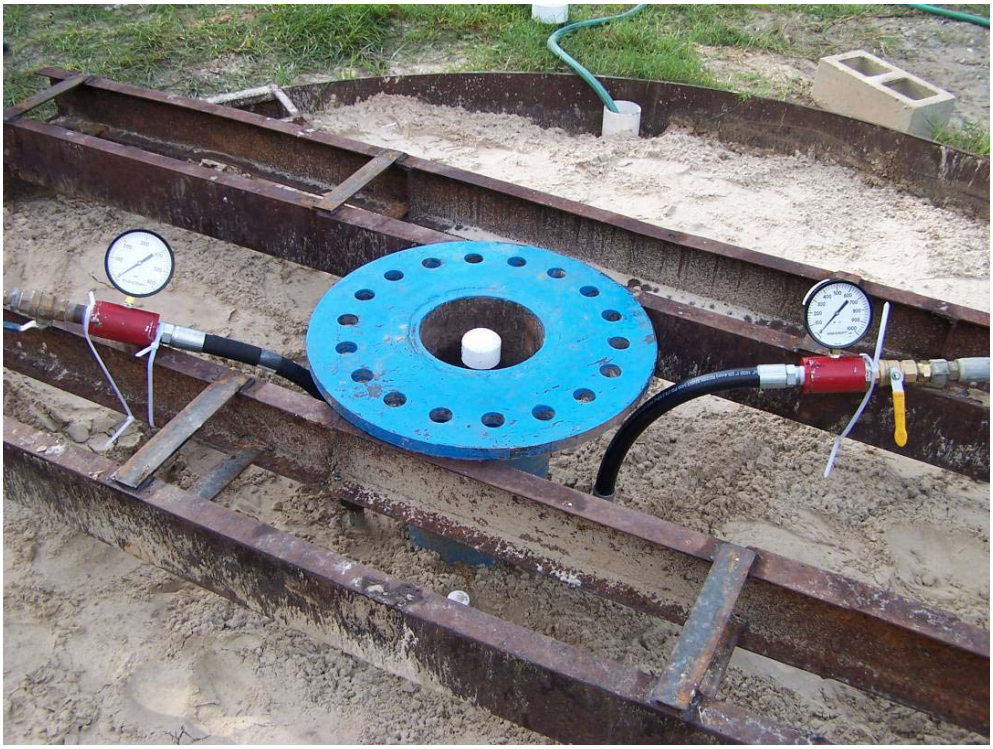

Figure 6.16 1000 psi gages to monitor inlet and outlet grout pressures.

Grouting of the pile commenced first with the top membrane (Figure 6.16). After placement of approximately 200 gallons of grout, the pressures at inlet and exit were approximately 70 and 60 psi, respectively. At this time, the ground surface began exhibiting a radial cracking pattern around the pile (Figure 6.17) to a distance of approximately 4′. Also at this time, the fluid grout began to flow upward through the ground surface near the pile. Grouting was ceased, and the grout delivery lines were flushed with water (Figure 6.18). Subsequently, the top 1 1/2′ of soil was excavated and the top of the pile was exposed revealing a tear in the membrane (Figure 6.19). It was decided to test if the tear could be repaired with fast setting cement (Figure 6.19). However, after pumping only 60 gallons of grout, leakage of grout to the surface was again observed. At this time, it was decided to stop grouting the top membrane, flush the system and re-grout the top system later after the grout had time to setup.

Figure 6.17 Radial cracking of the ground surface during grouting.

The grouting of the lower system began at a pressure of 80 psi for 100 gallons and gradually increased to120 psi (return gage Figure 6.16) at 200 gallons. After grouting 200 gallons, the pressures began to build up: 200 psi at 300 gallons and 300 psi at 350 gallons. At approximately 400 gallons, the grout pressures of 400 psi were observed (Figure 6.20). At this time, grout flow volumes began to diminish, and at approximately 450 gallons, the pressure gage spiked to the maximum gauge measurement and grout flow ceased.

Figure 6.18 Flushing of the top grout delivery system with water.

Figure 6.19 Tear in top membrane and repair with fast setting cement.

Shown in Figure 6.21 are the measured lateral soil pressures within the test chamber at a depth of 15′ and approximately 4′ away from the grout pile. Evident from the plot there occurred two major spikes in the stress measurements. The first was due to the initiation of the bottom grouting. At approximately 30 minutes into the bottom grouting it was noticed no grout flow was occurring, and a reduction of pressure was taking place (Figure 6.21). An examination of the grout pump revealed that a malfunction of the grout feed to the pump.

Figure 6.20 Grout pressure in bottom membrane at 400 gallons of grout.

The pumping was stopped, and the pump was repaired and grouting was subsequently reinitiated.

Also shown in Figure 6.21 was a 37-hour delay in measurements and another three-hour measurement. The latter is attributed to the regrouting of the top grout system after two days. The two other measurements (two weeks and one month later) represent long-term stress measurements.

A number of important observations may be made from Figure 6.21. First, the circumferential radial stresses (i.e., N, S, E, and W) were more uniform and larger than the 1st generation jet-grout pile measurements (Figure 4.28). The latter suggests that the expansion of the lower grout bulb was much more uniform or symmetrical and larger. Also of interest is the magnitude of peak horizontal stress change, i.e., $\Delta\sigma_h = 35$ psi, when added to the insitu horizontal stress (approximately 5 psi, $K_o \cong 0.44$) gives 40 psi which is equal to the passive stress state or with Kp = 3.53 times the minor principal stress equal to the vertical stress, σ_v, or 11.4 psi (for $\gamma = 110$ pcf). Evident is the fact that the horizontal stress near the grout pile must be much higher to agree with the measured grout pressures. The latter suggest that both the vertical and circumferential (i.e., hoop) stresses must be higher near the grout-pile as well, in order for them to satisfy the Mohr-Columb strength criteria. A further discussion of the stresses, especially values for design are presented in Chapter 7.

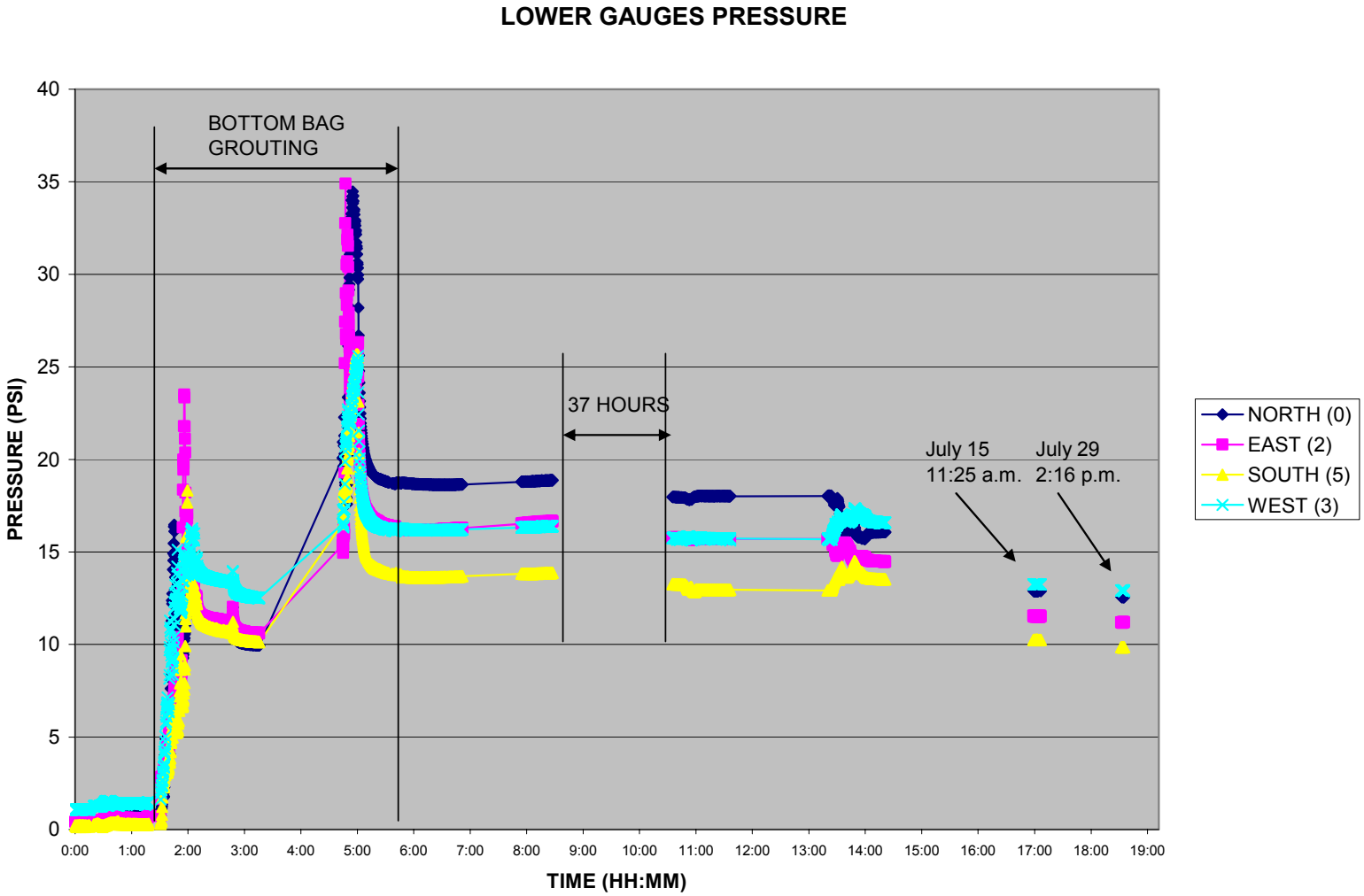

Figure 6.21 Measured horizontal stresses in test chamber at approximately 15′ depth.

Presented in Figure 6.22 are recorded horizontal stress changes at a depth of 6′ during the grouting process (top and bottom) as well as long-term. The first peak is associated with the pumping of 200 gallons into the top membrane whereupon the membrane developed a leak, a repair was attempted, more grout was pumped and leakage re-emerged and grouting of the top system stopped. Subsequently, the grouting of the lower membrane occurred and the changes in soil stresses at 6′ depth are as shown in Figure 6.22.

After grouting the lower system, the top bag was grouted again after 37 hours. Shown in the figure are the lateral stresses near the wall of the chamber during top membrane grouting. The process involved pumping approximately 125 gallons with grout gages measuring approximately 150 psi, and then pumping the final 150 gallons of grout with the grout gages measuring a gradual increase in pressure until 300 psi. It was decided to stop pumping at this point, since a total of approximately 450 gallons of grout had been placed around the top half of the pile, which met the design grout volume.

A comparison of the stresses at the upper level for the 1st generation jet-grouted pile (Figure 4.27) and the 2nd generation pile (Figure 6.22), showed that an increase of a factor of 2 to 3 in lateral stress and a more uniform stress around the perimeter of the 2nd generation pile. The higher pressure around the 2nd generation pile was the considerably larger grout volume around the pile (450 gallons/segment) than that of the 1st generation pile (100 gallons/segment). The significance of the latter will be evident in load response of both piles, which will be discussed next.

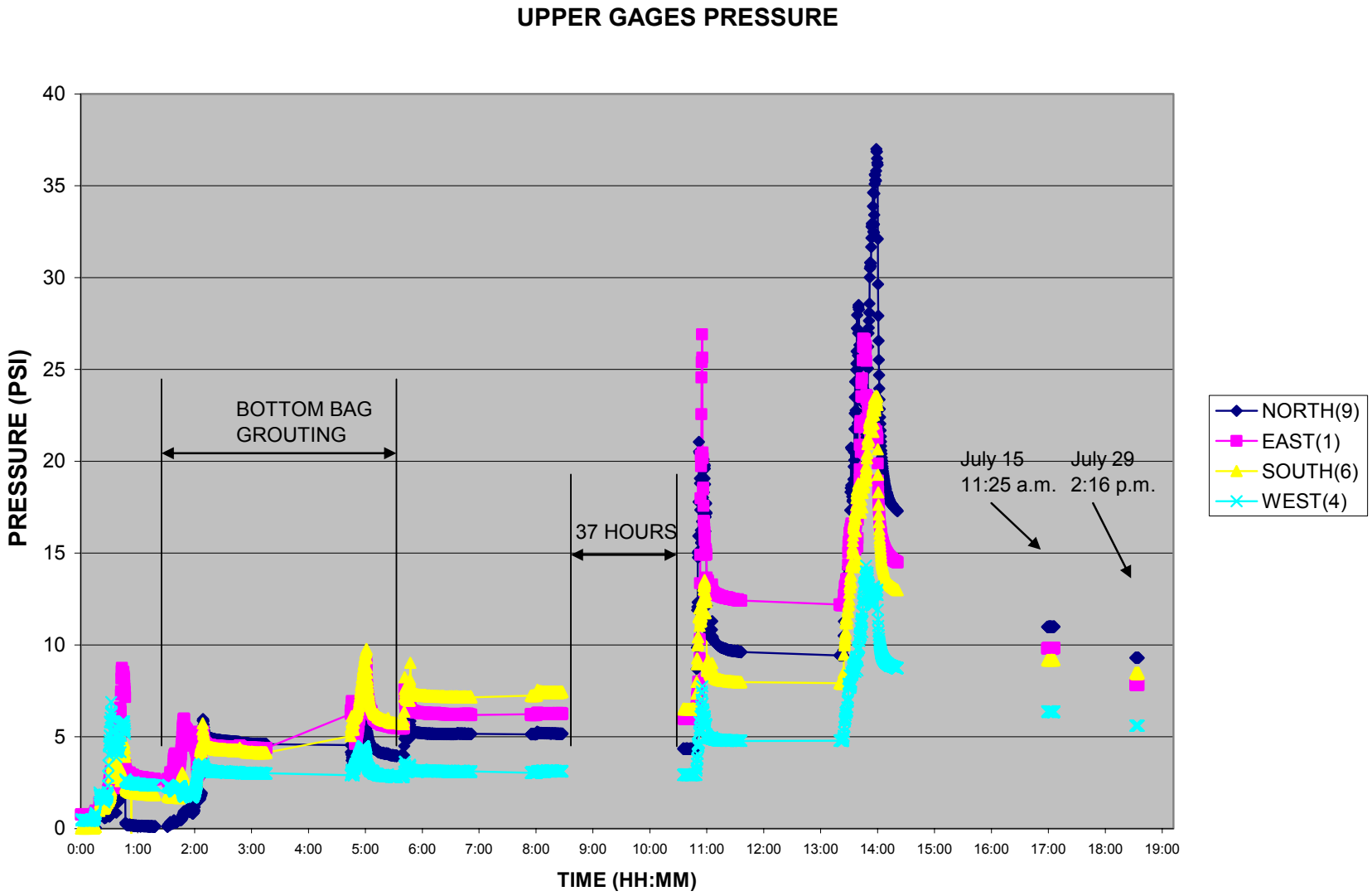

Figure 6.22 Measured horizontal stresses in test chamber at approximately 6′ depth.

6.5 Torque Test

Having jetted the 16″×16″×20′ precast composite pile into the ground to a depth of 20.5′ and grouting it to an effective diameter of 36″, a torque test was subsequently performed to measure its torsional soil-pile resistance. For this phase of testing, the tip of the pile was not grouted, so the torsional resistance could only be attributed to side resistance of the pile.

To perform the torque test, a mast arm (Figure 6.23) was constructed from a 12.5′ steel box section welded to a 12″ diameter × 1″ thick steel pipe. Welded to the bottom of the steel pipe was a 24″ diameter × 1″ thick steel plate. This mast arm assembly was bolted to the steel plate at the top of the pile using 18 grade 8 bolts.

Also shown in Figure 6.23 is a shear reinforced W section attached to a 1″ steel plate that was bolted to the 1 1/4″ Dywidag bars projecting from the east reaction shaft. The reaction was designed to carry 50 kips of shear (Figure 6.2) or provide 550 ft-kips of torque on the pile for 11′ torque arm. Due to actual placement of the jet-grout pile, the torque arm was only 10.5′.

Figure 6.23 Mast arm attached to 2nd generation jet-grout pile.

To provide torque to the mast arm a 50 kip hydraulic ram with a stroke of 36″ was required (15° of rotation). Unfortunately, most small hydraulic rams only have 12″ to 18″ of stroke. Consequently, it was decided to bolt two hydraulic rams together at their bases for testing (Figure 6.24). Also, of concern was the type of connection between the torque or mast arm with the hydraulic rams. Since it was not known or assured that the arm would simply rotated around the pile, a pin type connection (Figure 6.24) was used on both ends of the rams. Figure 6.25 shows the placement of rams for the torque test. The 4″ × 4″ wood members were used only to support the rams during the unloading.

Figure 6.24 Hydraulic rams used for torque testing.

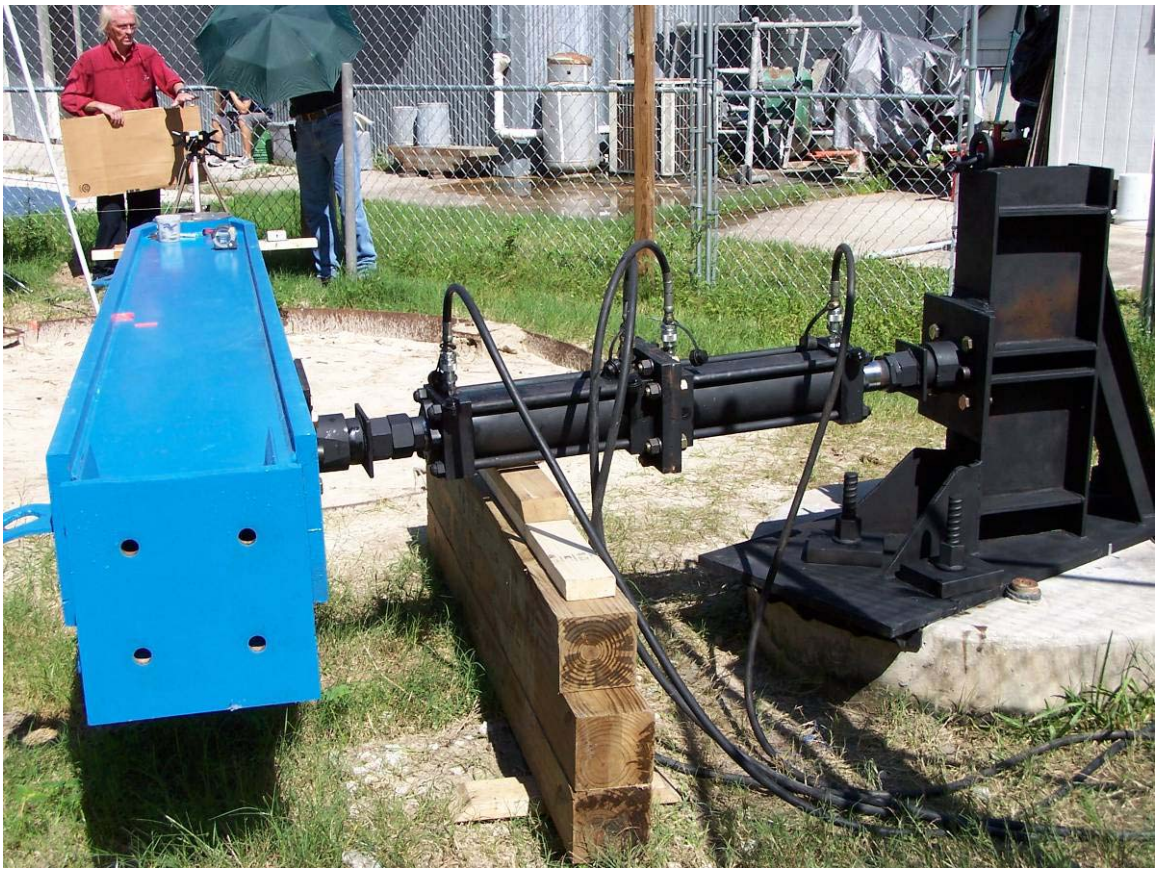

Figure 6.25 Torque mast arm and hydraulic loading rams.

Prior to the load test, the hydraulic rams (Figure 6.25) were placed within a reaction frame and a calibration to establish the relationships between hydraulic pressure and force. A number of different pressure gages and load cells were used in the calibration.

To monitor the translation and rotation of the jet-grouted pile, multiple levels of potentiometers were attached to the pile and stationary points (Figure 6.26). For instance, attached to the torque plates (Figure 6.23) were four aluminum tabs from which translation and rotation at one elevation may be ascertained. Using similar potentiometers at a second elevation, then rotation of the pile head in a cross-sectional view can be established.

Figure 6.26 Instrumentation to monitor translation and rotation.

Approximately two months after the jetting and grouting of the pile, the torque test was performed. Shown in Figure 6.27 is the applied torque versus the measured rotation from two separate systems. Using an average grouted shaft diameter of 36″, for a length of 20′, an average shearing resistance of 1.5 ksf between soil and pile is developed for 450 ft-kips of torque. Figure 6.28 shows radial cracking within the soil suggesting excellent shear transfer between the pile and the soil. Further discussion of torsional shear design is provided in Chapter 7.

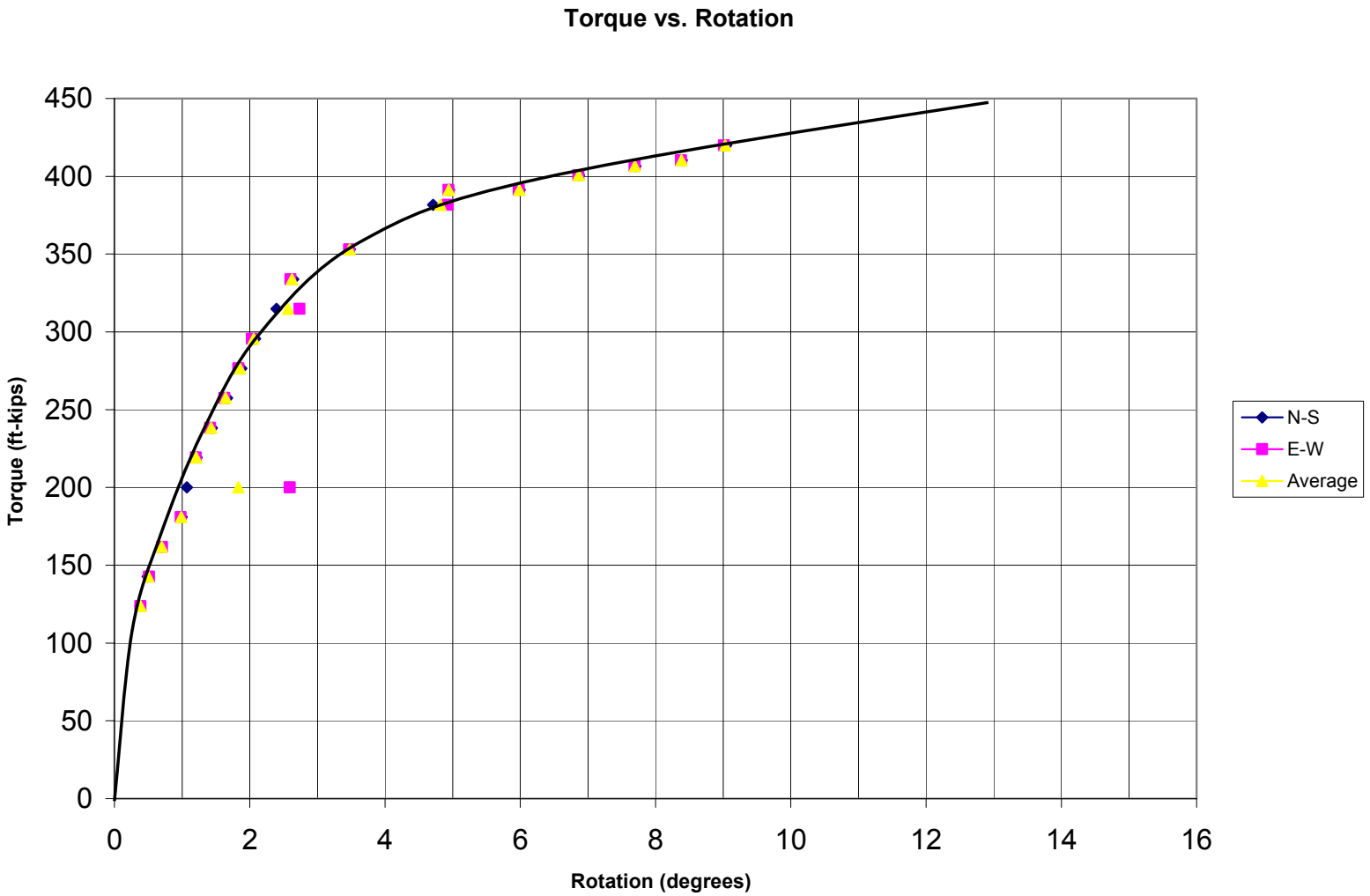

Figure 6.27 Torque vs. rotation of 2nd generation jet-grout pile.

Figure 6.28 Radial shear cracking in soil during torque test.

6.6 Tip Grouting of 16″ × 16″ × 20′ Pile and Top-Down Axial Load Testing

After successful completion of the torque test, it was decided to grout the tip of the pile and perform a top down axial compression test. Grouting the tip of the pile would give an indication of the axial shear resistance of the pile in tension (i.e., uplift) as well as an estimate of the total top-down capacity of the pile, if the reaction drilled shafts were insufficient to mobilize total resistance.

Approximately three weeks after the torque test, tip of the pile was grouted. The tip grout mix design was the same as the side membranes with the exception that the water cement ratio was reduced to 0.45. Shown in Figure 6.29 is measured grout tip pressure vs. time as well as the upward movement of the pile vs. time. Evident from the figure that at the 15 minute mark the grout pressure fell off. After a quick check of lines, valves, etc., it was found that no grout was being pumped to the pile due to hose cavitation from pump blockage in the holding tank. After 15 minutes to repair, the grouting continued with pressure increase vs. pumped grout volume. At approximately the 67 minute mark, the top of the pile began to move with a pressure of 500 psi. After 75 minutes, the grout pressure was 650 psi, the top of the pile had moved 0.075 inches upward, and 230 gallons of grout had been pumped to the pile tip. At this time grouting stopped due to a shortage of fly ash. It was decided to switch to just cement/water mix and continue grouting. However, when re-grouting commenced, the grout pressure spiked at 1000 psi, and the top of the center steel 2″ø grout pipe failed at the 2″ø PVC pipe connection (12″ into the precast pile), and thus ending the grouting process.

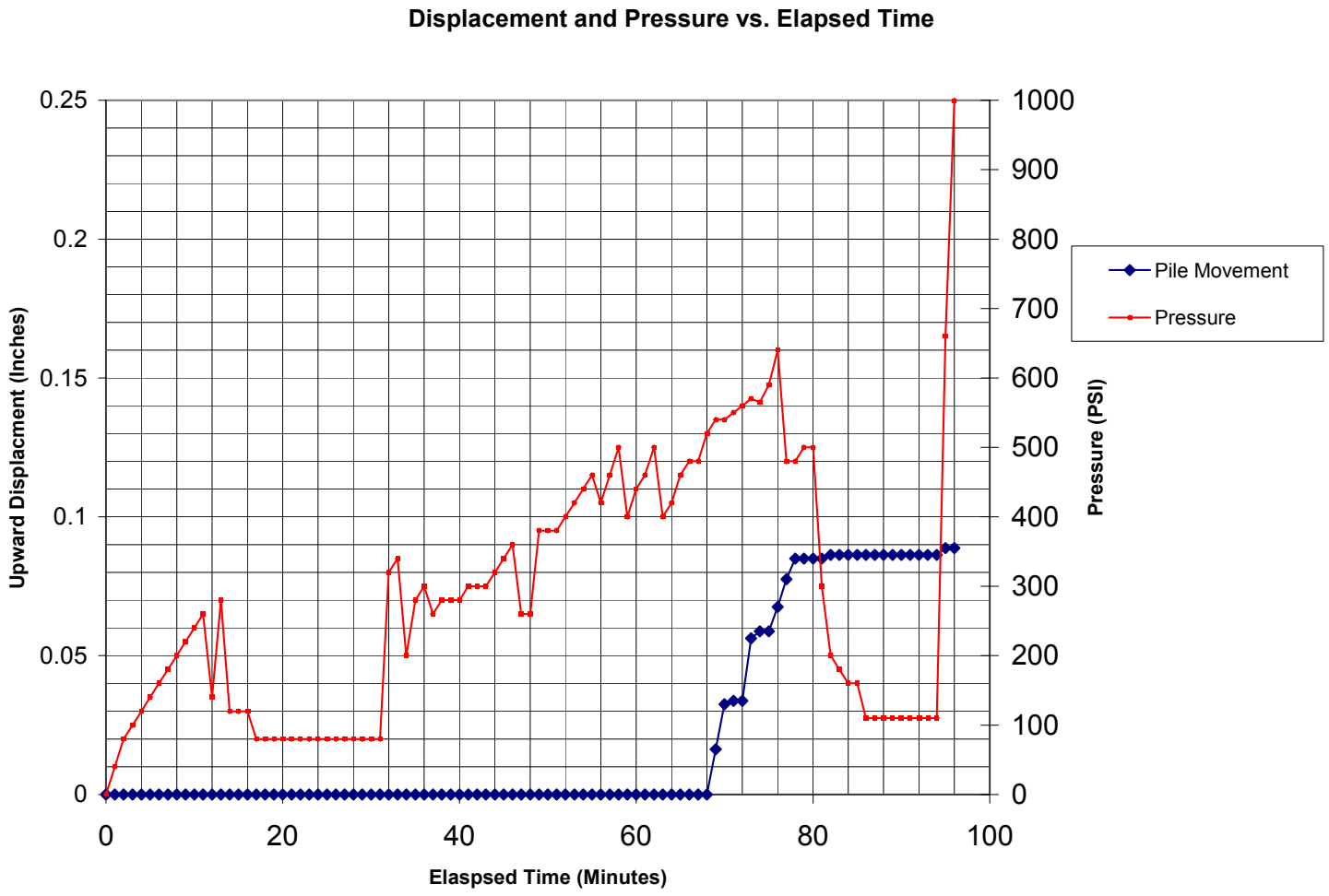

Figure 6.29 Tip grout pressure and upward movement of pile with time.

Assuming that axial skin friction is usually mobilized within 0.1 to 0.2 inches, then Figure 6.29 suggests that the ultimate axial skin friction of pile should be equal to the tip pressure of 650 psi times an effective tip area. For 230 gallons (30.7 ft^3) a grout cube of 3′ × 3′ × 3′ may exist at the pile tip. The expected minimum tip area should be the precast tip area (i.e., 256 in^2 = 16″ × 16″); however, grout generally assumes a circular shape. The maximum diagonal distance on the precast pile was 22.6″ (Area = 402 in^2). Consequently assuming an average area between square and circular (i.e., A = 329 in^2) and a pressure of 650 psi, then an uplift force 213.8 kips may have developed. The latter only represents the skin friction alongside the pile. One may conservatively assume that the uplift force is also the minimum tip resistance, consequently, the expected axial downward capacity should be twice this value or 428 kips.

Approximately three weeks after the tip grouting, the top-down test equipment was setup (Figure 6.30). Besides measuring load, vertical deformation of the pile head was monitored. Load was applied in 10 kip increments and held for approximately 15 minutes. The test was carried out until 300,000 lbs (300 kips) was applied and then unloading was initiated. The load did not exceed 300 kips even though axial deformation was less than 0.1″ because the 1″ thick steel plates (Figure 6.30) on top of the reaction beam (connect the Dywidag bars) began to bend. In addition, the reaction shafts could only safely provide 400 kips of axial uplift resistance without the potential of vertical movement.

Shown in Figure 6.31 is the resulting load vs. deformation of the 16″× 16″×20′ jet-grout pile. Evident from the figure, very little permanent deformation (less than 0.035″) occurred in the pile test, suggesting that the full capacity of pile may be well above 400 kips.

Figure 6.30 Setting up the top-down load test for 2nd generation jet-grout pile.

The latter is further supported by looking at the shape of the load vs. settlement response of the smaller scale test results given in Figure 5.17. Also shown in Figure 6.31 for comparison purposes is axial load vs. deformation response of an 18″ drilled shaft from FB-DEEP. Evident the axial capacity of the jet-grout pile is at least three times the drilled shaft. Further comparison of the capacity of the 2nd generation jet-grouted pile (Figure 6.31, pile 20′ long) with the 1st generation jet-grout pile (Figure 4.37, pile 27′ long), show 300 kips at 0.1″ vs. 100 kips at 0.1″, which showed an improvement of three times.

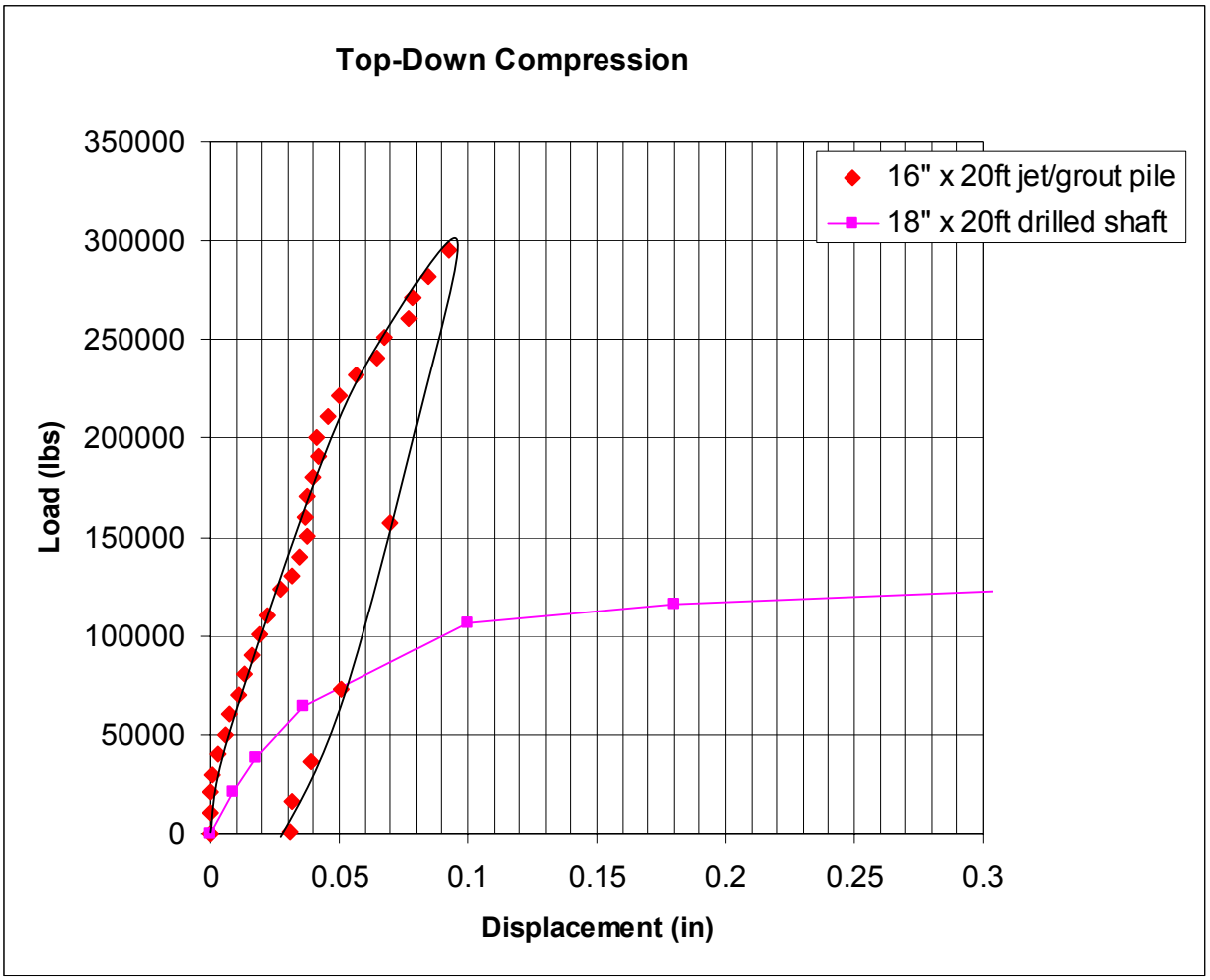

Figure 6.31 Axial load vs. displacement for 2nd generation jet-grout pile.

Also of interest were the measured horizontal stresses in the test chamber during the axial load test (Figure 6.32); the lateral stress which is initially constant, diminishes with increasing axial load. However, when the load is removed it once again increases. It is believed that the decrease in lateral stress is due to rotation of principal planes and the development of shear on vertical planes. A discussion of this is given in Chapter 7 on the design of the jet-grout pile.

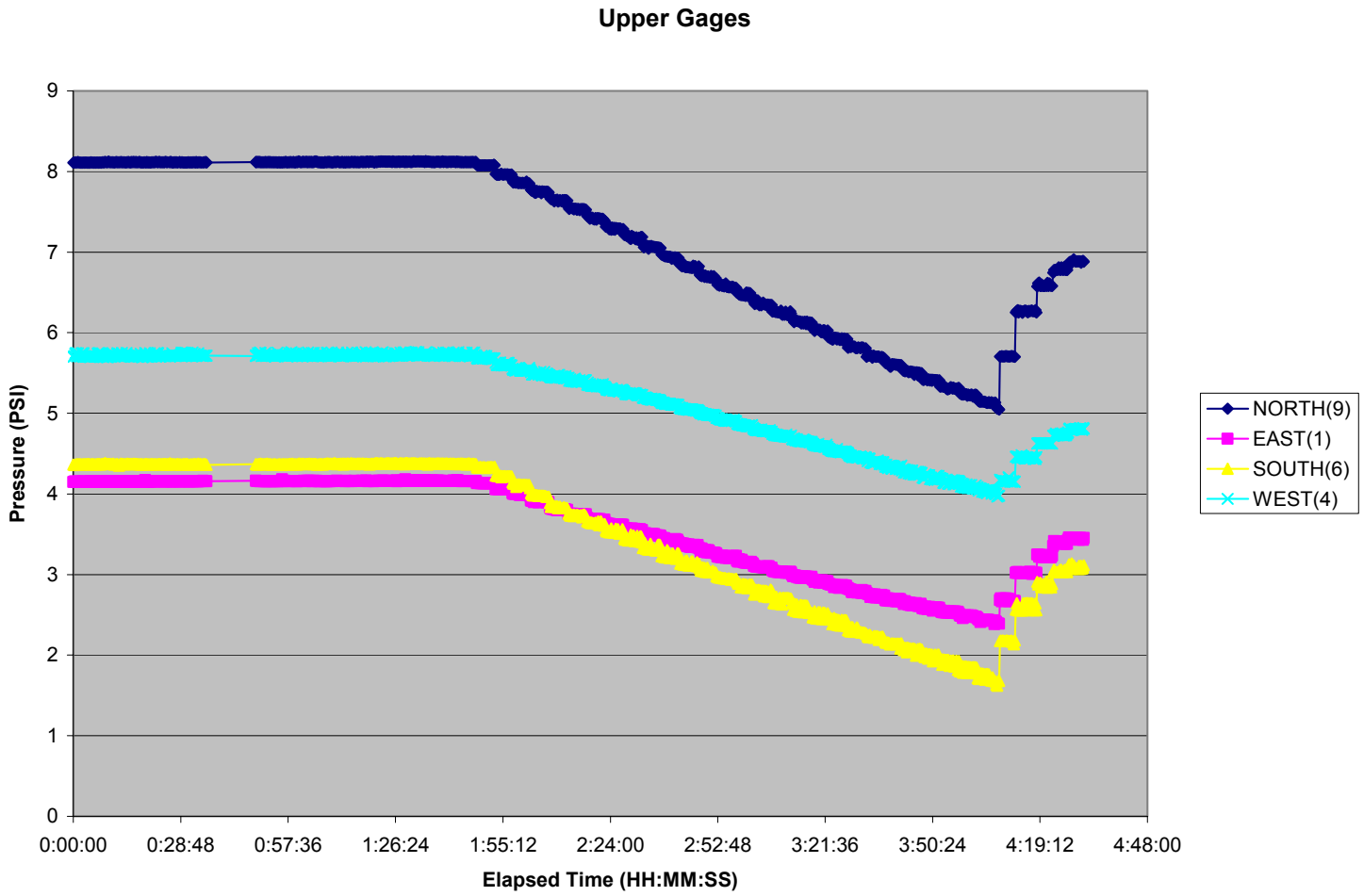

Figure 6.32 Change in lateral soil stress at 6′ depth due to axial top-down testing.

CHAPTER 7
DESIGN OF JET-GROUTED PILES

7.1 Estimation of Jet-Grouted Pile Grouting Pressures

In Geotechnical Engineering, the process of grouting a pile insitu falls within the study of cavity expansion theory. Research by Yu & Houlsby (1991), Salgado & Prezzi (2007) and Salgado & Randolph (2001) have contributed significantly to our understanding of soil stresses, and properties in the vicinity of an expanding cavity. For instance, shown in Figure 7.1 is an estimate of the change in soil properties and stresses as suggested by Salgado and Prezzi (2007). Away from the disturbance (r>A), the soil properties and stresses are typical at rest values; however, the nearer the cavity (R<r<a), the radial stresses increase quadratically, and the soil strength (ø) and shear modulus (G) decrease. The radial stress at the wall of the cavity is the maximum and is generally referred to as the limit pressure, as suggested by Menard in Pressuremeter Testing. Of interest for this work is the limit radial

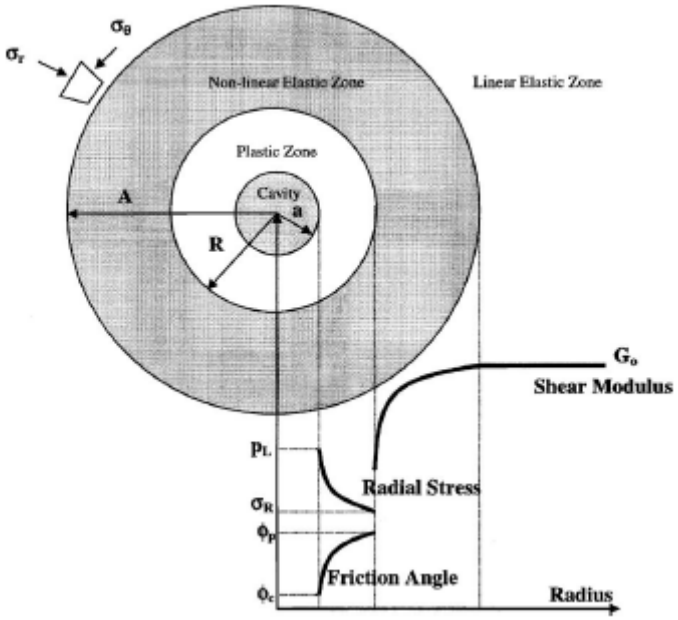

Figure 7.1 Change in stresses and soil properties with radius (Salgado, 2007).

stress (i.e., expected grout pressures), the circumferential (hoop) and the vertical stresses at the boundary of the cavity (i.e., grout membrane). For instance knowing the limit pressure allows one to identify the expected pump pressures needed for pile grouting. Similarly knowing all the normal stresses (i.e., radial, vertical and hoop) allows the assessment of expected axial and torsional capacity of the jet-grouted pile.

Recent work by Salgado et al. (2001) using stress-equilibrium, strength and flow assumptions have resulted in predictions of cylindrical cavity expansion limit pressures, P_L , as a function of soil strength, relative density (D_r), and depth or initial lateral insitu stress for sands (Figure 7.2). The critical state friction angle (øc) represent large strain strength (e.g., after dilation for dense sands) and generally is 0 to 5 degrees smaller than ϕ depending on density.

If one wanted to compute the limit pressure at 15′ deep(e.g., 2nd level in jet-grouted pile, Chapter 6), one would multiply the total soil unit weight of 110 pcf by the depth and by the coefficient of lateral earth pressure at rest (K_o = 0.44, for ø =34°, Chapter 6), for a hori-zontal stress of 34.7 kPa (726 psf), which when used in Figure 7.2 for D_r = 40% suggests a range of pL from 1500 kPa (218 psi) to 1700 kPa (247 psi) for øc of 30° and 33°, respectively . The actual measured grout pressure in the bottom membrane varied between 300 and 400 psi.

In the case of spherical cavity expansion, (Figure 7.3 for a typical sand) the initial mean stress is the sum of vertical stress and twice the lateral stress divided by three.

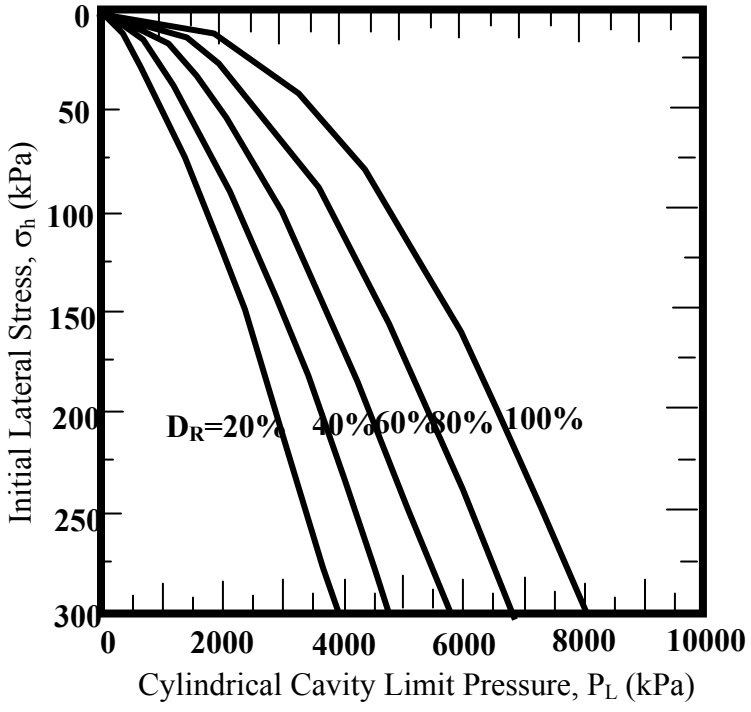

(a)

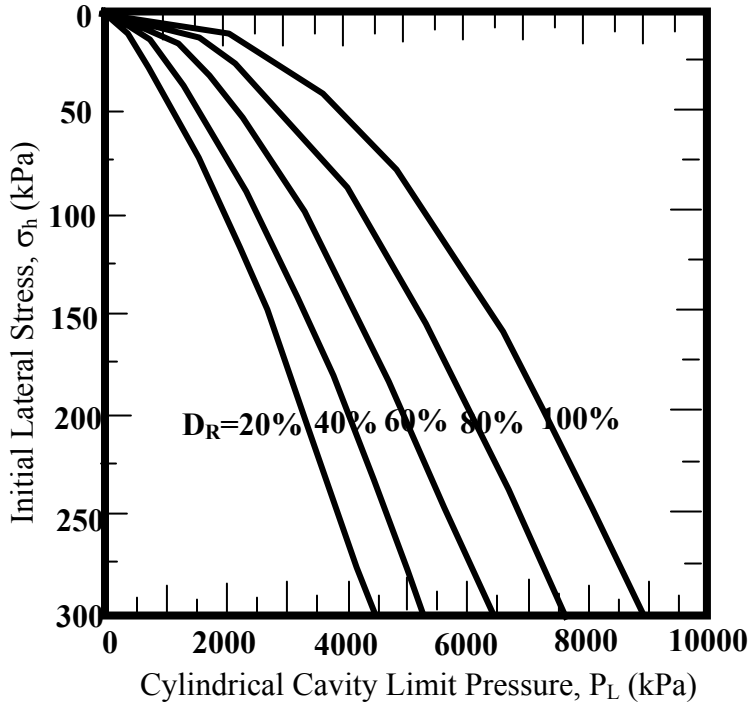

(b)

Figure 7.2 Cylindrical limit pressure as function of lateral stress, D_r, and øc (a) øc = 30°, (b) øc = 33° (Salgado, 2001).

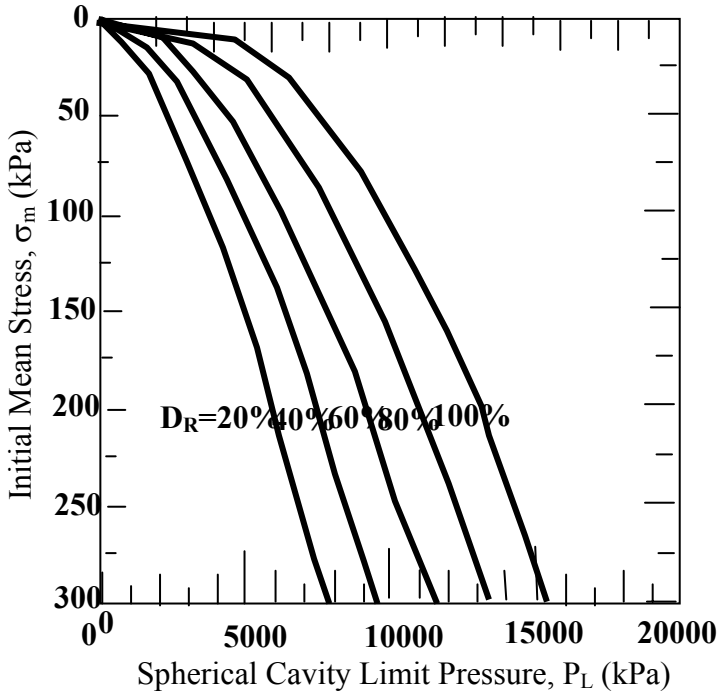

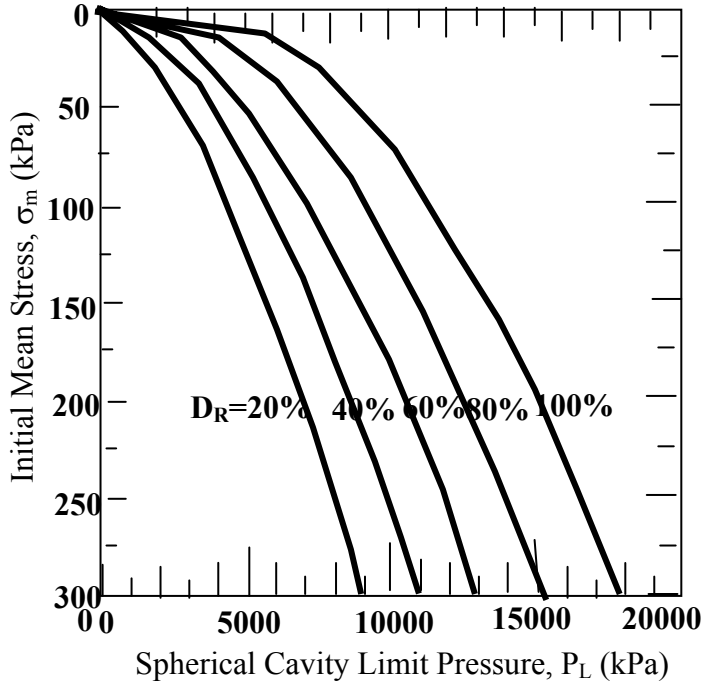

(b)

Figure 7.3 Spherical limit pressure as function of lateral stress, D_r, and Øc (a) Øc = 30°, (b) Øc = 33° (Salgado 2001).

For the case of 20′ pile (Chapter 6) jet-grouted pile, the mean stress at the pile tip was approximately 1400 psf (66 kPa) which gives a spherical limit pressure of between 4000 kpa and 5000 kPa or 580 psi to 725 psi for respective øc of 30° and 33°. The actual maximum grout pressure measured at the bottom of the jet grouted pile was 650 psi (Figure 6.29).

Evident from a comparison of measured membrane pressures, as well as grout pile-tip pressures, Salgado (2001) provides reasonable estimates of both cylindrical & spherical limit pressures that may be expected for variable length piles, soil densities and angle of internal friction in typical sand installations.

In the case of other soils or a mixture of soils it is proposed that Pressuremeter tests (PMT) be preformed at various depths on the site prior to the design and construction of the jet-grouted piles. Specific output from the PMT is the limit pressure, P_L. For instance shown in Figure 7.4 are PMT results for the silty-sand found in the test chamber at a depth of 6′, which was performed by SMO personnel. The limit pressure of 900 kpa (130 psi) compares very favorably to the 827 kpa (120 psi) measured when grouting the lower membrane (120 psi at 6′) for the 8′ length piles.

7.2 Estimation of Axial and Torsional Capacities of Jet-Grouted Piles

Besides estimating the required grout pressures required to form a jet-grouted pile, the design must assess the expected axial capacity of the pile. Of major interest is the expected skin friction on the pile, which may be verified in the construction process through tip grouting that is one of the major benefits of the pile. Similarly, it is expected that the total capacity of the pile will be at least double the skin friction or that the tip grout is capable of mobilizing the full side resistance of the pile.

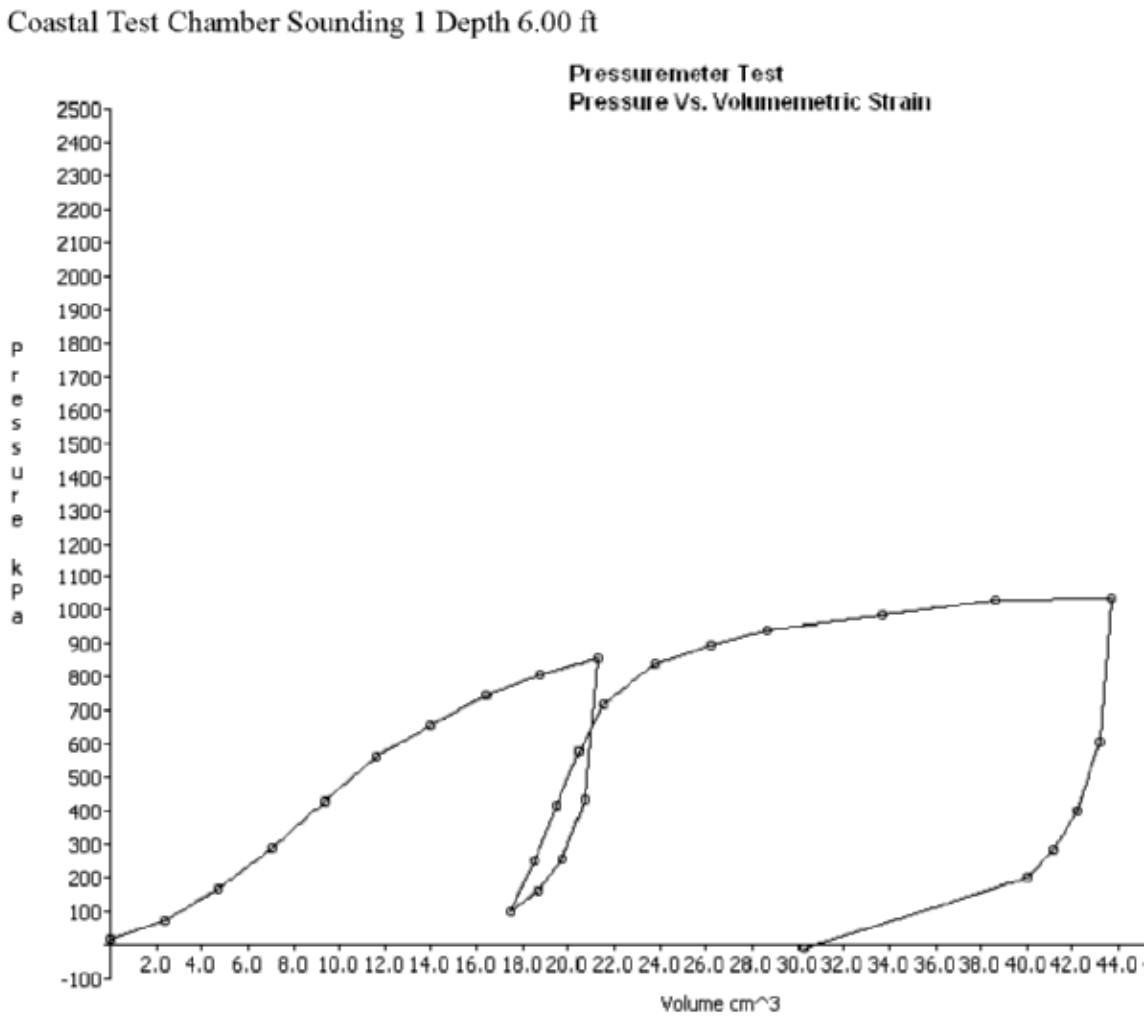

Figure 7.4 Pressuremeter results at 6′ for silty-sand in test chamber (SMO).

Consequently to estimate the expected side resistance of a jet-grouted pile, the expected normal stresses (i.e., radial, hoop, and vertical) adjacent to the pile need to be known. Yu and Houlsby (1991) have estimated the changes in the normal stresses around an expanding cylindrical cavity as shown in Figure 7.5.

The variable ***a*** represents the radius of the cavity (Figure 7.1) and ***r*** represents the radius outward from the cavity. The ratio ***a/r*** equal to one represents the stress change at wall of the cavity and the ratio of 0.1 represents the stress change 10 radii from the cavity wall. P_o (y axis) is used to normalize the results and represents the insitu stress prior to cavity expansion.

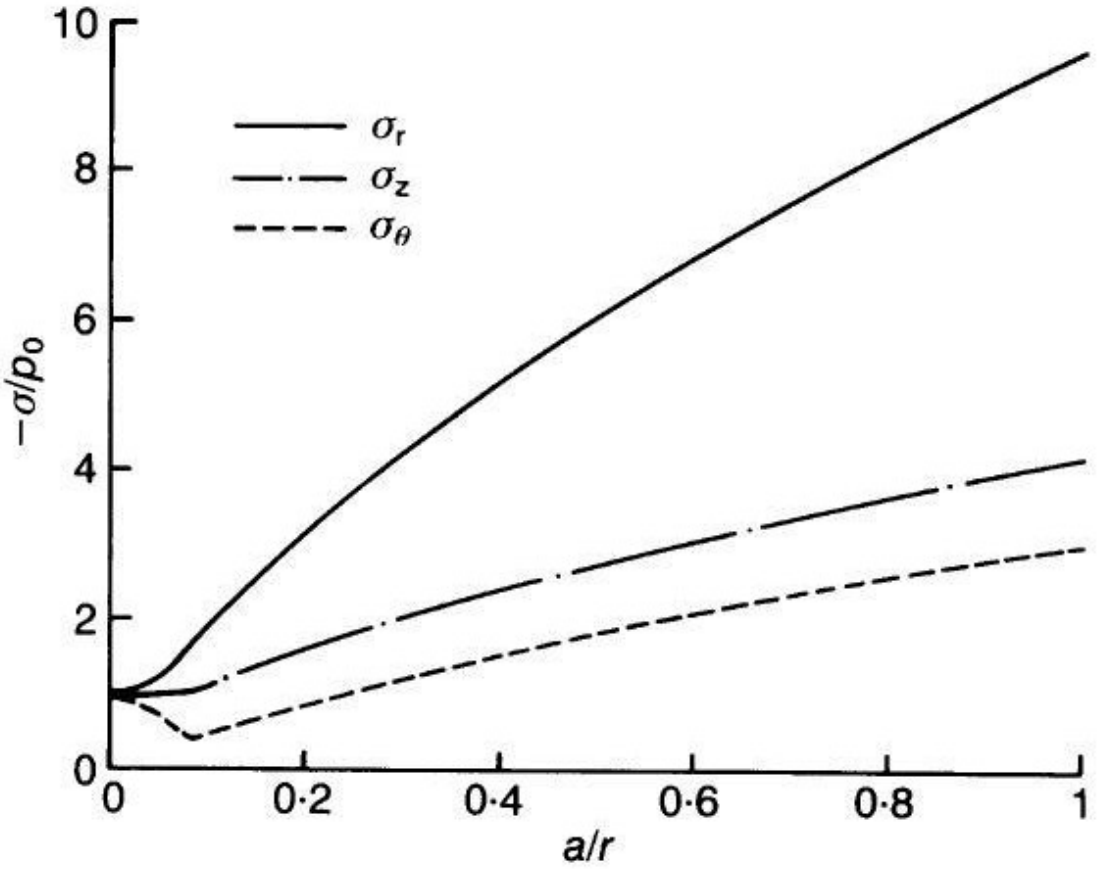

Figure 7.5 Changes in normal stresses around cylindrical cavity (Yu & Houlsby, 1991).

Evident from Figure 7.5, the radial stress, σ_r, is the major principal stress, and the minor principal stress, σ_θ (circumferential or hoop) is close to the intermediate principal stress, i.e., vertical (σ_z) stress. All of the normal stresses at the cavity wall (***a/r*** =1) have increased over the insitu stress (3 to 9 times). The difference between the minor/intermediate principal stresses and the major principal stress is controlled through the Mohr-Columb strength of the soil, i.e., Mohr circle of the major and minor principal stresses must be smaller than the strength envelope controlled by the sand's critical state friction angle ϕ_c, as shown in Figure 7.6.

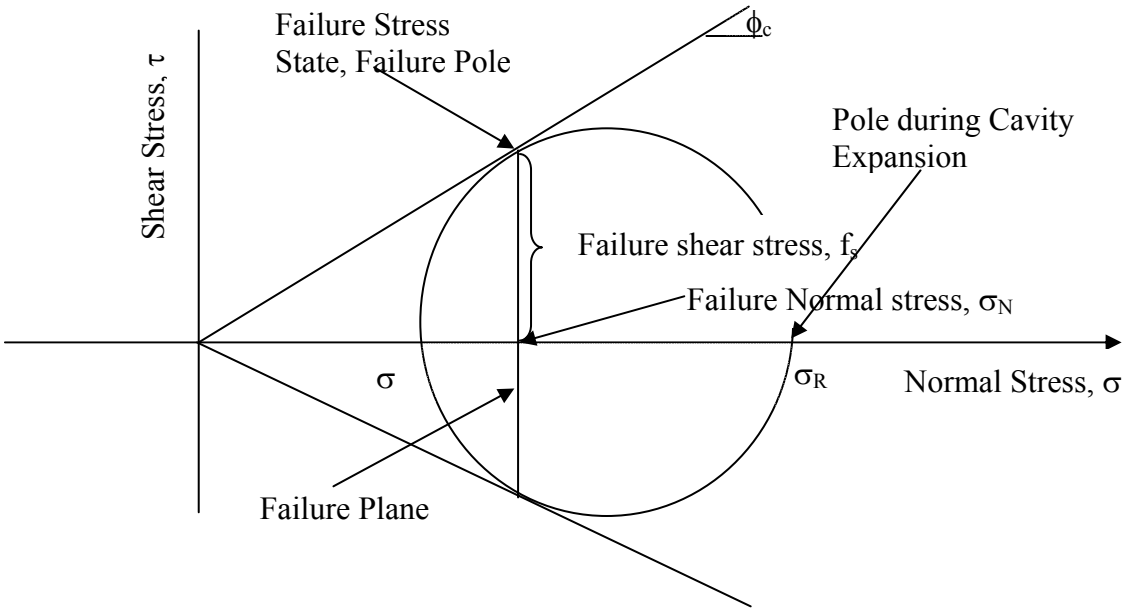

Figure 7.6 Normal stresses.

Based on the stresses, as suggested by Yu and Houlsby (1991), the pole of the Mohr circle during cavity expansion should reside on the far right of the circle. However, in the case of axial loading (Figure 7.7) the horizontal normal stress (σ_N) equal to σ_R initially (Figures 7.5 and 7.6) diminishes as the pole rotates around the Mohr circle until the failure plane is reached along with the failure stress state (Figure 7.6). At this point, the failure

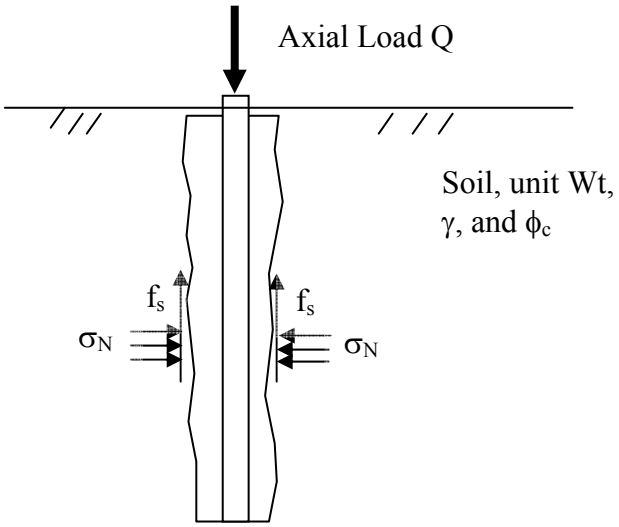

Figure 7.7 Normal and shear stress under axial load test.

plane is vertical, as shown in Figure 7.6 and the failure skin friction (fs, Figures 7.6 and 7.7) is fully developed. Note, for this development, it is assumed that there is no change in vertical stress, i.e., load transfer occurs only through shear (fs). Some validation of the reduction in horizontal normal stress is given in Figure 6.23 which shows the horizontal normal stress 1′ from the wall of the test chamber. Evident from the figure there is a significant reduction during the loading phase and a slight recovery during the unloading phase of the test.

Using the failure Mohr-Circle given in Figure 7.6, the value of the failure unit skin friction, fs, may be assessed in terms of critical friction angle, ϕ_c, and effective vertical stress as,

$$f_s = \sigma_{vg}\left[\frac{\sin\phi_c}{(1-\sin\phi_c)}\right]\sin(90-\phi_c) \qquad \text{Eq. (7.1)}$$

Evident from Eq. 7.1 the unit skin friction, fs, is a function of the critical state friction angle, ϕ_c, and the vertical effective stress at the wall of jet-grout pile, σ_{vg} which accordingly to Figure 7.5, may be 1 to 3 times its at rest condition (i.e., $\gamma \cdot Z$). Based on the small and full scale testing, Eq. 7.2 and Figure 7.8 gives an estimate of the vertical effective stress at the wall of the grouted pile based on depth (h), buoyant weight (γ') and grout vertical stress increase coefficient, K_g ,

$$\sigma'_{vg} = K_g\sigma'_{v0} = K_g\ \gamma'\ h \qquad \text{Eq. (7.2)}$$

The grout vertical stress increase coefficient, K_g (Figure 7.8) was estimated from pile test results at 5 and 10 ft depths, whereas the values at 20 to 25 ft were estimated from Figure 7.2. It should be noted, that the value of fs given in Eq. 7.1 could have also been developed in terms of the radial stress (Figure 7.6); however, the designer would still have to estimate the radial stress (e.g., Figure 7.2 or Pressuremeter Testing). Because the vertical (σ_{vg}) and hoop stresses (σ_θ) are similar (Figure 7.5), the torsional shear stress resistance, fs, give by Eq. 7.1 should be similar to its vertical value.

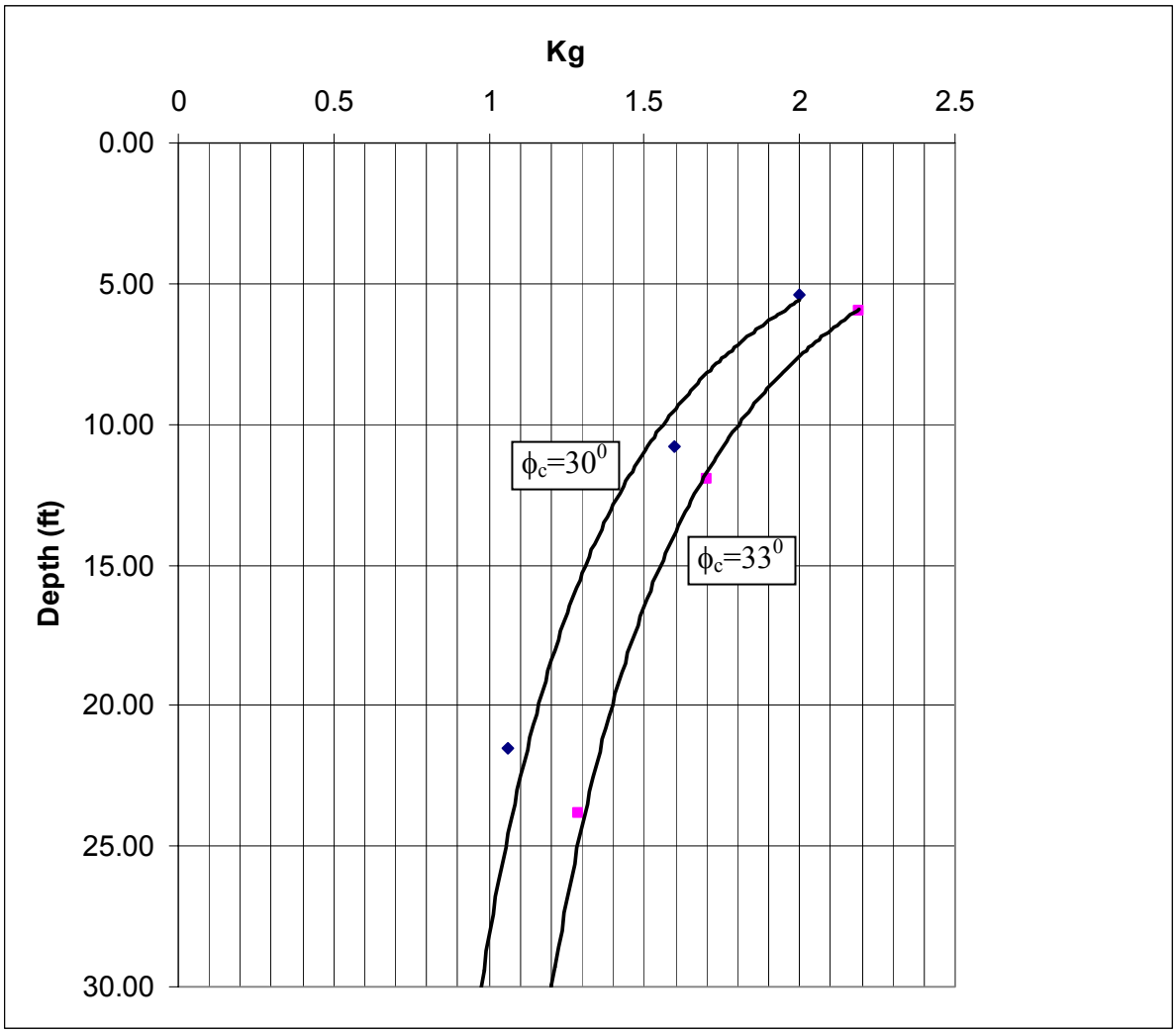

Figure 7.8 Estimate of grout vertical stress coefficient, K_g.

Using Eq. 7.1 and Figure 7.8 for K_g, the unit skin frictions for the small 6″×6″×8′ and 8″×8″ × 8′ jet-grouted piles were computed as shown in Table 7.1. Both of these piles were embedded approximately 9′ in the ground with an average at rest vertical stress of 495 psf (γ: 110 pcf × 4.5 ft). Next using an angle of internal friction of 34^0 and a critical state failure angle, $\phi_c \sim 31^0$, a grout vertical stress coefficient, K_g of 2.15 (Figure 7.8) is obtained for a depth of 5 ft. Multiplying the at rest vertical effective stress, σ'_{vo} = 495 psf by K_g gives σ'_{vg} = 1064 psf, and Eq. 7.1 gives a values of fs of 922psf (0.922 ksf). Using a surface area of the grout membrane of 33 ft^2 (6″) and 46 ft^2 (8″), gives skin frictions, Qs, of 33 kips (6″)

and 46 kips (8″) piles. Both of the latter predictions compare very favorably with the estimated skin friction from DeBeer Method (Figure 5.19) of 30 kips and 45 kips, respectively. If the end bearing is assumed to be equal to or greater than the side friction, than the total axial capacities of 66 kips (6″) and 92 kips (8″) would be obtained versus 65 kips (6″) and 110 kips (8″) from Figure 5.18.

Table 7.1 Estimated axial and torsional resistance of experimental test piles.

Pile Width (in)	H-Pile Length H (ft)	Initial Vertical Effective Stress σ'_{vo}(H/2) (psf)	K_g	Grouted Vertical Effective Stress σ'_{vg}(H/2) (psf)	ϕ_{cr} degree	fs Eq. 7.1 (ksf)	D_f Mem. Diam. (ft)	As Surf Area (ft^2)	Qs Side Resis. (kips)	Q_{torque} Torque Resis. (ft-kips)
6	9	495	2.15	1064.3	31	0.922	1.27	35.9	33.1	21.0
8	9	495	2.15	1064.3	31	0.922	1.77	50.0	46.1	40.7
16	20	1100.0	1.5	1650.0	31	1.42	3.0	188.5	267.7	401.5

In the case of the 16”× 16”× 20’ jet grouted pile (Table 7.1), the average at rest vertical stress, σ'_{vo}, is 1100 psf (H/2 × 110 pcf). Using the mid embedment depth (H/2) of 10 ft, Figure 7.8 gives a grout vertical stress coefficient, K_g of 1.5 for critical friction angle, $\phi_c = 31^0$. Multiplying K_g by the original insitu effective vertical stress, 1100 psf, at middle (H/2) of the pile gives a vertical effective stress of 1650 psf after grouting, and an expected unit skin friction, fs (Eq. 7.1) of 1.42 ksf. Multiplying the unit skin friction by the perimeter of the grout membrane gives a predicted side resistance of 267.7 kips. Unfortunately the top-down compression did not result in failure (Figure 6.31); however the torque load test did fail (Figure 6.27) at 420 ft-kips. Using the unit skin friction, fs =1.42 ksf, the torsional resistance may be computed as fs × π × D (diameter) × L (length) × R (radius) = 1.42 ksf × 3.14 × 3′× 20′ ×1.5′ = 401.5 ft-kips, which is within 5% of the measured 420 ft-kips. It should be noted

that the torsional test was performed prior to pile tip grouting (i.e., axial load testing) and torque resistance is due to side resistance alone.

For the case that the grouted membrane is not cylindrical or prismatic, e.g., spherically shaped, then the axial resistance of the grouted pile may be estimated from the cavity expansion pressures, as shown in Figure 7.9. For instance, in the case of the small scale 8′ piles, the measured grout pressures were 80 psi (5.7 tsf) and 120 psi (8.6 tsf) for the two grout membrane systems, respectively. Multiplying each of the grout pressures by the effective cross-sectional area of each membrane (Figure 7.8, i.e., cross-sectional area of D_F – cross-sectional area of D_i), which were 1.0 ft^2 (6″×6″ pile) and 2.0 ft^2 (8″×8″ pile) results in axial side resistances of 28.6 kips [(5.7tsf ×1ft^2 + 8.6tsf×1ft^2)×2 kip/ton] and 57.2 kips [(5.7tsf ×2ft^2 + 8.6tsf×2ft^2)×2 kip/ton], respectively, or a total resistance of 57.2 kips and 114.4 kips (for both skin and tip).

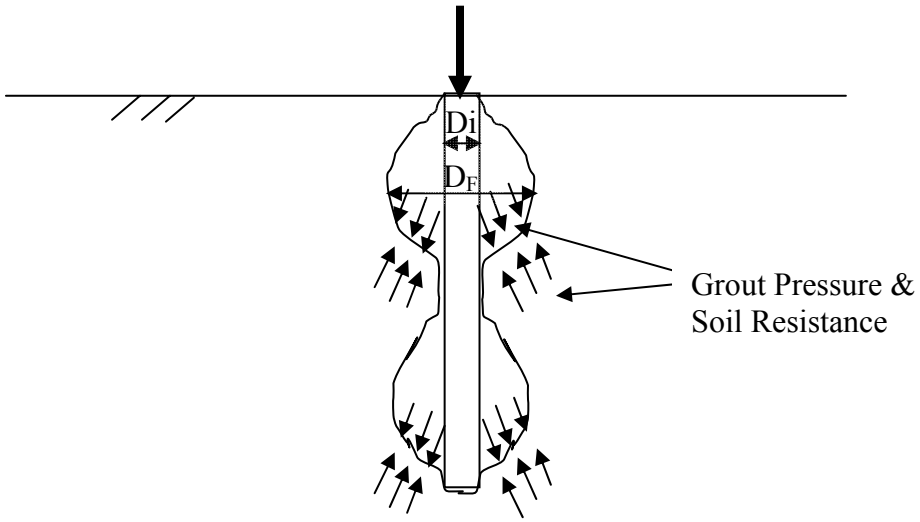

Figure 7.9 Barrel shaped membranes and soil resistance.

CHAPTER 8
SUMMARY AND CONCLUSIONS

A significant number of FDOT structures (e.g., bridges, signage, walls, etc.) are founded on deep foundations. In the past, the deep foundation of choice was a driven pile because of its high mobilized skin and tip resistance. However, as more and more FDOT structures are placed in metropolitan and/or businesses locations, the effects of pile driving vibrations and noise have become major issues.

To provide an alternative, FDOT began the use of drilled shafts which reduced both vibration and noise. However such foundations typically have reduced axial capacities (i.e., unit skin friction and end bearing) because of soil relaxation during excavations. Subsequently, to improve axial capacity, the Department introduced post grouted drilled shaft tips. The latter increased a shaft's tip resistance as well as ensuring a proof test on expected axial capacity. Even though the latter increased the axial capacity of a drilled shaft by as much as 1.5 to 2 times of the original value, the construction process suffers from the same issues, i.e., quality control as to the shaft's effective dimensions for structural analysis and limited or the lowest mobilized skin friction of any deep foundation.

Recently, a number of European and Asian contractors began grouting along the side of precast piles insitu (Figure 8.1). Capacity increases of 100% were reported for this type pile. However, installation vibration and noise still existed.

This research focus on creating a new foundation type that would utilize two commonly used construction techniques, i.e., jetting for deep foundation installation and grouting for soil improvement or foundation stabilization. The new foundation has a number of significant advantages: (1) use of precast reinforced concrete member eliminates the uncertainty of the cast-in-place drilled shaft quality; (2) jetting minimizes noise and vibration; (3)

grouting maximizes skin and tip resistance; and (4) tip grouting of the pile besides increasing tip resistance, provides a proof test, which increases confidence for design.

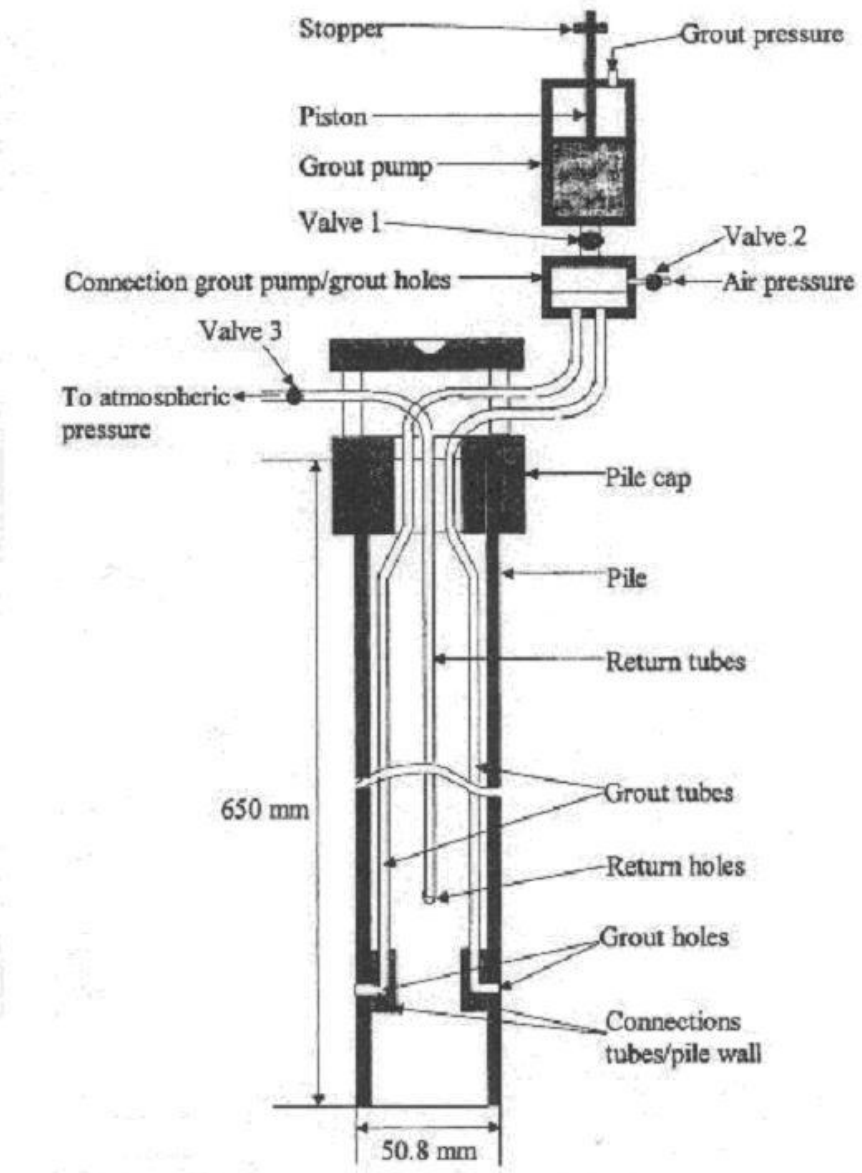

Figure 8.1 Side grouting system for precast pile (Jore et al. 1998).

The effort began with the installation of a large (12′ø × 35′) test chamber (Figure 8.2) where: 1) soil properties and moisture may be controlled; 2) soil stresses may be monitored; and 3) jet-grouted pile may be extracted and studied.

Based on several smaller scale pile jet-grouting efforts (Figure 8.1) two 16″ ×16″× 20′ precast piles were constructed and subsequently jetted-grouted in the test chamber containing

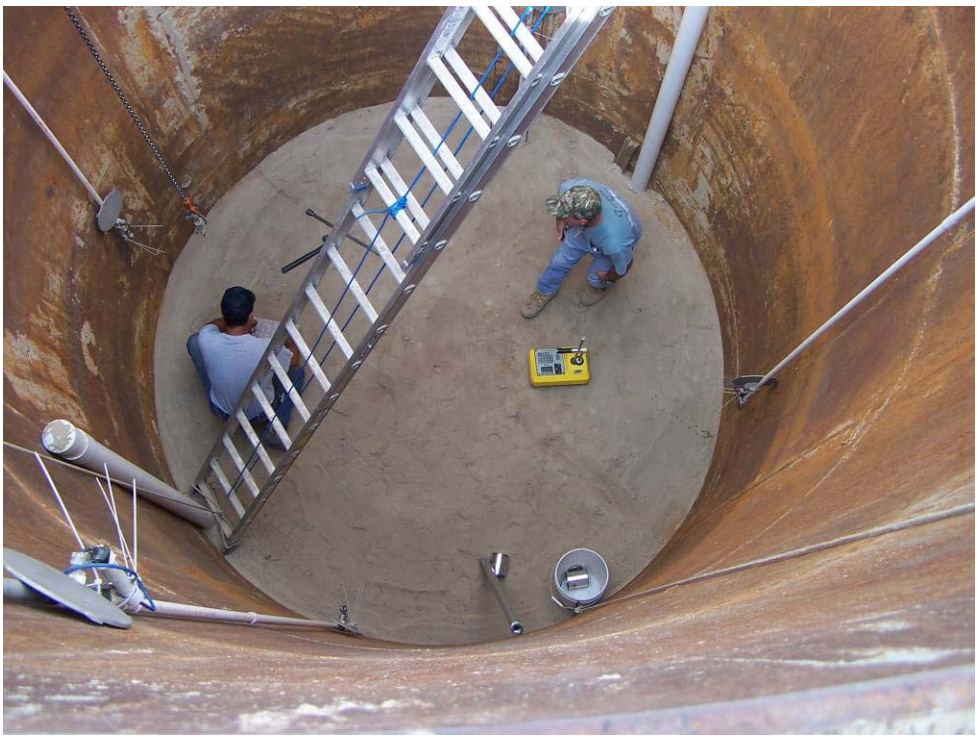

Figure 8.2 Filling the test chamber with Florida silty-sand.

(Figure 8.2) loose silty-sands. Axial load testing of the piles showed that the axial capacity of the piles were twice as that of a driven pile. Most of the increase was attributed to the earlier mobilization and greater tip resistance. Excavation alongside the jet-grouted piles revealed that grout bulbs did develop (Figure 8.3). However, there were poor bonding issues and grout flow problems, i.e., bulb expanded radially instead of vertically alongside the pile. Moreover, during the grouting process, a number of grout tubes became hydraulically locked (i.e., no flow, high pressure), clogged, and no way to clean in order to re-grout at a later date if required.

From these earlier experimental works, it was decided to redesign the grout delivery systems and introduce a semi-flexible high tensile strength permeable membrane around the precast pile to improve the grout flow problems. Influencing the grout mix design was the large cavity expansion pressures with depth (i.e., 100 to 1000 psi over 30′) and the limited cross-sectional size of the precast members. Specifically, the less fluid and larger particle

Figure 8.3 Side excavation of 16″× 16″× 20′ jet-grouted pile.

size grouts, i.e., compaction grout, which minimize soil hydrofracture, require larger diameter grout pipes and generally have no return lines for regrouting. Consequently, to allow for regrouting, grout return lines are needed which increase the number of tubes within a precast pile cross-section thus limiting the allowable tube diameters. In addition, even with the use of a compaction grout, the grout bulbs were observed to flow radially and not vertically. However, with the use of a semi-rigid membrane, and a colloidal grout, the flow was more vertical, because the membrane provided radial restrictions on flow and paths for it to flow vertical. To assist with the uniform grout flow, both the inlet and exit grout line were located diagonally at the pile corners and both the inlet and exit lines had grout exit ports. To provide one way valve action, each exit port was covered with a flexible membrane, which expanded under high pressure to allow the grout to escape and shut off under low pressure (i.e., cleaning with water) to prevent water escape into the fluid grout bulb (Figure 8.4). Ten to twenty of these mini- piles were constructed and jet-grouted into the ground to test various components of the new systems: 1) number of exit ports; 2) port

Figure 8.4 Development of grout delivery system.

valves; 3) membrane flexibility, strength and diameter; and 4) grout mix and pressure monitoring. Shown in Figure 8.5 is an example of the final grouted and excavated mini-pile demonstrating the excellent bond between the precast pile and the grout bulb.

After redesign of both the grout delivery system and grout mix, multiple small scale jet-grouted piles (8′ long) were tested in the test chamber under axial loading. Both developed excellent skin friction (0.92 ksf) and end bearing (Figure 8.6). Moreover, with lateral grout zones extending 2 times the perimeter of the precast member, significant axial side resistance, as well as excellent grout bonding was observed.

Based on the small scale pile tests, it was decided to perform a large scale pile test for both torsional and axial compression testing on the new jet-grouted pile design. In order to carry the torsional shear along the length of the 16″×16″ precast member, a 1″ thick ×12″ OD steel pipe had to be cast within the center of the concrete member. Shown in Figure 8.7 is the 16″× 16” × 20′ test pile being jetted into the test chamber. The same day, the sides of the pile

Figure 8.5 Installed and excavated jet-grouted pile.

Figure 8.6 8″× 8″ × 8′ Excavated jet-grout pile.

Figure 8.7 Installation of 16″× 16″ × 20′ jet-grouted pile.

were grouted with 800 gallons of colloidal grout. After one month, the test pile was subject to torque loading test (Figure 8.8). At approximately 15 degrees of rotation, the jet-grouted pile carried 420 ft-kips of resistance, or an average of 1.42 ksf of unit side shear resistance on the pile. The latter was carried at a diameter of 36″ (grout expanded diameter) and was transferred successfully to the 16″x16″ precast concrete member.

Following successful completion of the torsional testing, the tip of 20′ jet-grouted pile was pressure grouted. After pumping 220 gallons of grout (3′×3′×3′ bulb), a pressure of 650 psi was achieved with a vertical uplift of 0.1″ of the pile top. Attempts to pump more grout resulted in failure of a grout coupling connection. Subsequently, a top-down axial load test (Figure 8.9) was performed. A compression load of 300 kips was achieved with a downward movement of 0.095″ (Figure 8.10) before stopping at the axial uplift capacity of the 4′ diameter reaction shafts.

Figure 8.8 Torque test on 16″× 16″× 20′ jet-grouted pile.

Figure 8.9 Top-down axial loading jet-grouted pile.

Shown in Figure 8.10 also for comparison is the 20 ft jet-grouted pile with the estimated (i.e., FB-Deep) response of an 18″ ø × 20′ drilled shaft. It is estimated that the jet-grouted shaft should have an axial capacity between 400 to500 kips (torsional results and grout pressure × area of tip) as compared with the estimated 100 kips for the drilled shaft, i.e., 4 to 5 fold increase. In addition, grouting the tip of the pile is also a proof test on the pile capacity, so a higher LRFD ϕ for the pile than the value recommended for either drilled shafts (non tip grouted) or driven piles may be used.

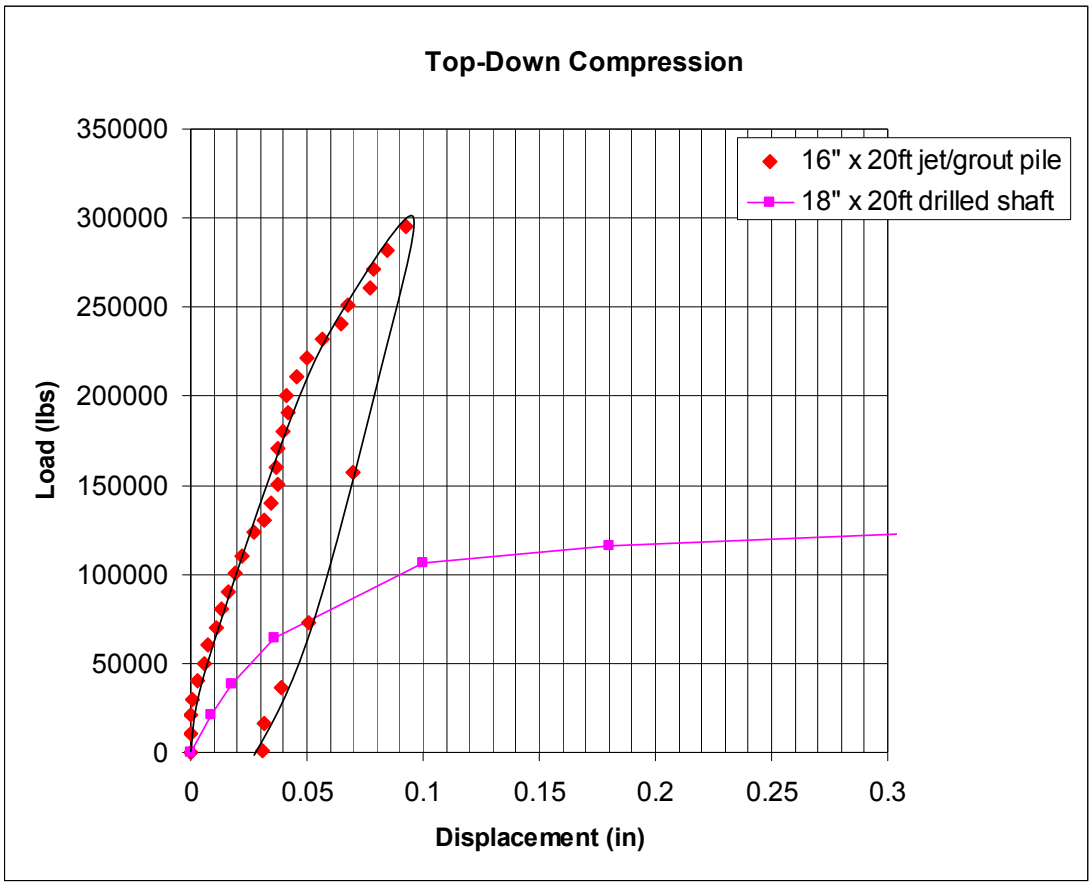

Figure 8.10 Axial load vs. deformation of jet-grouted pile and a drilled shaft.

For the design of the new jet-grouted pile, past works on cylindrical and spherical cavity expansion are very useful. For instance, published limit pressures from cylindrical cavity expansion theory as a function of depth, relative density and soil strength (critical state friction angle) agree quite well with measured side grout pressures for sands. Similar results

were obtained with spherical cavity expansion and measured pile tip grout pressures. In the case of other soils or a mixture, the limit pressures from pressuremeter testing is recommended based on testing within the test chamber.

Also based on cavity expansion theory, both the hoop (circumferential) and vertical stresses are similar, suggesting that both torsional and axial unit skin friction are quite comparable. The magnitude of the unit skin friction is controlled by the magnitude of the cylindrical cavity expansion theory, which is a function of depth, strength and relative density of the cohesionless soil. Based on estimation of the latter (e.g., cavity expansion theory, pressuremeter, etc.), and Mohr-Columb strength of the soil, the unit skin friction on a jet grouted pile may be estimated.

Based on the results of this research, it is believed that the jet-grouted has a number of distinct advantages: (1) use of precast reinforced concrete member eliminates the uncertainty of the cast-in-place drilled shaft quality; (2) jetting minimizes noise and vibration; (3) grouting maximizes skin and tip resistance; and (4) tip grouting of the pile increases tip resistance, and provides a proof test for which higher LRFD ø may be used in design. It is recommended that more testing of the pile be performed outside the test chamber in different soils so that a new LRFD ø may be established for this type of pile/shaft.

LIST OF REFERENCES

ACI Standard (2002). *Building Code Requirements for Structural Concrete (ACI 318-02),* Farmington Hills, Michigan.

Baker, A. C., and Broadrick, R. L. (1997). "Compaction Grouting." *Proc., 1997 ASCE Florida Annual Meeting*.

Best, J. F., and Lane, R. O. (1982). "Testing for Optimum Pumpability of Concrete." *Grouting in Geotechnical Engineering, Proc., ASCE Conf. on Grouting in Geotech. Eng.*, Vol. 1, 49-61.

Dapp, S. D., and Mullins, G. (2002). "Pressure Grouting Drilled Shaft Tips: Full-Scale Research Investigation for Silty and Shelly Sands." *Proc., ASCE Deep Foundations 2002: An International Perspective on Theory, Design, Construction, and Performance*, Reston, Va., 335-350.

Florida Department of Transportation Standard (2002). Section 455: Stuctures Foundations.

Fu, X.., and Zhou, Z. (2003). "Study on Bearing Capacity of Bored Cast-in-Situ Piles by Post Pressure Grouting." *Proc., ASCE 3rd Int. Conf. on Grouting and Ground Treatment*, Vol. 1, 707-715.

Hwang, N. H. C., and Houghtalen, R. J. (1996). *Fundamentals of Hydraulic Engineering Systems*, Prentice-Hall, ed. 3, 131-132.

Kuo, C. L., Heung, W., and Roberts, J. (1998). "Limited Mobility Displacement Grouting for a MSE Wall Foundation." *Proc., Grouts and Grouting: A Potpourri of Projects*, 70-82.

Naudts, A., and van Impe, R. (2000). "An Alternate Compaction Grouting Technique." *Proc., ASCE Geo-Denver: Advances in Grouting and Ground Modification*, 32-47.

Nichols, S. C., and Goodings, D. J. (2000). "Effects of Grout Composition, Depth, and Injection Rate on Compaction Grouting." *Proc., ASCE Geo-Denver: Advances in Grouting and Ground Modification*, 16-31.

Salgado, R., and Prezzi, M. (2007), "Computation of Cavity Expansion Pressure and Penetration Resistance in Sands," *International Journal of Geomechanics, ASCE, Vol.7, No. 4., ppg 251-265*

Salgado, R., and Randolph, M., (2003), "Analysis of Cavity Expansion in Sand," *International Journal of Geomechanics, ASCE, Vol.1, No. 2., pp 175-192*

Tsinker, G. P. (1988). "Pile Jetting." *J. Geotech. Eng.*, 114(3), 326-336.

Van der Stoel, A. E. C. (2001). "Grouting for Pile Foundation Improvement." Post-graduate thesis, Delft University of Technology, Amsterdam.

Warner, J. F., and Brown, D. R. (1974). "Planning and Performing Compaction Grouting." *J. Geotech. Eng. Div.,* 100(6), 653-666.

Yu, H.S. and Houlsby, G. (1991), "Finite Cavity Expansion in Dilatant Soils: Loading Analysis," *Geotechnique, Vol 41, No 2. pp 173-183.*